Spring 2008

Design and optimization of abrasive slurry feed system, control circuit and jet drilling tool for mining applications,

Pradeep Nambiath

Department: Mining Engineering

DESIGN AND OPTIMIZATION OF ABRASIVE SLURRY FEED SYSTEM, CONTROL CIRCUIT AND JET DRILLING TOOL FOR MINING APPLICATIONS

by

PRADEEP NAMBIATH

A DISSERTATION

Presented to the Faculty of the Graduate School of the

MISSOURI UNIVERSITY OF SCIENCE & TECHNOLOGY

In Partial Fulfillment of the Requirements for the Degree

DOCTOR OF PHILOSOPHY

in

MINING ENGINEERING

2008

Approved by

David A. Summers, Advisor
Samuel Frimpong
Greg Galecki
Jerry C. Tien
Leslie S. Gertsch

ABSTRACT

This dissertation focused on an investigation of small diameter hole drilling using abrasive slurry jet (ASJ) technology. The existing ASJ feed systems were reviewed and found inadequate to satisfy the requirements of an ASJ drill. A novel feed system was designed which improved on existing systems by resolving problems with the inability to perform stop/start operations and ensure precise metering of abrasive feed. This system met standards of consistency and evenness of feed required for machining aircraft component parts for Air Force Research Laboratory (AFRL). Theoretical and experimental analysis of the power of an ASJ stream yielded valuable design information that was then included in drilling tool design. The concept of introducing a swirl component in the nozzle before accelerating the slurry stream was used to design a Dispersed Abrasive Slurry jet (DASjet) nozzle. The influences of abrasive feed rate and pressure on the hole depth and diameter were studied. The effect of variation of the swirl angle on performance was found and an optimal angle identified. Material removal rates in air and under hole backpressure were determined. The loss in drilling performance when the drill operates against backpressure was overcome initially by the introduction of an air sheath around the jet. The cutting fluid and air shroud were then replaced with supercritical carbon dioxide. Supercritical CO_2 was shown to be a superior fluid medium to form the slurry jet because of the phase change which occurs at the nozzle orifice. Laboratory experiments conducted to validate this change successfully showed that this tool could drill holes to larger than two-inches in diameter, without nozzle rotation, and at rates of penetration of up to 400 ft/hour. As a result a novel drilling tool has been created for use in microhole drilling.

ACKNOWLEDGEMENTS

First, I would like to thank my advisor, Dr. David Summers for his confidence and belief in my abilities. This research would not have been possible without his support, patience and guidance. I am grateful to have been a part of his vision and quest for innovation and hope to continue along the path he has set me on.

I would like to thank Dr. Greg Galecki for his guidance through the initial days at the Rock Mechanics and Explosives Research Centre. His constant support and advice have helped through some difficult research problems and it has been a pleasure to work for and with him for the past 6 years.

I would like to thank my committee members, Dr. Samuel Frimpong, Dr. Jerry Tien and Dr. Leslie Gertsch for their time and value input towards the completion of my research.

I shall be ever indebted to Mr. John Tyler, Mr. Robert Fossey, Mr. Jim Blaine, Mr. Scott Parker, Miss Diane Henke, Miss Vicki Snelson and Miss Jo Blaine have supported and guided me through my years in Rolla with their advice and help in all matters.

This work was partially carried out under funding from the U.S DOE-NETL Microhole Technology Development for Ken Oglesby, Impact Technologies, LLC. This support is gratefully acknowledged.

TABLE OF CONTENTS

Page

LIST OF ILLUSTRATIONS

LIST OF TABLES

NOMENCLATURE

Symbol	Description
a	Constant
AFR	Abrasive feed rate
C	Mass concentration of abrasive
C_f	Coefficient of friction of the kerf wall
C_K	Characteristic velocity
D -	Nozzle diameter
d_j	Diameter of the jet
E_i -	Input energy
$\dot{M}_A$ -	Abrasive mass flow rate
m_a	Mass flow of abrasives
$\dot{M}_w$ -	Water mass flow rate
P -	Pressure
Q -	Total flow rate
R -	Loading ratio
R_f	Particle roundness factor
V_a	Velocity of the abrasive particles
V_c	Cutting threshold velocity
v -	Abrasive slurry velocity

η_t - Momentum transfer coefficient

μ_m - Momentum transfer parameter

ρ_a - Density of abrasive

ρ_w - Density of water

σ_f Work piece material flow stress

1. INTRODUCTION

1.1. BACKGROUND

Fluid jetting is the process by which power, created when a prime mover drives a pump, is transmitted as an energized primary liquid flow through an appropriately pressure-rated feed line, and delivered as a working tool from a nozzle. Traditionally water has been the primary phase resulting in use of term waterjetting to describe all such activities.

Waterjet applications in mining began with a need to remove soil cover from over valuable mineral deposits primarily gold, and then spread to the mining of the ore itself. Commercial mining of coal hydraulically began in 1952 [Ofengenden, 1980] and since then there has been substantial research and commercial development of hydraulic mining in Russia (Yufin, 1965), the United Kingdom [Jenkins, 1961], United States [Baker 1959], China [Wang, 1983], Japan [Wakabayashi, 1979] and Canada [Parkes, 1983]. Large volume flows at relatively low pressure are most effective for the majority of hydraulic mining. In this research program, the smaller flow rates and higher pressures that are required when waterjets are used for cutting rock are of greater interest. The classic modern application of waterjet cutting, which is in granite quarrying, is described in Bortolussi et al. [1989]. The use of a waterjet in cutting rock has allowed an easier path to understanding jet cutting behavior with other materials [Summers, 1995]. The relative large grain structure of many rocks results in the obvious development of a failure process. The use of a high pressure waterjet alone to cut through material required that

very high pressures be developed to penetrate through all rock types, and this was a requirement that in many applications made the process uneconomic.

1.2 ADDING ABRASIVE TO WATER

In 1980, Flow Research first commercialized a method for improving the cutting efficiency of waterjets by introducing abrasive particles into the jet stream. This development was initially for use as an industrial cutting system. The method for adding the abrasive centered around a nozzle that accelerated the water to a maximum velocity through a small orifice that fed the resulting waterjet into and through a mixing chamber, with the passage of the jet through that chamber creating a vacuum within it. As a result of this pressure drop, abrasive was aspirated into the mixing chamber from an external storage hopper through a feed pipe which led from the hopper to an opening in the side of the chamber. The abrasive is helped in movement from the hopper to the chamber by an air flow that is concurrently drawn by the suction, through the same feed pipe. The resulting mixture of water, abrasive and air combines in the chamber and as it leaves is refocused through a larger diameter, longer nozzle to form a secondary jet which the nozzle orifice will direct to the target, Figure 1.1. In the process of mixing there is a kinetic energy transfer from the fluid to the abrasive particles, and it is the particles, in this modification, that now have the energy to do the cutting. Because of their higher mass, and sharp-edged geometry they are able to effectively cut target material at a pressure much below that of the water alone. The technology although effectively successful in industrial applications for two-dimensional cutting metals and ceramics encountered a few problems when it was first applied to the cutting of rock.

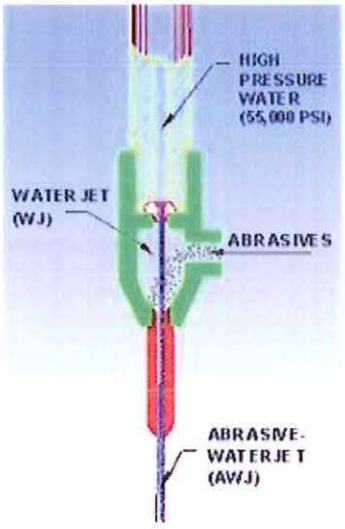

Figure 1.1 Operating mechanism of an AWJ

[http://www.stereovisionengineering.net/UHP%20Fluidjets_b.htm]

Because the abrasive must flow freely through the delivery tube from the hopper to the chamber, the initial Flow design (Figure 1.1) required that the abrasive to be supplied as a dry particulate to the point where it entered the mixing chamber. Any excess moisture before that point will cause the particles to agglomerate and block the feed line, stopping the process. Because the mixing chamber is located at the end of the cutting tool and very close to the cutting face, this requires that the feed line carry the dry abrasive to that point, as a secondary feed line (the waterline being the first). As will be discussed later, in conventional rock drilling the cutting head rotates, and thus a swivel would need to be developed that allowed feed and rotation of these two separate lines. Within the narrow confines of a drilled hole with a significant deflection of water back from the cutting face to the nozzle this design could be quite a challenge.

Several different ways to overcome this challenge have been proposed. One of the more promising research on works on using an abrasive waterjet as a rock drill was

carried out at the Bureau of Mines [Savanick, 1987]. This work focused on ways to resolve this problem of the multiple swivels and seals. Rather than do this upstream of the nozzle, the solution proposed was to send a non-rotating abrasive stream down a rotating pipe, at the end of which it struck an inclined carbide plate. This deflected the stream around the perimeter of the hole, where it cut into the rock and cut clearance for the tool to advance. Acceptable drilling rates of penetration (ROP) were achieved with the jet at a pressure of 10,000 psi, a flow rate of 20 gallons per minute and with 22 lb/min of abrasive added to the jet. Although the technique reached the point of commercial trials, the costs of tool wear, abrasive consumption, power and water usage made this tool somewhat expensive and difficult to operate, and the times were not right for the introduction to be successful.

It was clear that these initial methods for adding abrasive to the waterjet were somewhat inefficient, even through the resulting stream was powerful enough that it formed the basis for an entire industry. Thus, experiments continued to find alternate ways of adding the abrasive. In 1986 investigators at the British Hydromechanics Research Association (BHRA) published the first paper [Fairhurst, 1986] on an alternate means for adding abrasive to the jet fluid thereby providing a significant new milestone to this field. Fairhurst [1986] had shown that if a small quantity of the flow from the pump was diverted from the main flow, and used to transport abrasive from a pressurized container so that it could be subsequently remixed with the main flow, jets could be generated that were more powerful cutting tools than were the conventional abrasive-entrained jets. These new jets were called Abrasive Slurry Jets (ASJ) to differentiate them from the more-conventional entrained Abrasive Water Jets (AWJ).

Abrasive slurry jets are formed as a two phase jet with the abrasive particles mixed with the water before the fluid is accelerated to form a high velocity jet. There is no air phase to the fluid. Through time this definition has expanded to include those systems where the fluid and the abrasive are mixed before entering the high-pressure pump, as well as those more common systems where the abrasive is fed from a pressurized container into the line between the pump and the nozzle, Figure 1.2. The absence of the air phase in the ASJ jet stream results in higher efficiency of energy transfer to the abrasive (since none is expended on accelerating the air [Labus, 1989 and Tabitz, 1996]) and there is a more coherent jet structure to the jet after it leaves the nozzle, since *inter alia* there is no air expansion from within the jet to induce disruption of the flow.

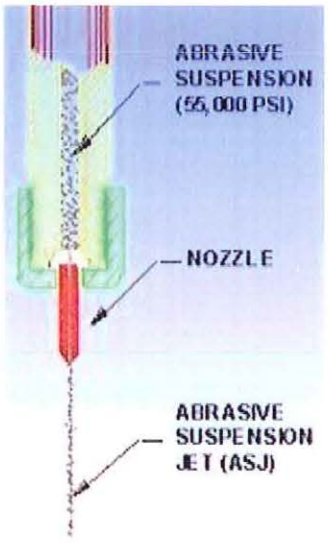

Figure 1.2 Operating mechanism of an ASJ

[http://www.stereovisionengineering.net/UHP%20Fluidjets_b.htm]

The higher efficiency and thus greater cutting performance of the ASJ, when compared with that of the AWJ has been discussed by Hashish [1989] theoretically and more recently Jiang [2005] explored the cutting capability of the ASJ both theoretically and experimentally. Yazici [1989] investigated the cutting and drilling of granite with an ASJ and used specific energy and erosion efficiency as metrics of cutting performance. More commonly, experimental studies of the cutting capability of abrasive slurry jets [Brandt, 1994] have largely used depth of cut as the measure of performance, in materials ranging from metals to ceramics and rocks. The effects of the change in abrasive concentration within the jet stream, the change in jet pressure, and the variation in nozzle size (and thus flow rate) on the depth of cut achieved, demonstrates how these parameters affect the effective application of abrasive power using an ASJ to penetrate or remove material.

An important distinction that needs to be made in the application of an ASJ, when compared to the use of an AWJ lies in the range of effective impact of the resulting jet. While both ASJ and AWJ systems can be used in short-range applications, that include metal cutting, and the cutting and singulation of precision parts for the semiconductor industry, where standoff distances are less than tenth of an inch. In contrast, oil well drilling or completion enhancement in the oil industry requires much greater standoff distances, which can exceed 20 inches. At such distances where directly pumped ASJ's [Fair, 1981 and Rach, 2007] can be used, the performance of the ASJ far exceeds that at which the AWJ is effective. This distinction gains additional importance in situations where the particles need to travel a significant distance in air or through fluid in order to impact and erode the target.

1.3 STATEMENT OF THE PROBLEM

In recent years, the need to drill smaller diameter holes over increasingly long distances has become an important requirement for the mining and oil and gas industry. Major research has been directed towards drilling wells that are around two inches in diameter, rather than the larger diameters of more classic drilling. For these new wells to be effective, the cost to drill them must be significantly less than that of conventional wells. Development of such tools will find application not only in the oil industry but also in the exploration and development of other resources, monitoring geothermal conditions and other uses where the smaller drill will have a reduced environmental impact. Current needs for the drilling industry include tools that can lower the cost and increase the performance in jobs such as these.

This research effort was therefore directed toward developing a non-rotating Abrasive Slurry Jet drilling tool capable of drilling a two-inch diameter well. In the process of developing this tool, it was necessary to overcome some of the barriers to progress that became evident as the design evolved. This included the interference that occurs in the conventional use of an ASJ system between the cutting jet as it travels toward the target surface and the rebounding jet and cut debris after impact. In addition, the benefit of a non-rotating design, one that would allow directional ASJ drilling in conjunction with coiled tubing, would be explored with the intent of creating a tool that can be used for multiple interval completions and drilling of horizontal laterals for coal bed methane extraction.

1.3.1. Abrasive Slurry Feed System. There is a need to evaluate the existing abrasive slurry jet feed systems and redesign the system, to overcome current limitations

in control. Specifically, a means for precise slurry metering is required, and a delivery system that can be switched on and off without concern. A controlled, consistent feed will allow drilling a hole with a constant diameter. The technology that evolves can also be applied for cutting materials (including metals) and the drilling of holes for rockbolt emplacement in methane rich environments.

In order to validate the design of a system that meets the above criteria, an experimental procedure must be developed that will determine and demonstrate consistency of feed. This means must be easily repeatable in a laboratory or field setting and be such that it can be specified as a standardized test with a defined material. The test should not be time intensive or difficult to perform in the laboratory.

1.3.2. Non-Rotating Nozzle Assembly. One of the considerable problems with the use of an abrasive-laden jet stream comes with the need to sweep the jet across the surface of the rock ahead of the bit, to ensure that all this rock is removed, thereby allowing the bit to advance. Historically this has been done by rotating the drilling tool over the rock surface. Where high-pressure fluid is involved, this requirement imposes the need for a high-pressure swivel. While such tools exist, they are vulnerable to damage in the hostile environment that exists at the bottom of a hole during drilling. The design of a drill that would not rotate would overcome these limitations.

Such a drill must, however, still remove, at an acceptable ROP, all the material from the face of the rock ahead of the tool, and function in the environment to be found at the bottom of a well that might be 5,000 ft deep or more. In such an environment, the cutting process must deal with the pressure of the surrounding fluid, and the rebounding fluid and debris from the cutting zone.

1.3.3. Fluid Medium for Dispersed Abrasive Slurry. Water has traditionally been used to transport abrasive in the slurry, and to form the resulting ASJ. The momentum transfer between the fluid and the abrasive provides the latter with the power that controls the cutting action of the system. There is only a finite amount of energy that can be conventionally transferred to the fluid by mechanical means, i.e. from a pump. Alternate sources of energy will therefore be explored, including ways to add and store energy in the liquid phase with the consequent ability to control and release this energy at the point of maximum benefit. One potential source for such an option is through the use of supercritical fluids. Initial investigations into the use of such supercritical fluids will therefore be undertaken, with liquid carbon-dioxide being used as an exemplary carrier fluid. Given that these studies will be the first attempt at utilizing this medium in abrasive assisted drilling the benefits and problems that develop with this new concept will be documented.

1.3.4. Theoretical Model for Determining Abrasive Power. While, experimental work is a validation of the concepts that evolve with this study, the potential of the technology, and the ultimate potential is better described with an underlying theoretical model of the process. Thus, it is important to determine the energy transfer efficiency of ASJ systems through the development of a descriptive theoretical model. This is particularly important in the assessment of the role of the concentration of abrasives in slurry cutting, and drilling applications and the optimization of that value for different conditions. Various parameters such as nozzle size, abrasive feed and pressures will have significant influence on the efficiency of the cutting system, and thus the descriptive analysis should determine optimal concentration values for ASJ systems. The

analysis should include energy transfer efficiency since it will have direct impact on economic viability of ASJ tool for cutting and drilling applications. The influence of quality of the nozzle is also of merit in this analysis.

2. LITERATURE REVIEW

Drilling in rock has been a key activity in the production of raw materials, as well as in construction and excavation. Current drilling methods rely on the use of hard metal or diamond drill bits thrust against rock, and where fragmentation is achieved by means of abrasion crushing and shear fracturing while the bit is rotating or impacting against the rock surface. Conventional drilling methods have issues with limited bit life coupled with high maintenance costs for the supporting mechanical assemblies. A high level of thrust is required to penetrate the rock, in order to drill the small diameter holes, which are of interest in the present research and so the drill bit which carries this load to the bit has a tendency to buckle. Drilling with continuous high pressure fluids has a distinct advantage since the thrust required for this tool is several orders of magnitude less, and there is little torque required for drilling. When the tool can achieve comparable drilling rates with existing equipment, this makes waterjet drilling a potentially viable option.

2.1. WATER JET DRILLING

Initial work in the development of waterjet drilling in the 1970s concentrated on the use of plain water as the cutting fluid, without any abrasive additives. Field experimentation, [Maurer, 1975] demonstrated the effectiveness of using water jet drilling in conjunction with conventional drills in oil field applications. Initial work with plain waterjets [Summers, 1968] led to the development of a waterjet drilling system where a single inclined rotating jet was used for drilling a straight hole. However, use of a single jet to cover the entire face of the bit was inefficient, and considerable

improvement was achieved when a second orifice was added to the nozzle. This jet was axially located and directed to remove the central core of rock ahead of the bit. Adding this smaller jet, half the diameter of the main orifice, improved penetration rates by two orders of magnitude. Subsequent experimentation, showed that the optimum angle of inclination for this jet was in the range from 20 – 25 degrees to the hole axis [Summers, 1976]. As originally configured, however, the jets could not drill through all the rocks that they might encounter underground.

Two different solutions have been pursued to resolve the difficulty of drilling through a harder suite of rocks, both were initially funded by the-then U.S. Bureau of Mines. Work at the Colorado School of Mines (CSM) proposed a hybrid bit combining high pressure waterjets and mechanical cutting [Bonge, 1982]. The other option, followed by Flow Research used higher jet operating pressures for cutting, and was able to achieve up to 50% greater productivity when compared with mechanical drilling systems [Veenhuizen, 1978]. A commercially available drilling system the Jet-Bolter, marketed by Jarvis-Clark, resulted from this approach. On a larger scale, CSM then went on to provide waterjet assistance to tunnel boring machines and this was picked up in a number of countries [Hoshino, 1976].

Two alternatives have been conceived to obtain material removal rates that would be several orders of magnitude higher than plain waterjets, particularly in harder rock. The first of these was the mixing of abrasives with high velocity waterjets by entrainment – known as Abrasive Waterjetting (AWJ) and this was followed by the second where premixed slurry was pressurized and forced through a nozzle. This latter has become

known as Abrasive Slurry Jetting (ASJ).These two methods revolutionized the range and impact of waterjet drilling.

2.2. ABRASIVE WATER JET DRILLING

The first use of solid particles in a stream of fluids was aimed at improving the drilling rates of oil field bits [Eckel, 1955]. The principle used was similar to one subsequently developed in a conventional AWJ where particles would be drawn into a jet stream using a suction effect. One advantage of running this tool at the bottom of a developing oil well is that the confining condition allowed spent solid particles, after impact with the target, to be reintroduced into the cutting jet stream until the particle size became too small for the tool to perform efficiently. Unfortunately a fire destroyed the major equipment being used for this research and the program was discontinued.

Alternate methods of introducing abrasive into a jet stream involved surrounding the abrasive flow with a jet and one in which abrasive surrounds the jet [Chatterton, 1975]. The development of a rock drill based on the AWJ concept, but without the need for a high-pressure swivel, directed a mixture of water and abrasive towards a deflector at the end of a collimating tube [Savanik, 1987]. This design did not use a second collimating tube to bring the jet back together, reducing the pressure and downstream range. But it enabled the creation of a rotating device by putting a low pressure swivel into the water feed line. Although the concept was reviewed commercially, it found no ready market.

Analysis of a number of potential designs [Hashish, 1989a] to use a non rotary drill stem, included designs with multiple waterjets being used to form a single AWJ, as

well as two AWJs mounted in a rotary drill stem. It was concluded that drilling with non rotary drill stem with either fixed or rotating waterjets would require much higher power and abrasive concentration levels than were conventionally practical, if one were to aim to achieve faster rates of penetration (ROP) than with conventional tools. Also, the use of multiple small waterjets rather than a single waterjet of equivalent power was found to be more efficient in terms of material removal ahead of the bit. The suite of designs examined in this approach all required that a separate feed line be provided to the cutting bit, through which dry abrasives is supplied. This presented an increasing problem at greater depths as back pressure and cuttings recycling made it an impractical feature for a deep-hole drilling tool.

2.3. ABRASIVE SLURRY JET DRILLING

The genesis of ASJ drilling can be traced back to the same oil field research that led to the AWJ evolution. In contrast with the AWJ work, studies where the abrasive particle was accelerated with the drilling fluid showed significant better drilling performance [Anon, 1971]. Subsequent research undertaken by Gulf Research and Development Co. presented improved techniques for this drilling method [Fair, 1981]. This approach was revisited for drilling small diameter holes in mining applications [Summers, 1991]. Nozzle design is an important component in this drilling method and Yazici tested different configurations of nozzles in the drill body, both to evaluate abrasive acceleration potential and to influence the shape of the hole being drilled [Yazici, 1989a].

The superior cutting capability of an ASJ system over the more conventional and widely adopted AWJ system [Fairhust, 1986] spawned research aimed at using this efficient cutting technology in cutting processes. Subsequent work, [Brandt 1994], [Alberts, 1995], [Shimizu, 1998], [Fowell, 2000] has reinforced the superior cutting capability of ASJ systems. An ASJ cutting system has two major components; the abrasive slurry feed system and a nozzle assembly. The abrasive slurry feed system supplies a suspension containing abrasives to the nozzle assembly which accelerates this suspension; the subsequent cutting action is a result of the abrasive particles exiting the nozzle at velocities that are determined by the process parameters.

2.3.1. Abrasive Feed System. According to the method of generation, ASJ feed systems can be divided in to three main categories:

- Direct pumping systems
- Indirect pumping systems
- Bypass systems

Despite the different generation mechanisms, Figure 2.1, the most important difference between the two systems is the ability in bypass systems to control the concentration of solid abrasives in the slurry flow stream and the inability to do so in direct pumping systems. Historically, direct pumping systems have operated at higher pressures than bypass systems [Brandt, 1994], [Hashish, 1991].

2.3.1.1 Direct pumping systems. In direct pumping systems, the abrasive is mixed with water at normal pressures and fed into the low pressure inlet side of the pump and exits as a high pressure suspension through the nozzle. Despite the relative ease of operation of this system, the high wear in internal components of the pump has prevented

widespread commercialization of this concept. For example, where such a concept is used in generating the high-pressure sand-laden fluid used in hydrofracking an oil well, the cost of the operation has, in the past, included the cost to replace the high-pressure end of the pumps, since passage of the abrasive during a single operation, is sufficient to erode them beyond further practical use.

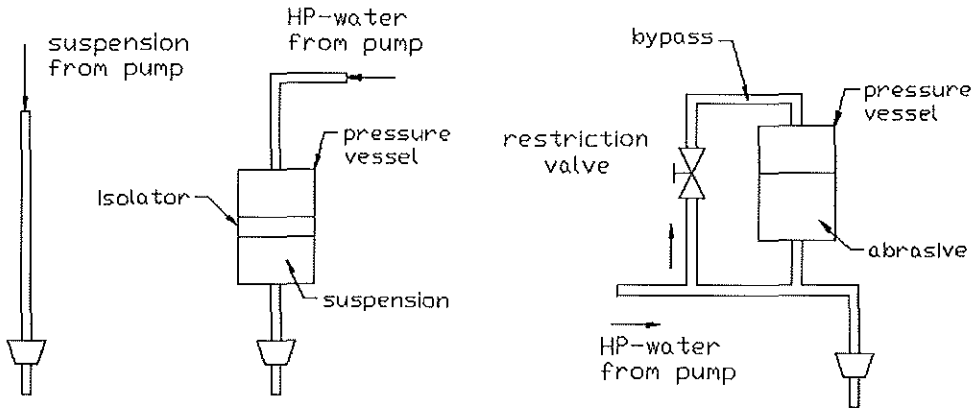

Figure 2.1. Mechanisms of ASJ [Brandt, 1996]

2.3.1.2 Indirect pumping systems. In indirect pumping systems, the water abrasive slurry is separately charged under low-pressure into a pressure vessel that is then installed between the high-pressure pump and the cutting nozzle. This vessel is then brought up to operational pressure by use of the high pressure water feed line, which brings the slurry to the pressure of the cutting system. There is a separator between the abrasive slurry and the high pressure water supplied from the pump to prevent mixing and dilution of the abrasive slurry. In some designs of this system, the abrasive is held in suspension using a polymeric additive.

One of the main reasons why direct pumping systems have not been popular is the inability to change abrasive flow rate independent of the system operational parameters, primarily pressure, nozzle and suspension characteristics. The settling of abrasives in the storage vessels can be remedied by mixing the abrasive with high viscous additives to suspend the abrasive particles. The viscosity of the polymer solution is generally four times that of water. The effect of these additives was investigated [Hollinger, 1991] on the coherence and cutting capability of the jet [Zakin, 1976].

2.3.1.3 Bypass systems. The abrasive is stored under pressure in a cylinder and a portion of the water flow from the pump is used to extract a controlled amount of abrasive from the vessel and to mix this with the remaining water flow on its way to the nozzle, generating an abrasive suspension of the desired concentration. The main difference between the different systems proposed has been in the working parameters and the mechanism of abrasive mixing with the main fluid flow to the nozzle. The work in Brandt [1996] gives a detailed description of these existing systems. The various configurations can be seen in Figure 2.2 and are described below.

The original DIAJET system [Fairhurst, 1986] was fitted with a special bottom outlet configuration, a combination at the bottom of the tank as seen in Figure 2.2 is used to achieve an even supply throughout the discharge of abrasive from the storage vessel. This design ensures that the abrasive is not gravity fed, but pushed as a result of the bypass flow through the opening. The abrasive exits through the bottom of the tank and has to be controlled by opening and closing of a valve, resulting in excessive wear during stop start operations.

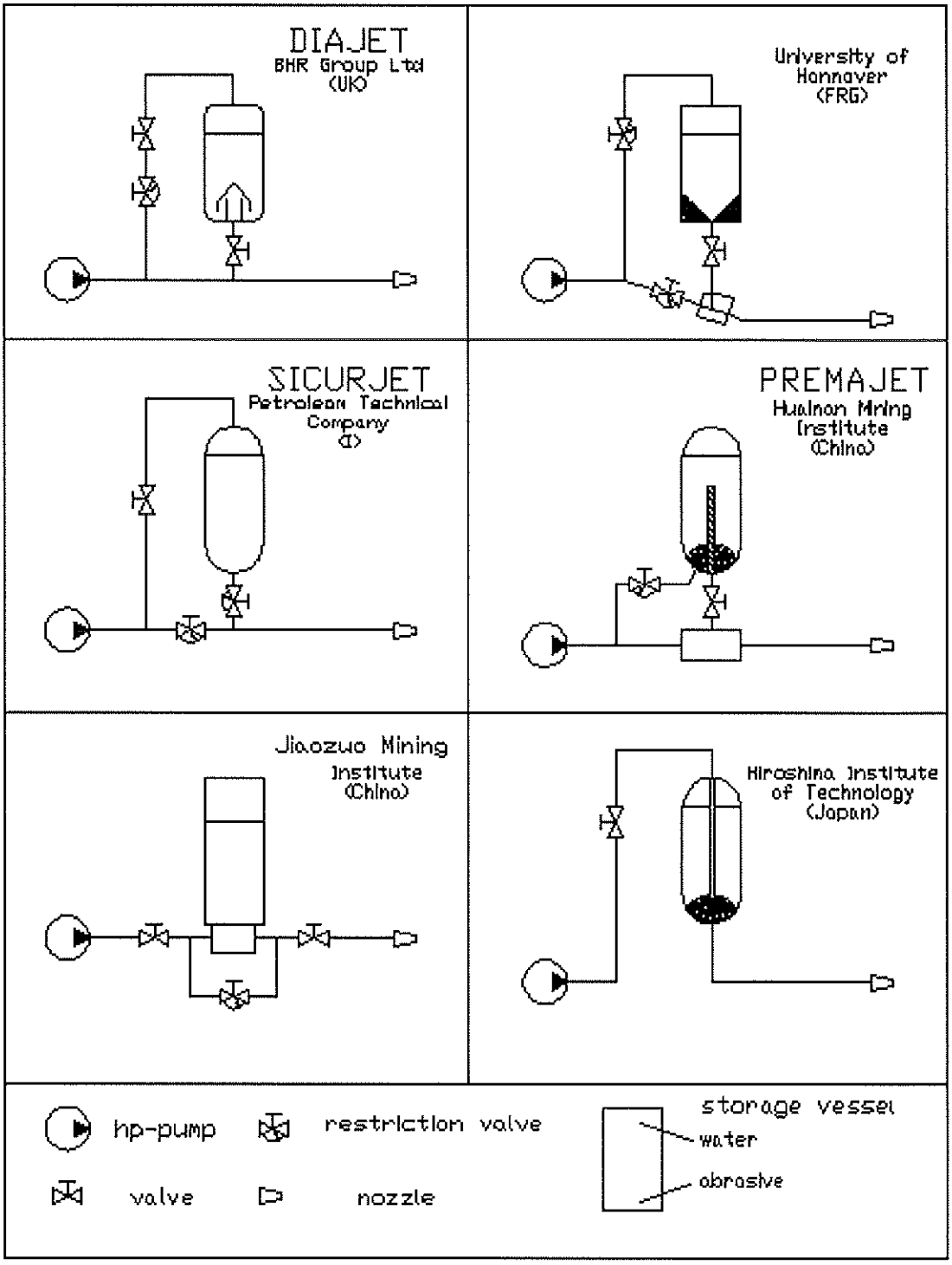

Figure 2.2. Configuration of existing ASJ feed systems

The system developed at the University of Hannover [Brandt, 1994] had a cone at the outlet of the storage vessel and the bypass flow was mixed with the main water in a special mixing cell. Water is pumped from a piston pump and splits into two lines, the bypass feeds top of the storage vessel to control the flow and the abrasive feed rate. The flow of abrasive from the bottom of the storage vessel is controlled via a valve to a junction where it mixes with water from the second line before exiting the nozzle. The abrasive flow rate was determined by the weight loss of the pressure vessel. This is a very difficult system to monitor within the precision required for accurate control of abrasive feed rate. Also, it is not possible to shut the abrasive flow without depressurizing the system because of abrasives in the line.

The PREMJET system [Liu, 1992] has a screw fitted at the bottom of the storage vessel to ensure a constant abrasive flow and to avoid any blockages. The flow from the pump is divided into two- the bypass line and the main line. The bypass line is fed through the bottom of the storage vessel and is used to partially fluidize the abrasive. This flow line is regulated to obtain precise regulation of the abrasive flow rate. The fluidized abrasive is metered into the main line to obtain a slurry jet. This arrangement was successful in metering the abrasive flow but again a gate valve at the bottom the tank controlled the abrasive flow and it is not possible to start/stop the system without flushing the valve with clean water to remove abrasive particles.

The feed system developed at the Jiaozu Mining Institute [Zhang, 1995] utilizes a special mixing chamber beneath the storage vessel. The abrasive falls from the storage tank under gravity while the water permeates up through the abrasive into the vessel. The feed is very much dependent on gravity and there is no flow to push down on the

abrasive. Evenness of abrasive feed cannot be guaranteed and is very much dependent on the amount of abrasive left in the tank.

The Hiroshima Institute of Technology [Shimizu, 1995] design uses a single flow line to extract the abrasive. The pressurized water discharges through a mixing nozzle into the storage vessel. The nozzle location above the outlet channel of the vessel causes the abrasive at the bottom to be fluidized and the resulting slurry to flow down through this channel and towards the nozzle assembly. The concentration of slurry decreases with time but is constant over short periods.

2.3.2. Nozzle Geometry. The basic design of an ASJ nozzle is shown in Figure 2.3. The nozzle can be divided into three main sections, the pipe section, the acceleration section with decreasing cross section and focus section with constant or increasing cross section. Optimizing of nozzle performance is generally a balance between cutting performance and nozzle lifetime. The cutting performance increases with increase in abrasive flow up to a certain point after which performance decreases. This excess flow of abrasive through the nozzle erodes the nozzle body reducing nozzle lifetimes. The type of nozzles used is dependent on the type of feed system that is used. With the indirect pumping system, low profile short nozzle designs are used. Nozzle diameters for this type of application range from 0.229mm [Hashish, 1991] to 0.6mm [Alberts, 1995]. Nozzles that are used with the bypass feed system have larger diameters and are longer. The inlet section is designed with a radius [Brandt, 1994] or a taper [Yazici, 1989b] with the convergent angles between 12 and 60 degrees. Four methods have been proposed by researchers to reduce the wear of these nozzles.

- A shoulder, where the particles are deflected by the tapered surface towards the interior of the flow with the carrier fluid in contact with the internal surfaces [Bloomfield, 1991].
- A two step tapered nozzle, that prolongs nozzle life and helps accelerate the particles more efficiently [Mingqing, 1996].
- Use of porous nozzle through which the fluid may percolate to form a protective layer between the slurry and the wall [Tan 1991], [Anand, 2003]. This design was tested at MS&T and works as long as there is flow, but rapidly erodes away when the flow stops [Summers, 2008].
- A central body in the nozzle to create a downstream wake to help entrain abrasive particles into the core of the jet [Hashish, 1993].

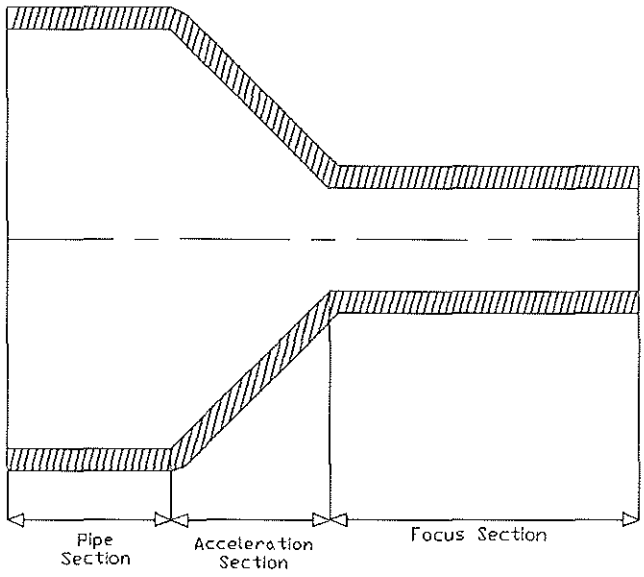

Figure 2.3. Abrasive slurry jet nozzle

The optimization of the nozzle design is very much a function of demands of the application. The cutting efficiencies of short nozzles have been found to be higher than longer nozzles, where as the longer nozzles have greater jet coherence and therefore range [Brandt 1998a, 1998b].

2.3.3. Operating Parameters. The ASJ cutting process is affected by different process parameters. Figure 2.4 gives a symbolic representation of the interaction between different operational parameters and the depth of cut [Yazici, 1989a]. A significant amount of work has been carried out by different investigators examining the role of each of these parameters in a series of attempts to understand how they influence the cutting performance and the consequent best way to optimize cutting performance

2.3.3.1 Pressure. The relationship between depth of cut and pressure is linear. This was experimentally verified [Yazici, 1989b], [Hashish, 1991], [Zhang, 1995] and [Brandt, 1996] but the trend reduces at higher pressures because of mixing inefficiencies at higher pressure [Hashish, 1986].

2.3.3.2 Standoff distance. Two effects govern the variation of depth of cut with standoff distance. The jet spreads with increase in standoff distance and correspondingly the frequency of impact of abrasive particles decreases per unit area of the target material. Secondly, as the particles exit the nozzle they are subject to drag forces and the particles begin to decelerate. This effect on the depth of cut was experimentally verified [Liu, 1992], [Laurinat, 1992] and [Brandt, 1996]. This effect is consistent over the different abrasive sizes [Seiji, 1996].

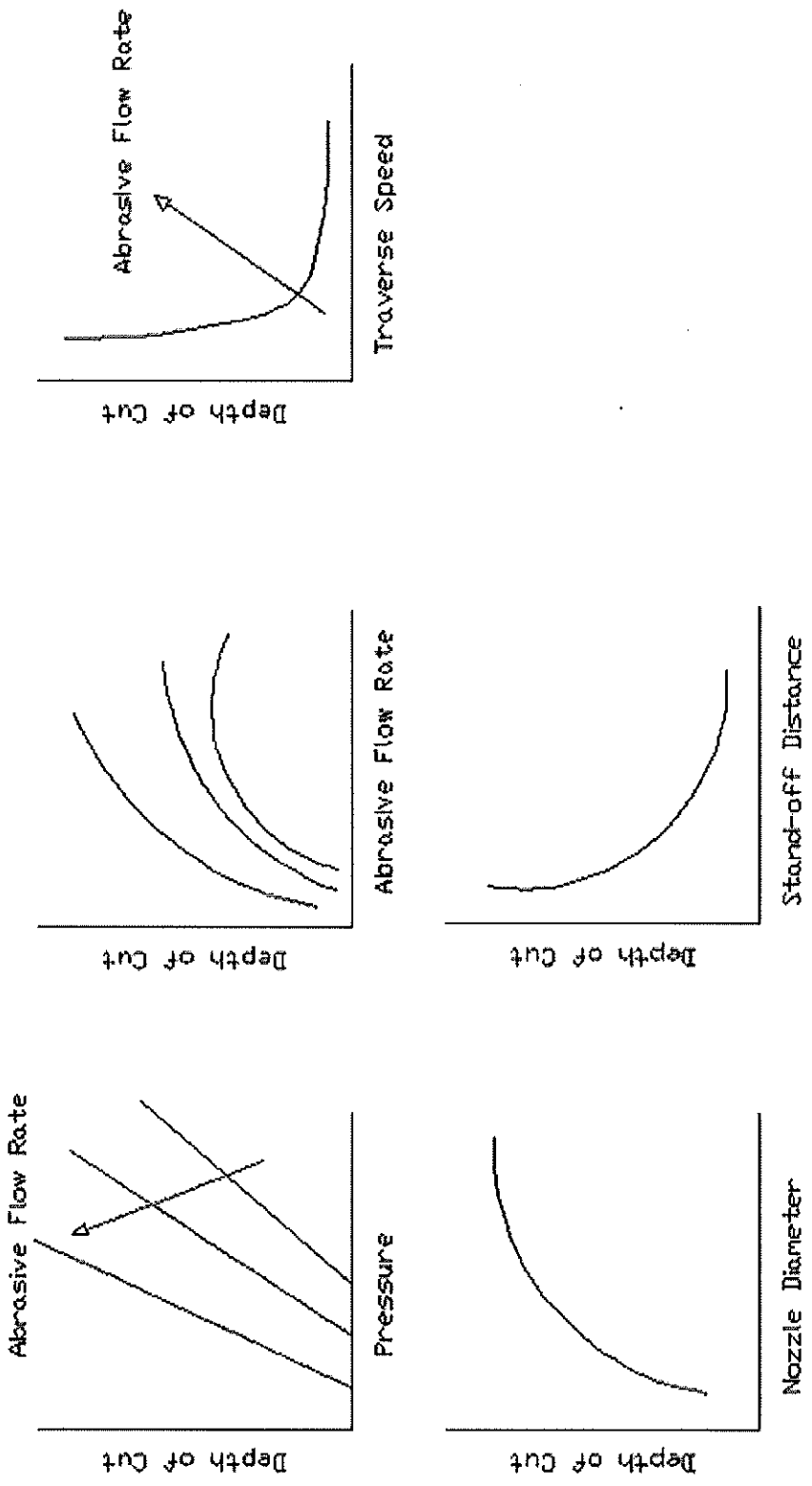

Figure 2.4. Effect of operating parameters on depth of cut

In testing conducted at MS&T to determine the throw distance of abrasive particles the finer particles decelerated faster and was found closer to the nozzle than larger particles which were carried further [Summers, 2008]. Under water the drilling capability of ASJ is severely reduced with increased standoff distance as compared to that in air [Weng, 1996], [Shimizu, 2002].

2.3.3.3 Abrasive concentration. The cutting capability of a slurry jet increases linearly with increase in abrasive concentration until its reaches its maximum. In ASJ literature the measure of abrasive in a jet stream is defined by either concentration by weight or Abrasive Feed Rate (AFR). Abrasive concentration is the mass percentage of abrasive in total mass of the slurry jet. AFR is defined as the mass of abrasive exiting the nozzle in a slurry jet stream in unit time. Researchers have observed a plateau after a point for increased concentrations [Hashish, 1991], [Hai, 1995], [Brandt, 1995], [Laurinat, 1992] and [Hashish, 1997].The data from previous research does not show a consistent maximum optimal concentration. This is in part due to the different nozzle designs used for testing. Nozzle design characteristics have an important part to play in optimal concentrations because it determines the momentum transfer efficiencies and the energy lost as a result of particle interactions and disintegration [Bortolussi, 1988].

2.3.3.4 Traverse rate. Increasing the traverse rate will result in a hyperbolic decrease in the cutting capability of the jet [Yazici, 1989a], [Hai, 1995], [Brandt 1995], [Laurinat, 1992] and [Hashish, 1997]. Decreasing the traverse rate will result in greater cutting depth till a certain point beyond which further decrease with not result in increased depth of cut. This has been proven with titanium cutting at different speeds at the waterjet lab in MS&T [Zhang, 2006].

2.3.3.5 Nozzle diameter. With an increase in the nozzle diameter for a given concentration, the amount of abrasives impacting the cutting surface increases, resulting in increased erosion rates [Hai, 1995]. It is important to note that with increased nozzle diameter, the utilization ratio of abrasives decreases. Larger nozzles will result in greater material removal by increasing the kerf width without significant increase in depth of cut, demonstrated in cutting of granite by Yazici [1989a]. Smaller nozzles at higher pressures is a better option if available.

2.4. DISCUSSION

In order to choose a method of mixing abrasive for drilling applications, it is necessary to review the comparisons that have been carried out to date on both AWJ and ASJ systems. For the same hydraulic power, the ASJ has been able to achieve twice the cutting depth of an equivalent AWJ system [Brandt, 1994].

Hashish confirmed these results by comparing the AWJ and ASJ systems up to pressures of 345 Mpa [Hashish, 1991]. An advantage with the ASJ is the absence of air in the mixture which becomes a two-phase flow as compared with AWJ which is a three-phase flow. As a consequence, there is less particle disintegration as the slurry is accelerated through the nozzle with an ASJ system [Galecki, 2000]. There is better recycling potential for the abrasive with the ASJ because drying is not required and up to 90% of the original particle sizes can be recovered as compared to 25% in case of an AWJ system, which also requires that the abrasive be dried.

3. DESIGN OF ASJ FEED SYSTEM

Although ASJ systems have been in existence since before BHR first publicized the idea in 1986 (Fairhurst, MSc thesis), a number of drawbacks have become evident in some of the different designs for this system that have been proposed over the years. The ASJ feed systems reviewed in the previous chapter were all bottom feed systems. A bottom feed system can be defined as one where the high pressure fluid is bypassed from the main line into the top of the pressurized vessel filled with abrasive. This high pressure fluid pushes the abrasive slurry out of the bottom of the vessel, Figure 3.1. There are two disadvantages to this system

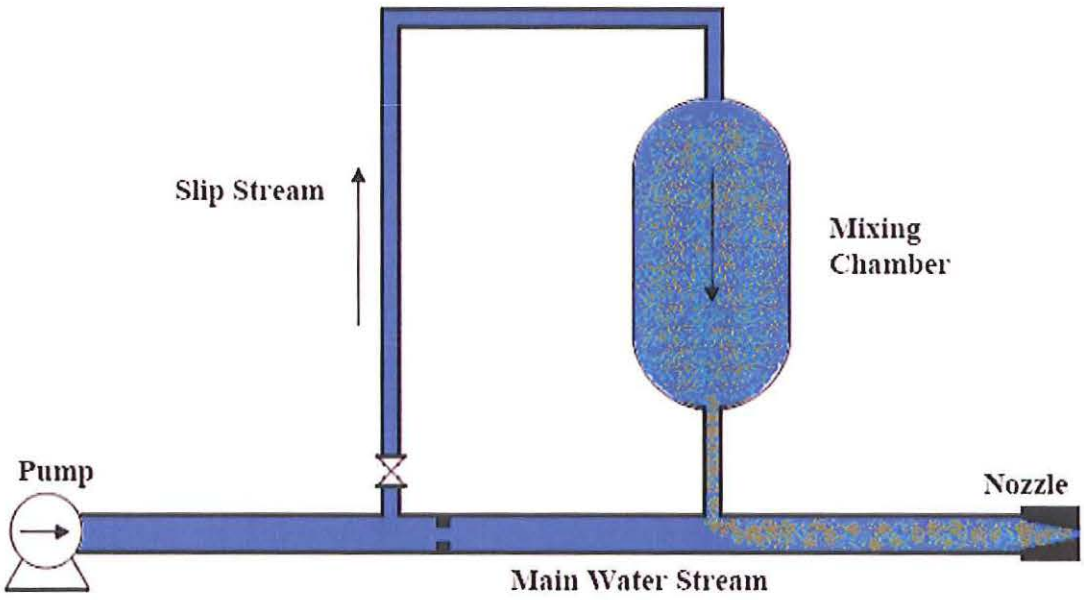

Figure 3.1. Initial bottom feed ASJ system

- Start/Stop operations is only possible by opening/closing the valve at the bottom of the tank while the fluid is still flowing through it at high pressure, and with abrasive content. Abrasive particles trapped in the valve during closure will result in accelerated wear of the valve components, resulting in unacceptably short valve lifetimes.
- Feed rate of abrasive out of the bottom of the tank is predominantly gravity controlled and this configuration does not assure consistency of feed rate.

In order to eliminate these shortcomings of the bottom feed design, a series of experiments and proto-type construction tests were carried out leading to a new circuit configuration. One of the major advantages of the new design is that it relies on a feed of abrasive slurry out of the top of the pressure vessel. Here a controllable portion of the high pressure fluid is bypassed from the main fluid feed line from the high pressure pump, and this is fed in through the bottom of the abrasive holding tank. This fluid injection displaces abrasive which is entrained in the cross-tank flow, and then fed back to the main fluid supply line through an exit port on the top of the tank. This design was created to ensure consistency of abrasive feed rate as well as to provide flexibility in adjusting the abrasive concentration in the feed to the cutting nozzle.

3.1. EVALUATION OF EXISTING BYPASS SYSTEMS

ASJ feed systems have traditionally had two major problems that have limited their commercial use

- The inability to rapidly cycle through Jet On/ Jet Off cycles: This is a major requirement for precision cutting in many manufacturing facilities where

detailed cutting operations often have short cutting cycle durations. ASJ feed systems were originally bottom feed systems i.e. the abrasive slurry was released through the bottom of the pressurized vessel in which it was held. In this system, when turning the abrasive feed to the jet off, a valve must be closed in the line from the pressurized slurry tank to the nozzle. And when abrasive feed is required again, this valve has to be re-opened. During cutting operations, which typically require the cutting of a number of segments on a sheet, this valve must be opened and closed under pressure at frequent intervals, and in a condition where abrasive particles are in the stream being controlled. The wear from these particles leads to an accelerated erosion of the valve components. Regular replacement of the seat and ball as part of maintenance of this expensive component makes this configuration commercially impractical for use in operations with a high cycle rate. This has limited the use of ASJ feed systems to applications which are continuous, i.e. once the cutting process is started, the abrasive flow is not stopped until all the abrasive in the pressurized reservoir has been drained.

- Precision control of the abrasive concentration as it is metered into the cutting jet: In many cases the concentration of abrasive changes over the use of a single batch loading of abrasive, and, as a result, there are unacceptable changes in the quality of the abrasive jet, giving an uneven performance. This problem exists with many of the bottom feed designs that have been developed for existing ASJ feed systems. These systems are designed so that

gravity controls the rate at which the abrasive is fed from the tank into the nozzle feed line.

A reliable ASJ feed systems requires a solution to both these major problems. The performance of any newly designed ASJ feed systems in these solutions can be categorized using four main indices [You Ming-qing, 1993]

- Flow control – Requires that the concentration of abrasives in the flow can be varied to meet designated levels.
- Evenness of Abrasive Feed – The concentration of abrasives is constant when sampled at intervals during operation.
- Repeatability – For the same flow settings the feed rate of abrasives is constant and consistent.
- Feasibility – The system must be buildable in a way that is economically viable and physically realizable.

3.2. A REDESIGNED ASJ SYSTEM

Within the constraints of the basic design, and following a series of exploratory constructions and evaluations, a novel slurry feed circuit has been developed which addresses the two major design problems and has been demonstrated to satisfy the four indices of performance.

The proposed new ASJ feed system is a top feed system, Figure 3.2. The flow into and out of the tank is controlled by the 7 valves that are shown in the figure. The high pressure tank is initially filled with abrasive. This step requires that valves #1, #4, #5 and #7 are kept open and all others are closed.

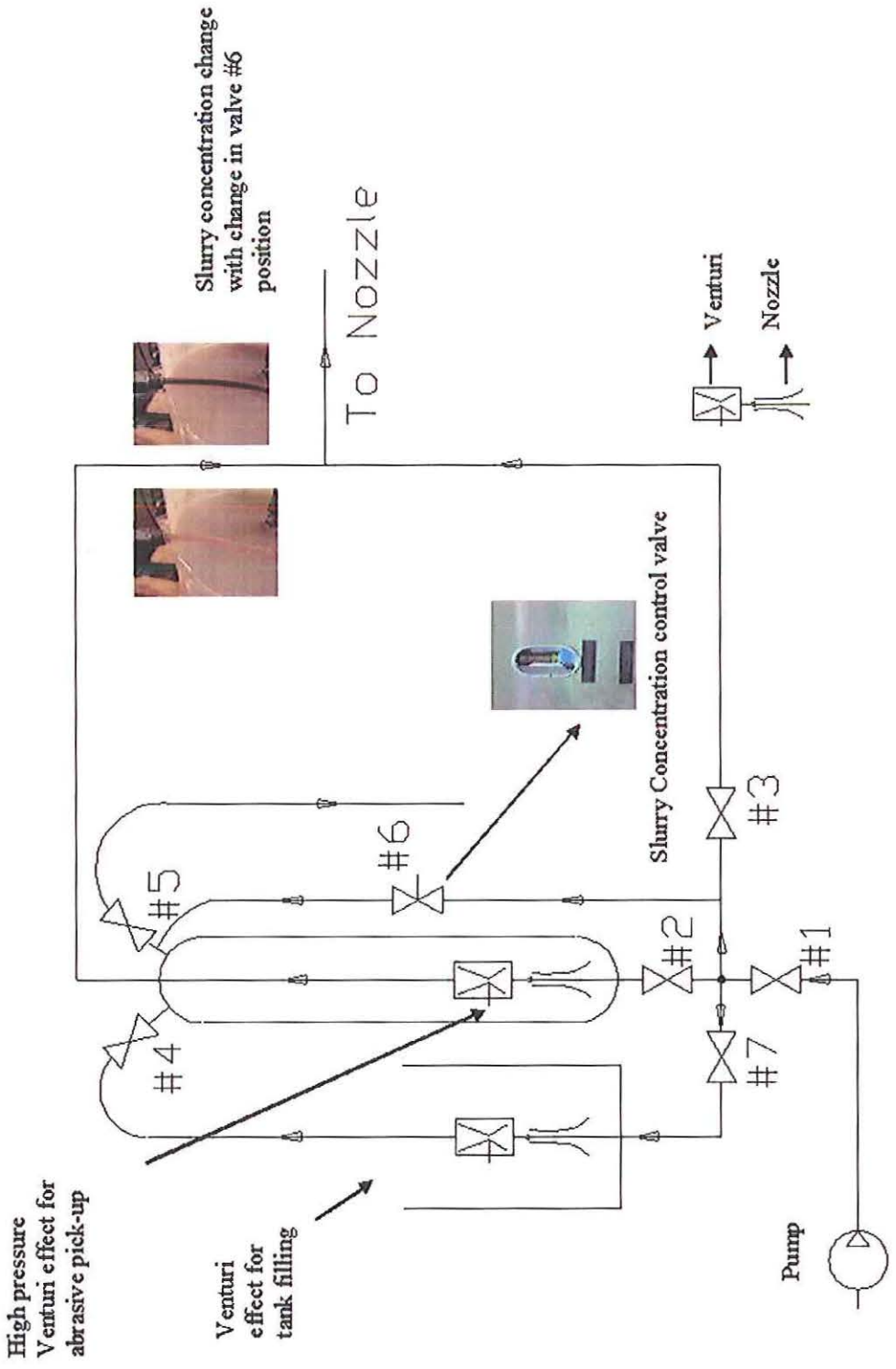

Figure 3.2. Novel abrasive slurry feed system

A new supply of abrasive is first dumped into the adjacent loading reservoir, where it is mixed into the water already in the reservoir. A modified jet pump design then uses the venturi- effect of a conventional jet pump to pick up the abrasive from this reservoir and transport it, through a delivery line into the tank, entering through valve # 4. The abrasive settles to the bottom of the tank and the transport medium (typically water) overflows from the tank through valve #5. Output from valve 5 is monitored, so that when abrasive is seen to be coming out of the tank, it is presumed to be full. At that point, valves # 7, #4 and #5 are closed.

The critical part of the operation of a successful ASJ feed system is the ability to pick up a controlled volume of abrasive. This is achieved by using a modified jet pump design, within the tank, so that the venturi effect picks up abrasive from around the jet pump location. This is positioned as close to the bottom as possible to enable maximum utilization of abrasive in the tank.

During cutting operations, valves # 1, #3 and #2 are opened, and the high pressure water flows through valves #3 and #2. Without an additional step, the water flowing through the modified jet pump in the tank is not capable of picking up any significant amount of abrasive since its extraction would result in a vacuum being created inside the tank. To control the amount of abrasive fed from the tank into the nozzle feed line, the flow of replacement water into the tank is adjusted by regulating valve # 6. Opening this valve, allowing water to flow into the pressure vessel, allows the modified jet pump to pick up abrasive from inside the tank and mix this with the water released by valve # 3. Together these form an abrasive slurry flow that passes up, and out of the tank. Thus, the

control of abrasive concentration in the resulting cutting stream is achieved by controlling the flow through valves #2, #3 and #6.

Once the system had been validated by manual operation of these valves, they were replaced with electronically controlled flow control valves which provide a better and more responsive way to monitor and control the abrasive concentration exiting the nozzle. A flow meter was also added to the circuit at this time, in order to better monitor conditions and provide input to the controlling software operating the valves.

3.3 COMPONENTS OF REDESIGNED ASJ SYSTEM

The redesigned system described in the above Section 3.2 was constructed using a combination of specially machined components and off-the-shelf parts. The major components of the system include

- High pressure tank
- Jet Pump
- Pneumatic On/Off valves
- Medium pressure ball valves
- Turbine flowmeter

3.3.1. High Pressure Tank. The high pressure tank was part of an older ASJ system that was purchased from US Jetting Systems. The maximum operating pressure for this tank is 69 MPa, and it holds a total of 90 kg of abrasive.

3.3.2. Jet Pump. The design of a top feed system requires that the abrasive be metered out from the top of a pressurized container into the high-pressure line feeding the nozzle. There is therefore a requirement for particle conveyance from the bottom of the

tank to the top of the tank against gravity. The pick up point for the abrasives was selected to be close to the lowest point inside the tank so as to achieve nearly 100% utilization of the stored abrasive. Based on an evaluation of the different options available, and on prior experience with abrasive movement at the RMERC, it was decided to use an internal jet pump within the holding tank as the solution to the design problems. A jet pump has no moving parts and utilizes the motion of fluid under controlled conditions as its power source. This has advantages, since operational maintenance of the assembly, once constructed, is not easy. Figure 3.3 shows the configuration of a typical jet pump.

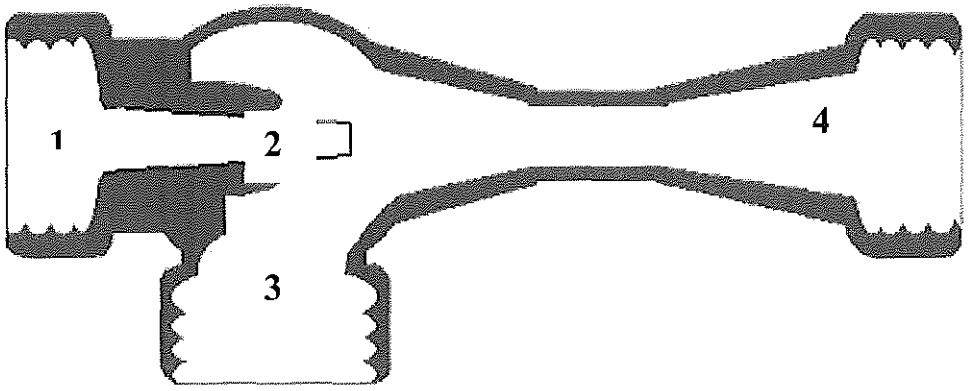

Figure 3.3. Configuration of a typical jet pump

[Image from www.pumpsofoklahoma.com/eductor.htm]

High pressure water enters the system in section 1; as the cross-sectional area decreases the velocity of the fluid increases as it passes through section 2 which

represents the nozzle section of the configuration. This fluid under pressure passes into the venturi tube creating a partial vacuum within the upper chamber by nature of its passage. The material which has to be transported (in this case the abrasive in the surrounding vessel) is drawn into the stream through section 3 in response to creation of this partial vacuum. It is at this point that there is an exchange of momentum between the driving fluid and the aspirated abrasive. The diffuser, section 4 allows the velocity of the mixture to be gradually converted back into pressure. This reduced velocity mixture continues its motion through the outlet piping losing pressure as it moves further away from the diffuser section.

3.3.2.1. Jet pump for ASJ feed system. Based on the operating principle of the jet pump outlined in Section 3.3.2, a design for the transport of the abrasive slurry from inside the tank through the top is shown in Figure 3.4. This system was manufactured to the authors design in the RMERC machine shop. All components except the throat section were machined from stainless steel. Because of the abrasive nature of the cutting particles aspirated into the cutting fluid, the throat section of the jet pump was made of high strength carbide material.

The jet pump is threaded into an assembly that is, itself, threaded into the bottom access port of the abrasive holding tank. The tank is sealed at the top using a Teflon crush seal, Figure 3.5 that must be replaced each time the internal feed system is disassembled and rebuilt. This design makes it easy to remove the nozzle section of the pump and to empty and clean the tank if required. The abrasive slurry that is picked up by the jet pump is fed into the vertical, 4.3 mm internal diameter, feed pipe that passes through the top of the tank, Figure 3.6.

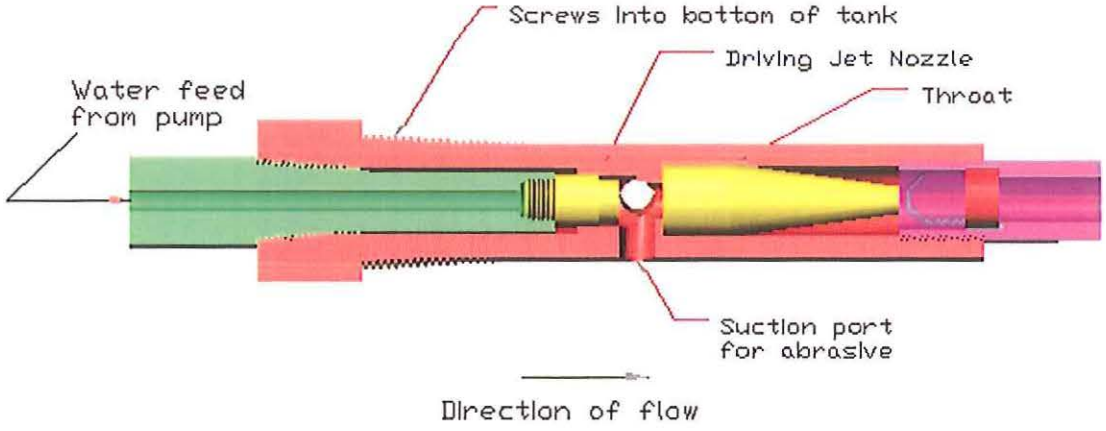

Figure 3.4. Jet pump design for ASJ feed system

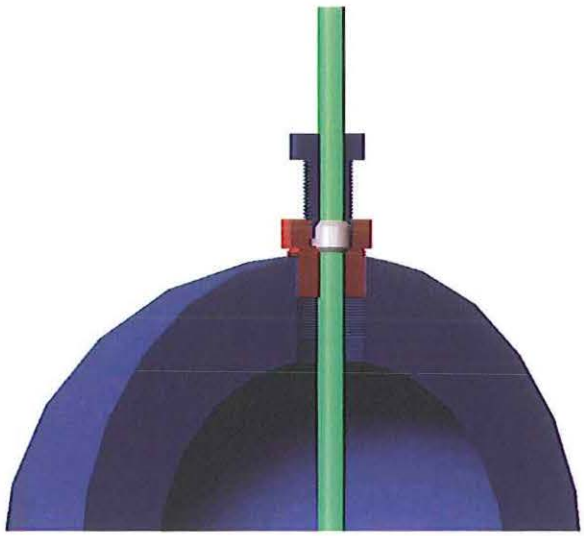

Figure 3.5. Teflon crush seal for slurry transport pipe

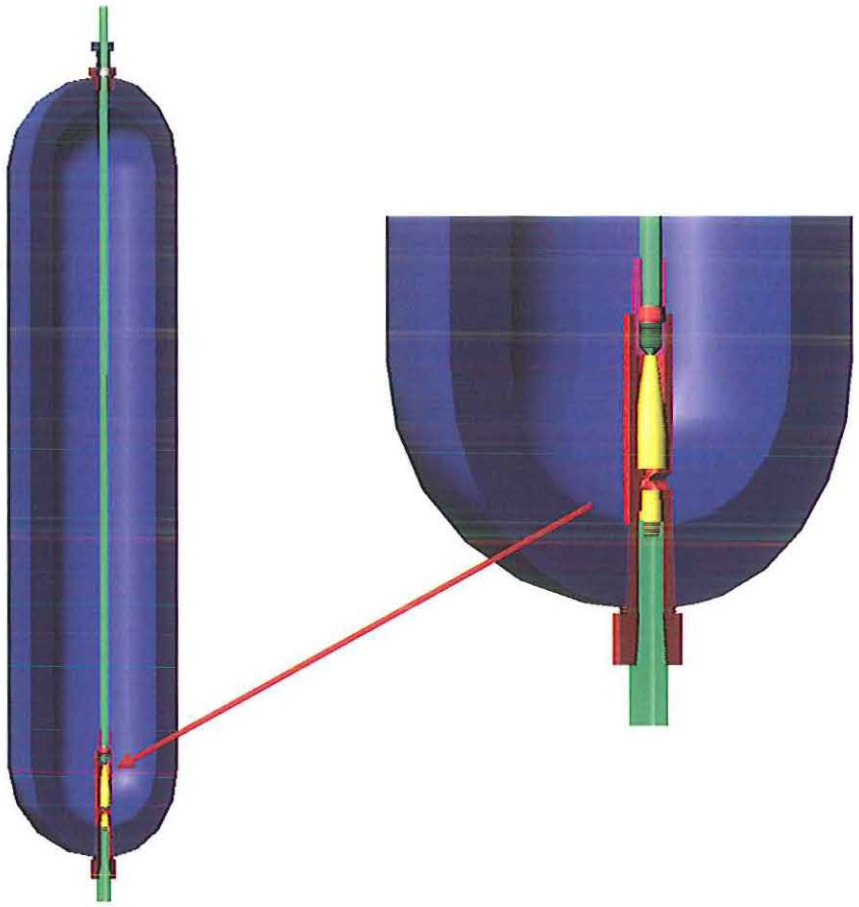

Figure 3.6. ASJ feed tank with jet pump placement

3.3.2.2. Testing the jet pump. It was important to validate the operation of the newly designed system, and to calibrate its performance comparing the change in inlet pressures and nozzle diameters on delivered abrasive feed through the jet pump. As an intermediate step in this process, the amount of vacuum generated under the different pump operating conditions was first established. A pressure transducer was fitted into one suction port of the designed jet pump and the other ports were sealed. The pressure drop was measured using a voltmeter, Figure 3.7. Nozzle sizes of 1.651mm, 1.143mm, 0.889

mm and 0.635mm were tested. Pressures tested ranged from 0 psi to 69 MPa at 3.45 MPa increments. For the largest nozzle tested, 1.651mm diameter, it was not possible to reach a pressure above 45 MPa because of the horsepower limitations of the pump. The 1.143 mm, 0.889mm and 0.635mm nozzles were not able to perform at the lower pressures because there was a certain minimum performance below which the pump could not operate. Performance data is plotted in Figure 3.8. It can be seen that the initial 13.8 MPa inlet pressure provides the controlling pressure differential created in the suction port of the jet pump. No significant variation in the pressure differential could be observed as the nozzles size was reduced from 1.651 to 0.635 mm.

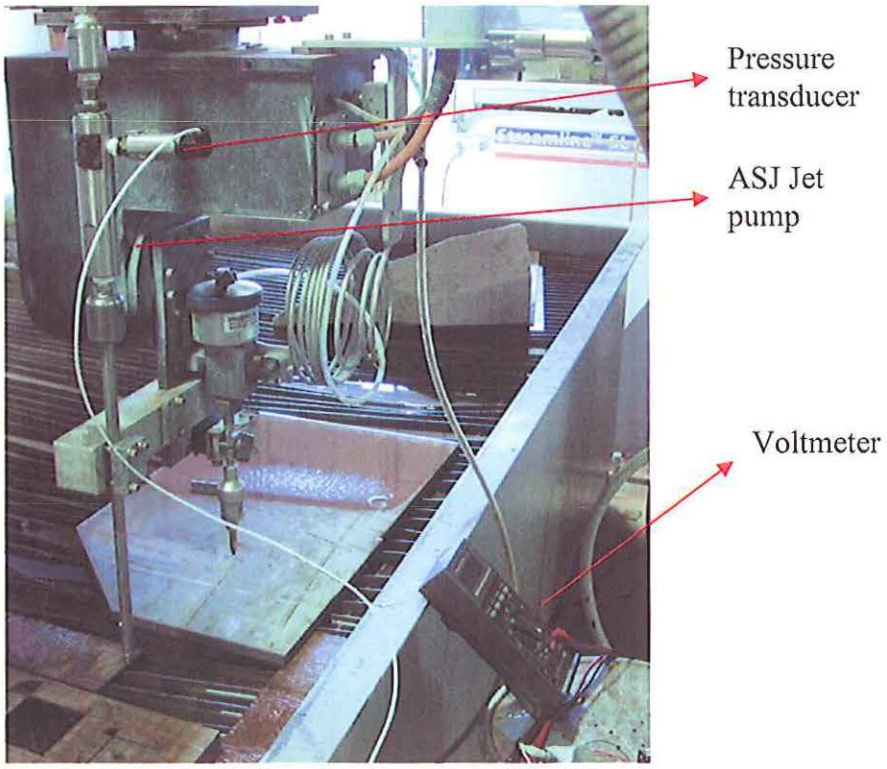

Figure 3.7. Experimental setup for evaluating the slurry jet pump

(Note that this is built around a 5-axis PAR cutting table).

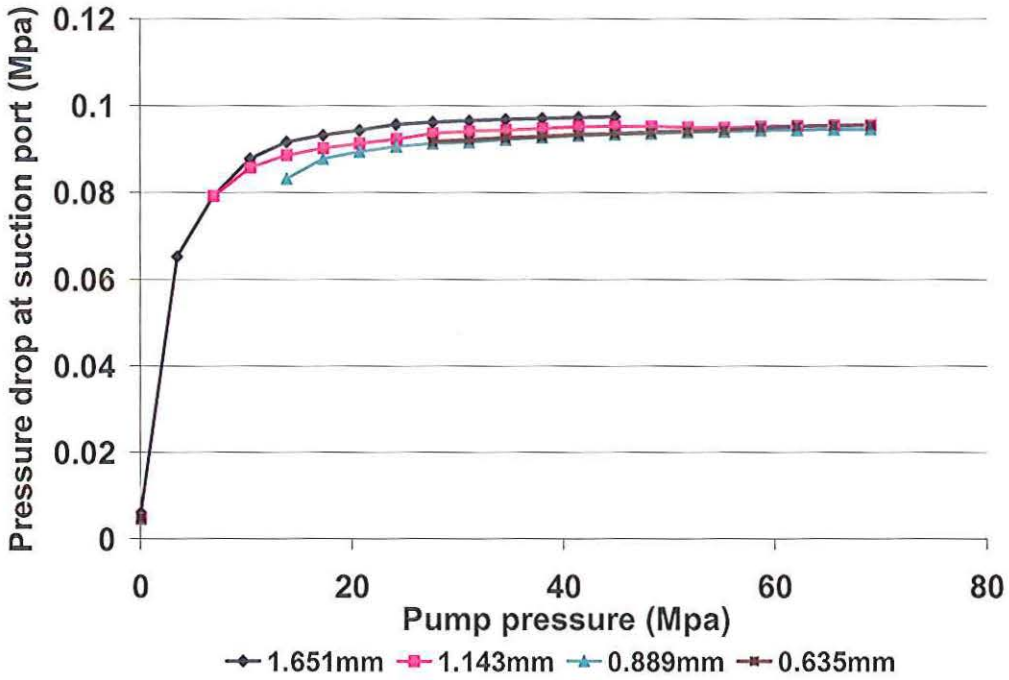

Figure 3.8. Effect of pressure and nozzle sizes on pressure drop at suction port

It can be inferred from these results that at operating pressures above 13.8 MPa, that the inlet pressure into the jet pump does not influence the amount of abrasives delivered from inside the tank into the jet stream. In order to test this observation the system was run at 20.7 Mpa, 27.6 MPa and 34.5 MPa at bypass flow rates of 0.4, 0.7, and 1.0 liters/min and the abrasive was collected after it had passed through the cutting nozzle. The plotted results can be seen if Figure 3.9. This data reinforces the conclusion that the inlet pressure into the tank does not affect the abrasive flow rate out of the tank but that it is the bypass flow rate (controlled by valve #6) that causes the required changes in this variable.

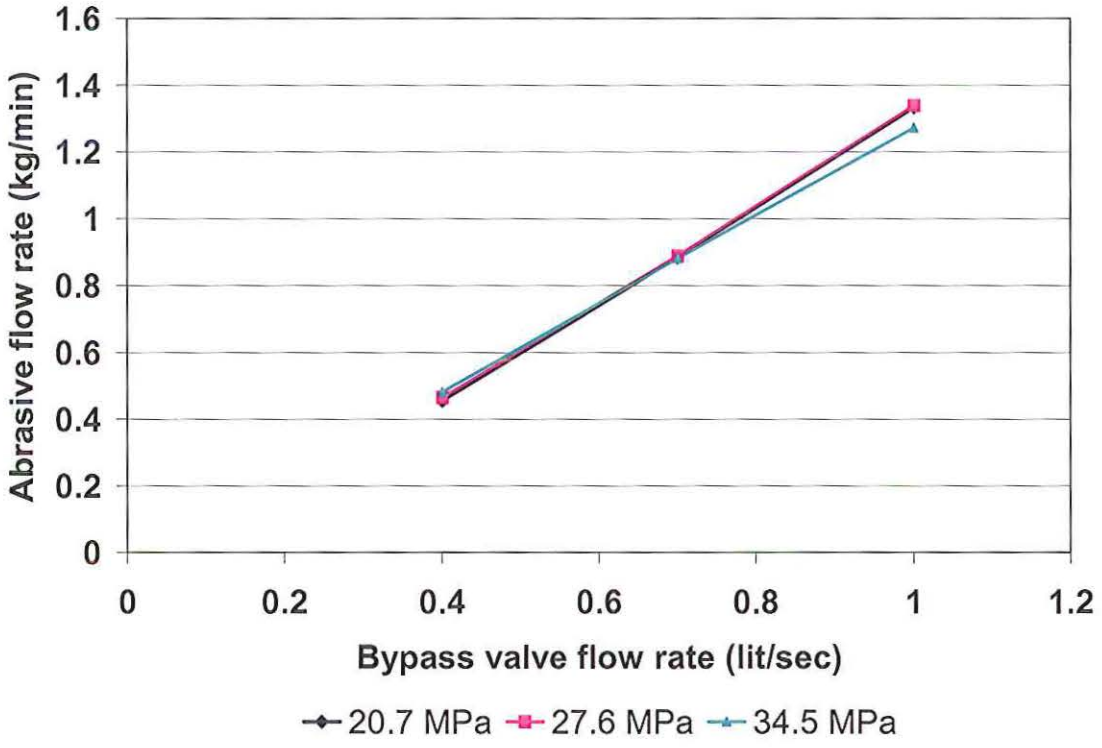

Figure 3.9. Effect of pump pressure on abrasive feed rate

3.3.3. Pneumatic On/Off Valves. These valves are rated up to 86 MPa. (The system operational pressure is at 69 MPA and below). In Figure 3.1 valves # 2 and #6 were selected to be operated using pneumatic power. The start /stop operation of the feed system is controlled by the opening and closing of these valves, which are therefore critical to the operation. A solenoid mounted over these valves, is powered by a 12 volt D.C. circuit, and used to activate the valves. Because the valves must open and close against the pump delivery pressure, and because of intrinsic safety issues, pneumatic power was considered to provide the best option for these components.

3.3.4. Medium Pressure Ball Valves. In the design, valves # 1. #3, #4, #5, #7 are medium pressure ball valves. Maximum operating pressure for these valves is

100MPa. This design is considered acceptable for these components (and proved to be so) because the new circuit design only passes high pressure water – without abrasive – through these valves, negating the wear problem which had previously been one of the major disadvantages of their use.

3.3.5. Turbine Flowmeter. The meter is mounted between valve #5 and #6 in Figure 3.2 It is used to measure the amount of fluid metered into the tank to replace the volume of abrasive removed by venturi action of the jet pump. This flow controls the abrasive mass flow rate out of the high pressure tank. Figure 3.10 shows a cross sectional view of the turbine flow meter with its major components.

1. Flow rectifier with bearings
2. Spacers
3. Ring nut
4. Turbine wheel with shaft
5. Ball bearing

The metered flow passes through the turbine flowmeter in an axial direction, spinning the turbine. The speed of the turbine is proportional to the mean flow velocity of fluid. The sensor is mounted on the flow meter, reads the turbine RPM, amplifies and modifies the alternating voltage produced, which is proportional to the instantaneous flow. This flow rate is then displayed on the local display unit, Figure 3.11 and the signal can be monitored by a controlling computer, which can, as necessary, adjust the flow through the control valves, to bring the value back to the required level.

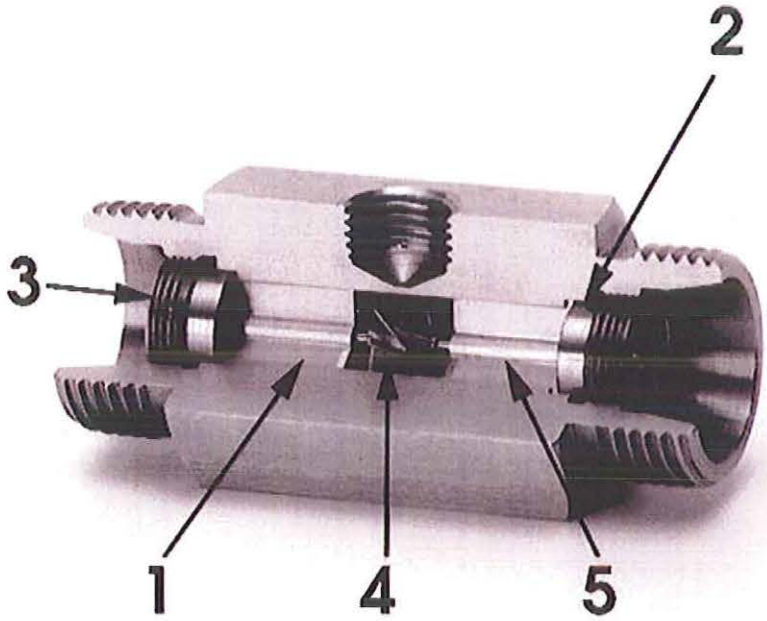

Figure 3.10. Sectional view of the turbine flowmeter

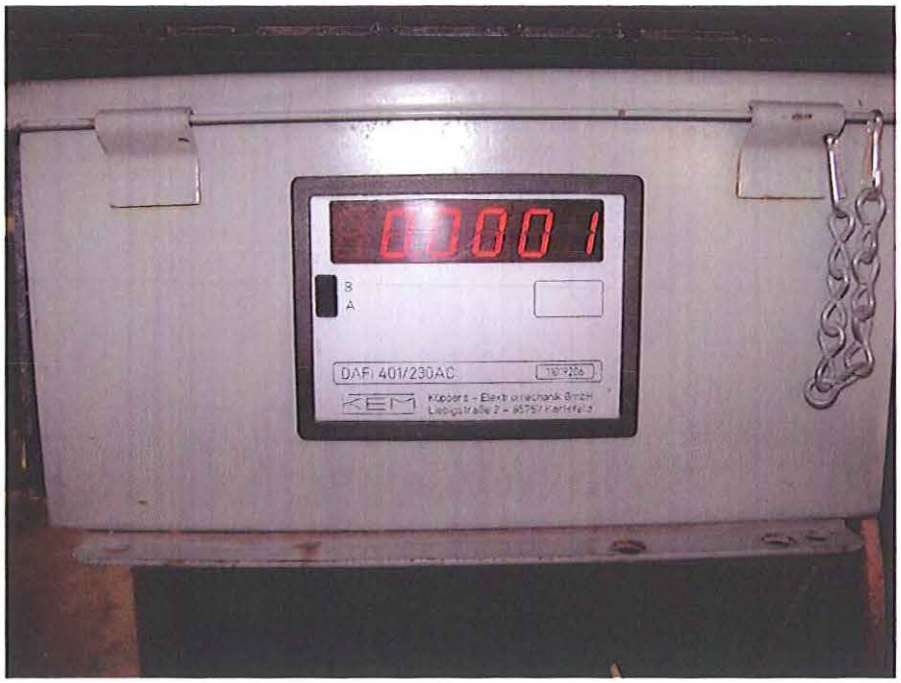

Figure 3.11. Display unit for flow through turbine flowmeter

3.4 PERFORMANCE OF THE NOVEL ASJ FEED SYSTEM

In evaluating the stability of the abrasive flow rate (AFR) from the tank with time, it was difficult to determine the most effective metric of performance. And yet it is a critical issue since Ming-qing [1993] identified interruption of the abrasive water jet as being caused by abrasive choking resulting from air in the tank, and variations in abrasive concentration impact the quality of the cut that the jet can make. The first step in determining the effectiveness of the system was to compare the performance of this new system, based on criteria set using tests carried out by researchers in the past.

3.4.1 Effect of Abrasive Feed Rate and Traverse Speed. The factors that govern the influence of abrasive feed rate and traverse speed on the depth of cut have been discussed in Section 2, a standardized test had been developed at Missouri S&T to evaluate nozzle performance, and this was now used to test the novel MS&T ASJ system. Test samples were prepared from strips of ASTM 108 steel 6mm thick and cut into triangles 15 cm long. These samples were oriented vertically and the jet aligned to cut down through the center axis of the 6mm thickness (Figure 3.12). The top face of the triangle was kept horizontal (to maintain standoff distance) and the jet started cutting at the pointed edge, moving into a thicker depth of material over the traverse. This gave a good measure of the achievable depth of cut being the point at which the jet stops cutting through the hypotenuse. Figure 3.13 shows one of the sides of the tested samples after test. One side of the cut has been removed by milling to expose the full cutting face of the jet. Tests were carried out with a 1 mm diameter nozzle at 65.8 MPa.

Triangle tests with abrasive feed rates of 0.5, 0.8 and 1.2 kg/min were performed to study the effect of traverse speed and abrasive feed rate on depth of cut with this

system and the data plotted. Figure 3.14 and Figure 3.15 show trends similar to the symbolic curves shown in Figure 2.4. These preliminary tests also validated that the MS&T system cutting performance is comparable with that of earlier designs.

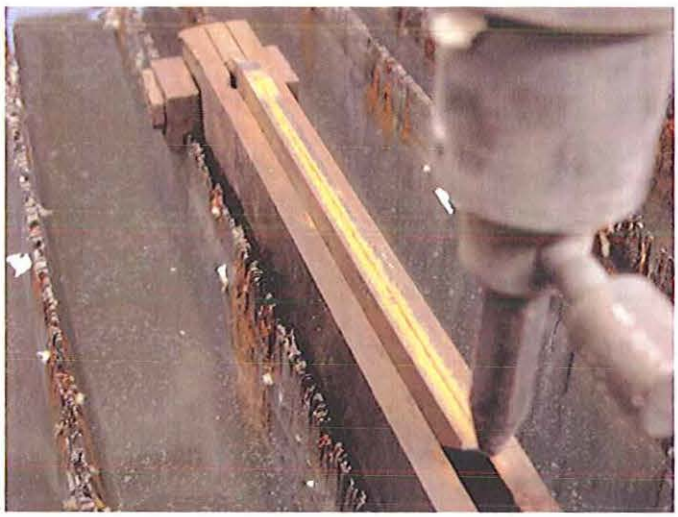

Figure 3.12. Triangle test setup

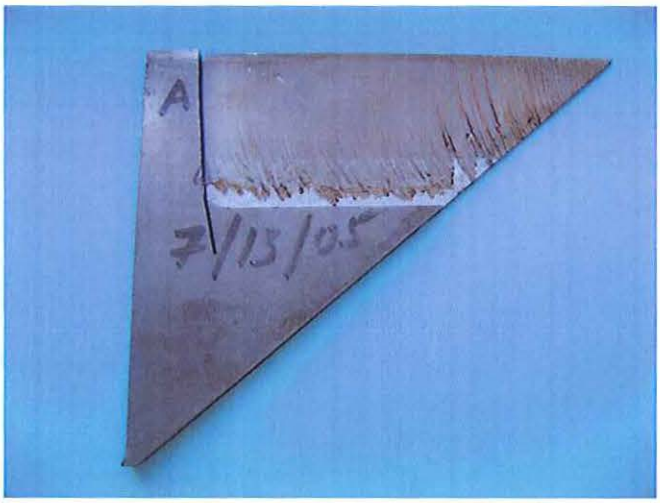

Figure 3.13. Triangle test with the cut surface exposed after milling

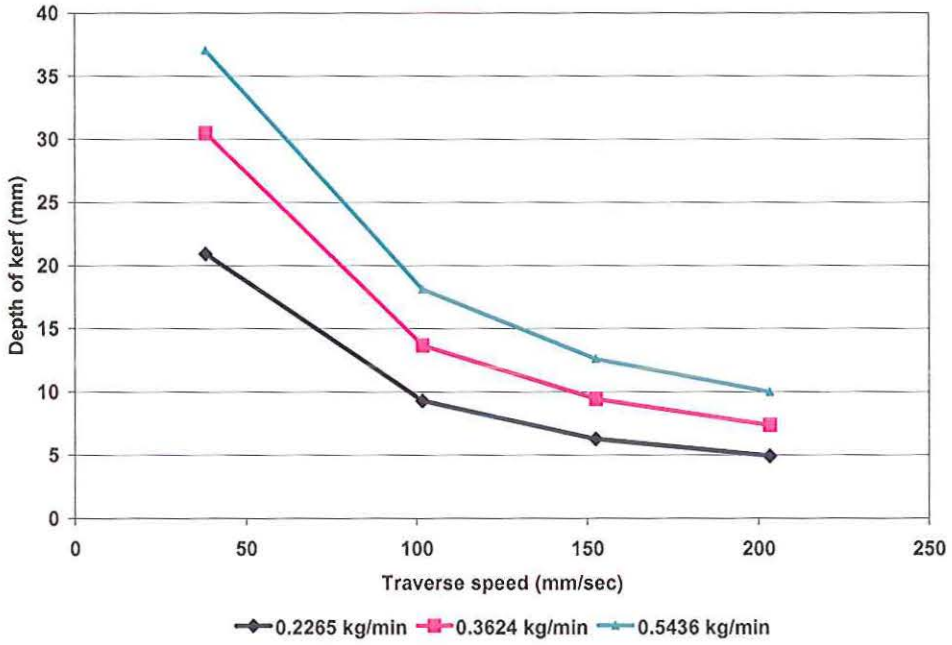

Figure 3.14. Influence of traverse speed on depth of cut

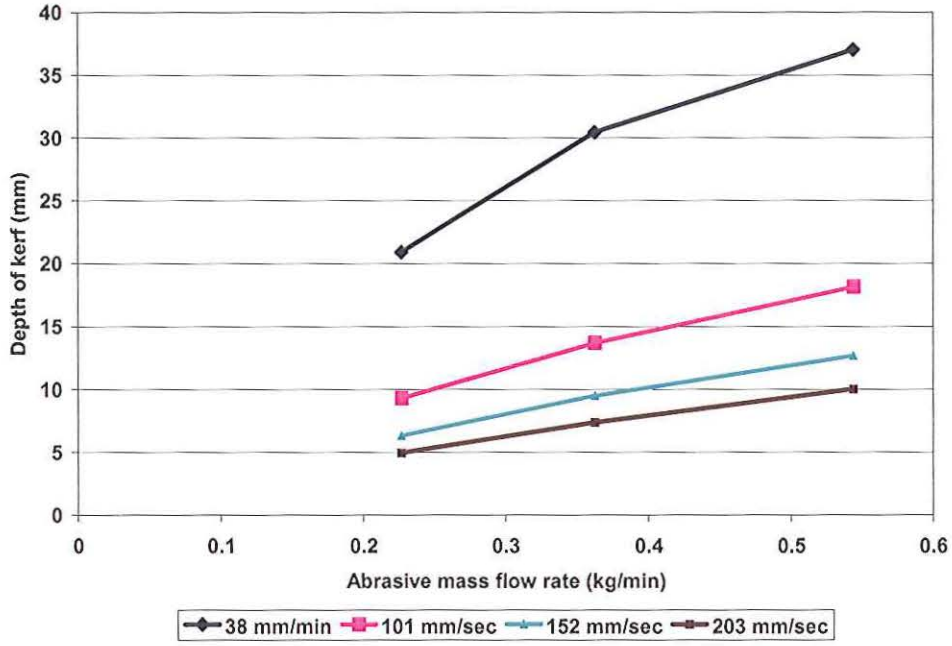

Figure 3.15. Influence of abrasive feed rate on depth of cut

3.4.2 Repeatability and Consistency of Abrasive Feed Rate. Determining the evenness of the abrasive feed within the injection tank is difficult because there are no real time measurement systems available. Work by [Gadd, 1996] proposed use of ultrasonic equipment in determining the abrasive flow rate in real time but at present this method has not been developed to an extent that it can be used during cutting. Attempts to monitor the weight of the tank during the cutting operation (and thus by weight loss to determine AFR) have not been successful. One of the more effective methods for measuring abrasive concentration is by the collecting samples coming from the nozzle. While there are various ways of achieving this, the method used at Missouri S&T is based on mounting the nozzle horizontally on a lance and directing the resulting jet axially along a partitioned tube where the particles can be collected as they lose energy, Figure 3.16. This method was modified from earlier test protocols. The system was operated under the designated test conditions (jet pressure and AFR) with the jet being redirectable so as either to pass down the tube or not. For each test, abrasive was collected over a 30 second period and then the jet redirected away for 30 seconds. During this interval the earlier set of samples was collected and removed. A total of 9 samples were thus collected for each test run, which lasted for a period of 9 minutes. The abrasive samples collected were separately dried in an oven and weighed to determine the amount of abrasive in the delivered jet. The data is plotted in Figure 3.17. It can been seen that, with the new design, the abrasive feed was consistent over the interval that the test was carried out, for each of the test conditions.

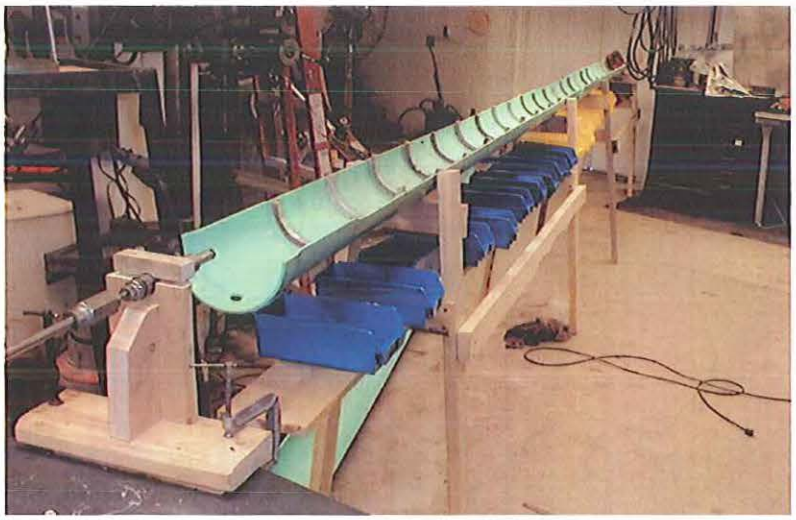

Figure 3.16. Present setup for abrasive concentration measurement

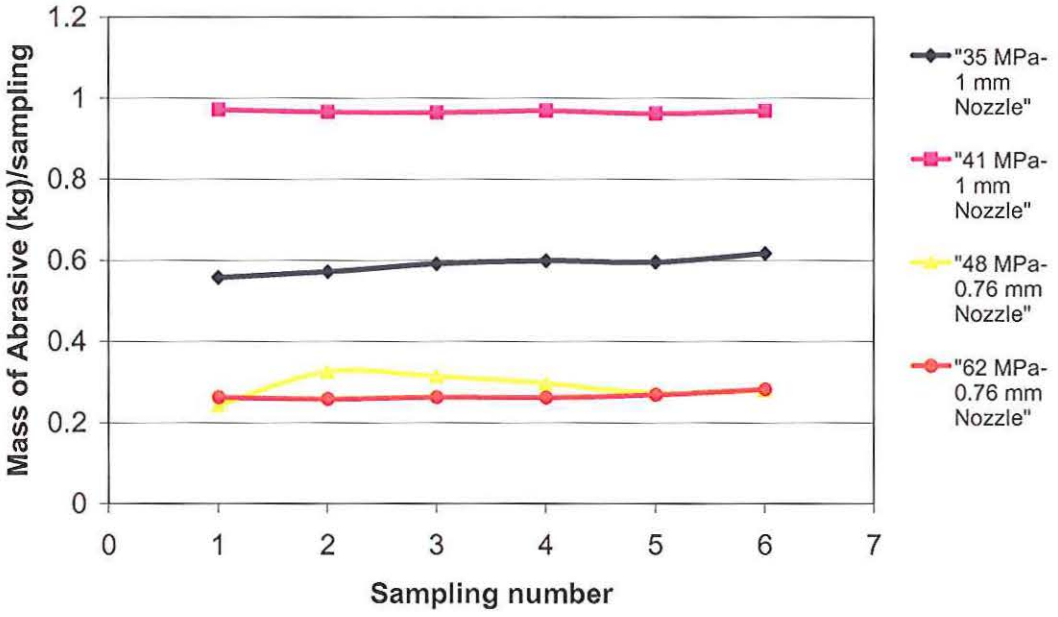

Figure 3.17. Abrasive feed consistency over a single run

This technique, while effective as a laboratory tool, is not practical during an actual cutting operation. The quality of the cut surface in abrasive cutting is, for both types of abrasive feed, a direct function of the pressure, traverse speed and abrasive concentration. Control of abrasive concentration with the ASJ during a prolonged cut is thus a critical factor in commercial use. The tests showed that this could be controlled with the new design.

3.5 SURFACE ROUGHNESS -METRIC OF PERFORMANCE

Of the three parameters controlling cut quality, the traverse speed and the pressure can be maintained at a constant value fairly simply, the latter through valve adjustment. The surface quality thus becomes hostage to the steadiness of the abrasive concentration as a function of time.

To correlate ASJ performance as a function of abrasive slurry concentration, a real–time measurement of the slurry concentration had to be found. (The method described above is an indirect one and not a real time indicator of conditions during cutting itself). At present, there exists no instrumentation for real time measurement of abrasive slurry concentration in a mixture exiting the nozzle, concurrent with the jet cutting in real time. Since this is an important step in evaluation, a method had, therefore, to be developed. One potential approach is to consider is the indirect measurement of the evenness of the cut, since this is affected by the AFR and changes in quality would potentially indicate a change in ARFR, all other parameters being equal. It would thus provide a metric, although, due to nozzle wear, the cut surface quality changes even with

no change in AFR over time. For these considerations that change is much slower than the one under discussion.

In order to validate the potential benefit of this metric, an ASJ was moved at 0.254 mm/sec to through-cut 13.5 mm thick titanium sheet at a known AFR. Initially, a different pump was used to that used in the earlier part of this dissertation. The replacement pump had been in use in the High Pressure Waterjet Laboratory of Missouri S&T for over 20 years. In that time, the high pressure end has been replaced more than once, due to internal wear. It immediately became clear that such a change was again required. Until the time that these experiments were carried out, pump performance had been considered more than adequate for the work being carried out in the Laboratory.

However, when the cutting tests to monitor precision cutting in titanium were started, it was found that a slight difference, almost undetectable, in the flow produced from the three cylinders was, in turn, inducing a slight variation in the flow into the abrasive holding tank, and thus changing the pressure of the water entering the abrasive tank, and its velocity. This variation induced a non-uniform feed of abrasive into the feed line, and thus generated a time-varying change in the cutting ability of the jet. Note that this change in flow would also change the jet characteristics, and this may have also had an influence on the result. Figure 3.18 shows the cut surface when this varying inlet pressure was used to feed the system and the cut surface when a pump with a correct, steady non- pulsating pressure source was used. Note that the pressure fluctuation from the replacement pump was not detectable by simple pump observation.

In order to use the new metric a protocol had to be established, as follows. The surface roughness was measured at 25mm intervals over a cut length of 125 mm.

Measurements, were made using a Mitutoyo Surftest SJ-201P surface type profilometer with a range of 7880μin to 5900μin. Readings were taken along a traverse line set at the top middle and bottom of the cut surface. The data presented in Table 3.1 is an average of three R_a readings, and is given in micro inches. At the designated traverse speed, the roughness measurements were at time intervals of 1 minute. The cut gets rougher with depth, and thus the limiting roughness that determines an acceptable surface is that over the bottom section. The standard deviation of the bottom section is 7.69 μin and this is over a run time of 9 minutes. Standard deviation of roughness value for the top middle and bottom indicate an even cut, which as discussed earlier is a function of the evenness of abrasive feed. U.S. Air Force Research Labs and Boeing specifications for an acceptable cut quality require a surface roughness profile of less than 125 μin.

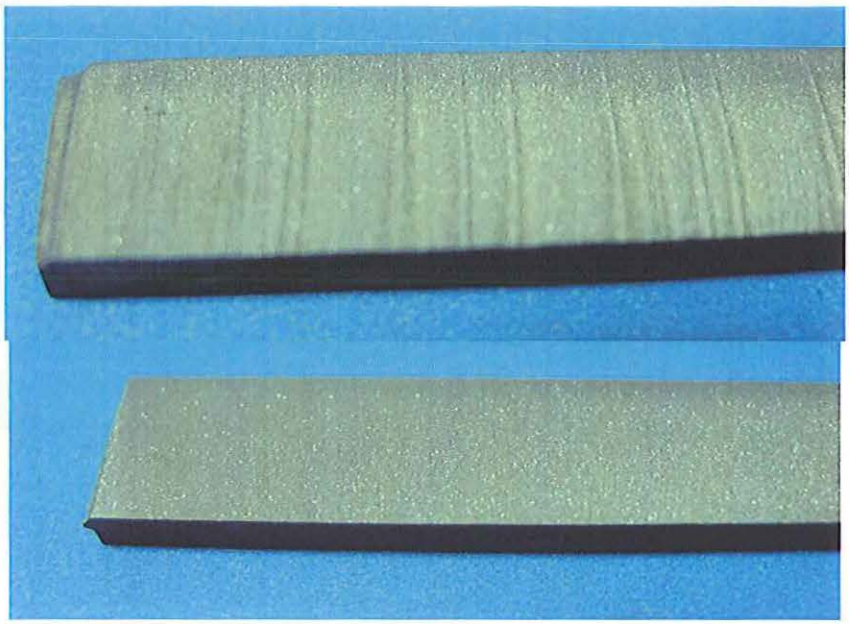

Figure 3.18. Titanium cut surfaces using unsteady and steady abrasive feed under equivalent conditions, when cutting 12.7 mm thick titanium

Surface roughness is a function of the traverse speed, abrasive concentration and nozzle diameter. Maintaining any two of these parameters constant and varying the third makes it possible to assess the effect of the varying parameter on the cut surface quality. It is also well known that the surface roughness is not constant throughout the depth of cut. The cut surface roughness at the top is significantly better than that achieved at the bottom and hence the bottom roughness is the limiting value for an acceptable surface quality of cut.

Table 3.1. Surface roughness values at each section

Section	Top	Middle	Bottom
1	78.6	98.0	112.5
2	75.7	86.9	106.2
3	74.6	86.3	97.3
4	79.6	94.8	103.4
5	72.1	79.5	100.7
6	67.1	87.5	92.3
7	67.3	83.7	89.4
8	63.8	80.5	99.1
9	69.3	79.8	90.3
Mean	72.0	86.3	99.0
Std Dev	5.5	6.5	7.7

To determine these effects, the ASJ unit was used with a 1mm diameter nozzle, at a pressure of 65.5 MPa to find the influence of slurry concentration and traverse speed on

the generated cut surface roughness when slicing 6.35 mm thick plates. Abrasive slurry concentrations of 0.5 kg/min, 0.8 kg/min and 1.2 kg/min were used for these tests and the speed was varied from 0.423 mm/sec to 2.12 mm/sec at 0.212 mm/sec increments. The variation in the resulting surface roughness can be seen in Figure 3.19.

These roughness tests were conducted in order to assess weather the ASJ could achieve cut quality levels comparable to that of AWJ cutting that the Centre for Aerospace Manufacturing Technology (CAMT) program required [Zhang, 2006]. The data points were used to plot exponential trend lines for different slurry concentrations as shown in the Figure 3.19. The trends for three different abrasive concentrations showed a definite, and anticipated, trend towards an increase in surface roughness with faster traverse rate. The surface roughness also decreases with an increase in abrasive concentration except at lower speeds where the traverse rate seems to have a stronger influence.

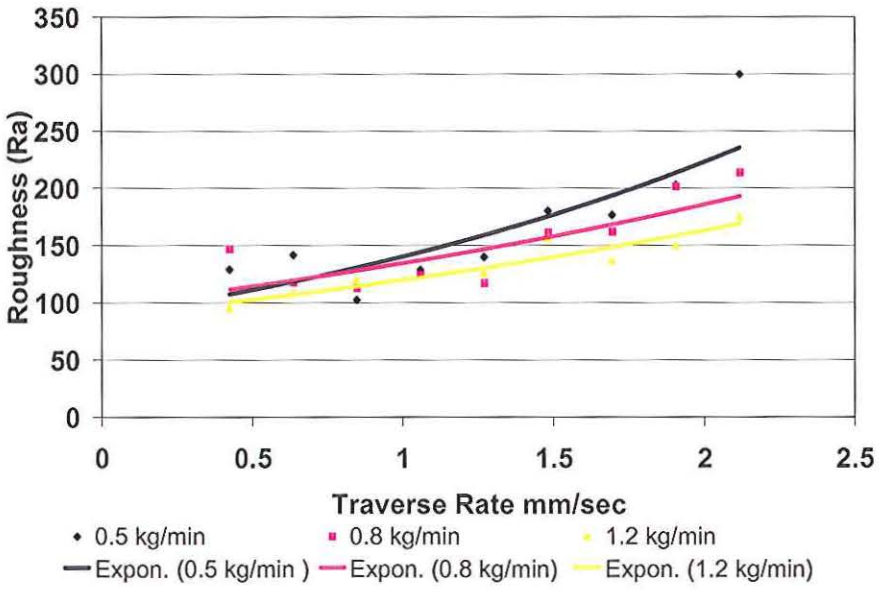

Figure 3.19. Surface roughness variations with change in AFR, traverse rate

3.6 DISCUSSION

A top feed abrasive slurry feed system has been described in this chapter. A prototype built based on this design is being used at UMR for ASJ testing. The system has satisfied the four indices of performances defined in Section 3.1. Future improvements on the system include computer control of opening/closing of the valves as a means to designing an autonomous drilling system. It should be noted that future improvements should be accompanied with higher operating pressures to enhance its potential.

The objective of the new design was to improve the control and consistency of abrasive in the slurry fed out of the system. Reduction in wear of the high pressure components and ability to start/stop the system without causing accelerated wear of the valves was targeted and achieved with this design. High precision machining standards of the Department of Defense were satisfied with this design thereby exceeding initial expected standards of performance.

4. EXPERIMENTAL ANALYSIS OF POWER OF ABRASIVE SLURRY JETS

4.1 INTRODUCTION

The cutting power of the abrasive in an ASJ is a function of the energy that the abrasive particles have when they exit the nozzle. Ideally, all the exiting particles should have the same optimal velocity with perfect momentum transfer, steady state uni-directional flow and equal particle size. However, under less ideal real conditions, the flow analysis must also include particle interaction and the effects of nozzle design, both of which can cause considerable loss in particulate energy. To assess the impact of such changes it is necessary to be able to measure this velocity.

4.2 PARTICLE VELOCITY MEASUREMENT

One successful method for indirectly measuring abrasive particle velocities and their distribution is by the collecting the abrasive after it has left the nozzle, but without allowing it to impact a target. To achieve this, the nozzle is mounted horizontally and directs the resulting jet along the centerline of a tube, divided in 30 cm divisions, so that as the particle velocity drops the particles will fall, and settle to the bottom of the tube, with insufficient residual energy to cut the tube. Figure 4.1 show the test setup. The loss in individual particle kinetic energy with distance controls the particle trajectory and the distribution of particles along the tube thus mirrors the velocity distribution in the jet.

Tests of nozzle performance have been carried out for different jet pressures, nozzle designs and abrasive flow rates. In each case, to simplify measurement, the abrasive particles collected over each 30-cm increment were combined. The samples

were then dried separately in an oven and weighed. For purpose of analysis the mass measured in this way was designated as having reached the center point of that interval along the tube. The kinetic energy of the particles was then calculated, both by increment and in combination using this averaged travel distance and the incremental mass collected in that interval, The tests were carried out at jet pressures of 35 MPa, 69 MPa, 103MPa and 138MPa with abrasive flow rates of 0.272 kg/min, 0.453 kg/min and 0.68kg/min. Nozzle sizes of 0.5 mm and 0.7 mm were used. Barton garnet at a mesh size 80 was used throughout the tests.

Figure 4.1. Tube tests for measurement of energy of ASJ

4.3 EFFECT OF PRESSURE ON KINETIC ENERGY

The velocity of the particles was calculated based on their respective distance traveled from the nozzle, using the average mass and average distance values. The mass of abrasives at each point was plotted against the square of the derived respective calculated velocity that would be required to reach that point along the tube. The area under the curve then becomes proportional to the contained abrasive energy within the jet. Figure 4.2, Figure 4.3 and Figure 4.4 show the distribution of the particle velocities

for the 0.5 mm nozzle, at 0.272, 0.453 and 0.68 kg/min feed rates. It can be seen that as the pressure increases a higher percentage of the abrasive particles reaches the upper levels of velocity.

The energy contained in the particles was also calculated for the 0.7 mm nozzle at the same feed rates. The total energy contained in each jet, at different pressures, for both nozzles was then plotted with Figure 4.5 showing data from the 0.5 mm diameter jet and Figure 4.6 the data from the 0.7 mm diameter nozzle. It is clear from both graphs that an increase in abrasive flow rate produces an upward increase in the energy curve for the same range of pressures and in both nozzles.

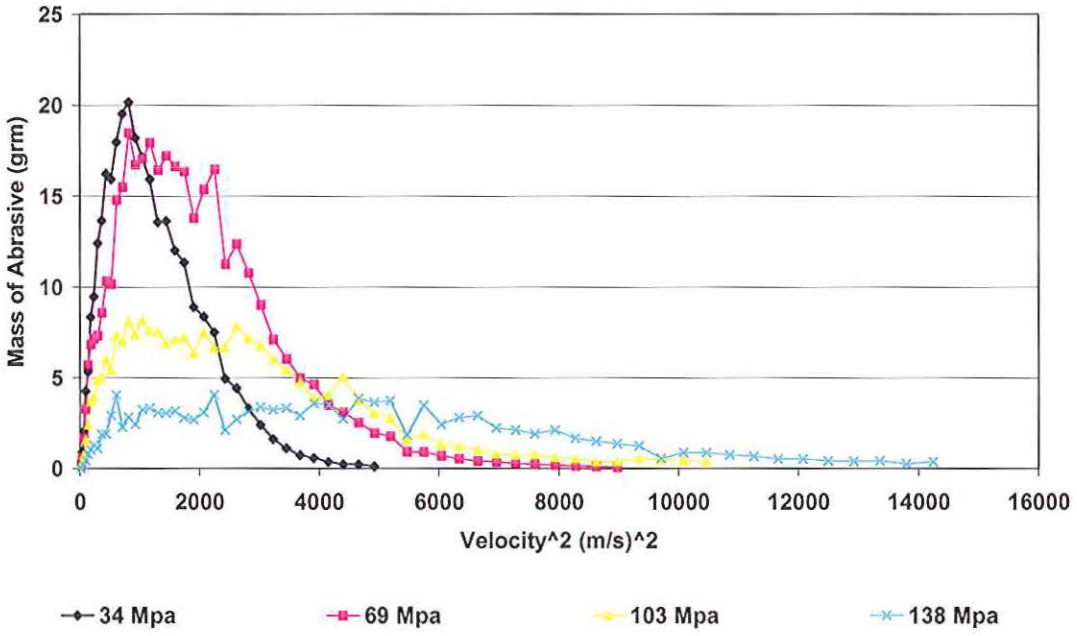

Figure 4.2. 0.5 mm nozzle at 0.272 kg/min AFR

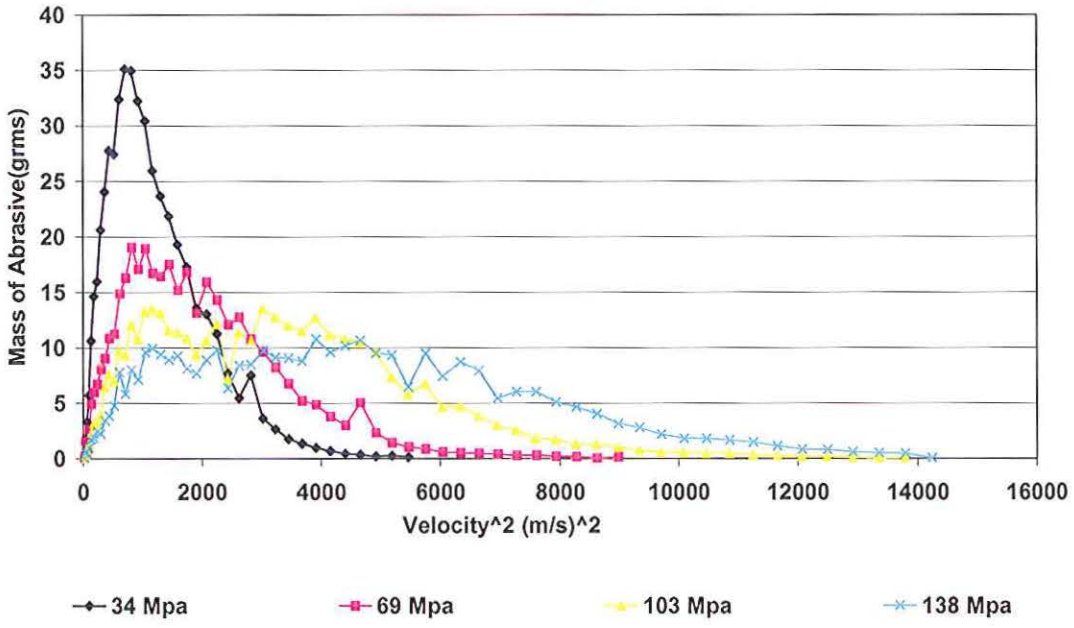

Figure 4.3. 0.5 mm nozzle at 0.453 kg/min AFR

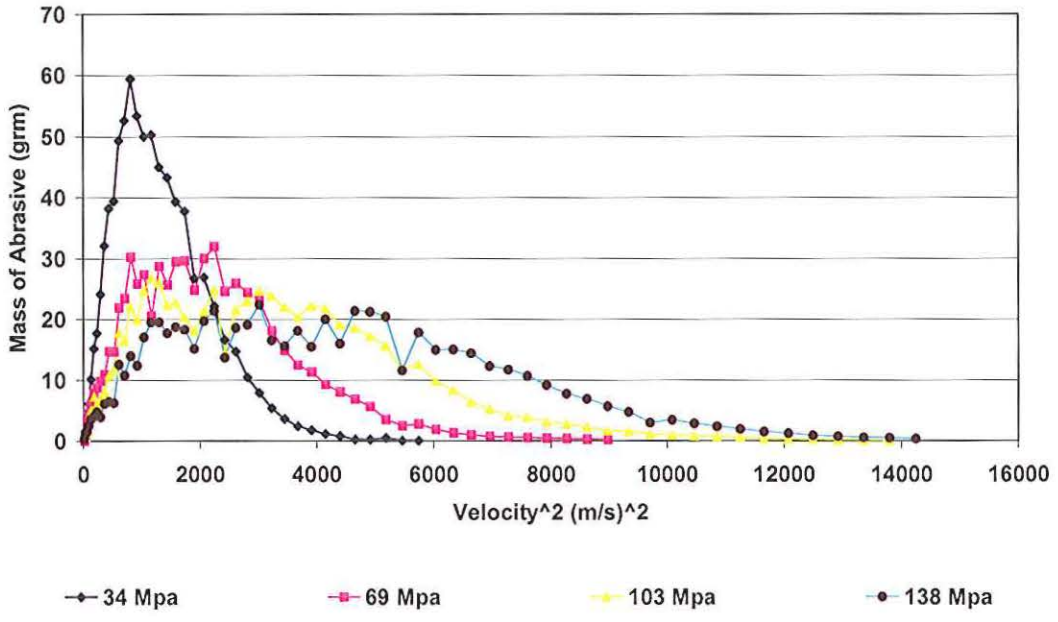

Figure 4.4. 0.5 mm nozzle at 0.68 kg/min AFR

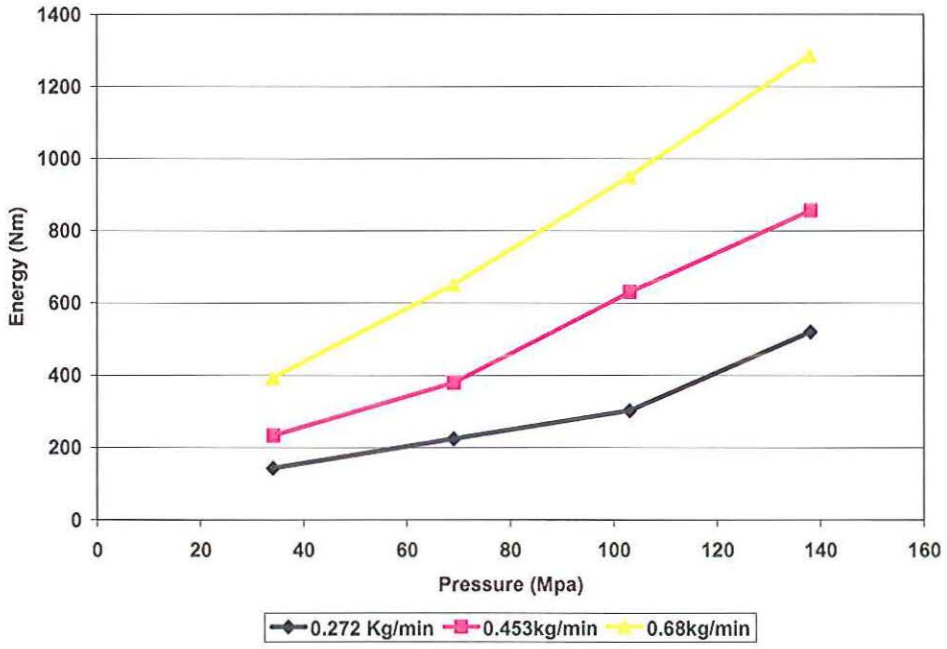

Figure 4.5. Total energy contained in the 0.5 mm nozzle at different feed rates

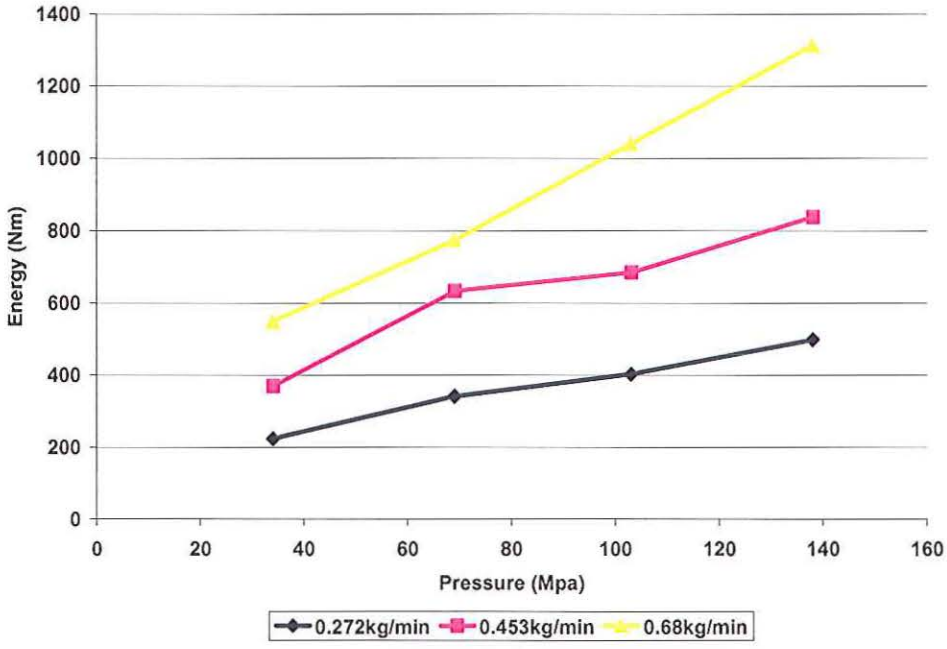

Figure 4.6. Total energy contained in the 0.7 mm nozzle at different feed rates

4.4 EFFECIENCY AS A FUNCTION OF PRESSURE FOR DIFFERENT AFR

Once the combined energy contained in the particles for a given jet had been computed, the relative efficiencies of energy transfer, with respect to the input energy from the pump were calculated. The equation for input energy is given by

$$E_i = P \cdot Q \tag{1}$$

where P is the pumping pressure and Q is the total flow rate which values includes both the mass flow rate of the abrasive and that of the water.

$$Q = \frac{\dot{M}_a}{\rho_a} + \frac{\dot{M}_w}{\rho_w} \tag{2}$$

Figure 4.7 and Figure 4.8 show the variation in energy transfer efficiency with an increase in jet pressure for the different abrasive flow rates using either a 0.5 or a 0.7 mm nozzle. It can be seen that the higher the abrasive feed rate, the higher the energy transfer efficiency. The efficiency values seem to level out above a critical pressure, though the value of that pressure differs for the two nozzles.

4.5 CONCLUSIONS

Initial experimental investigations reveal that the particles show an increase in kinetic energy with both an increase in pressure and an increase in abrasive flow rate.

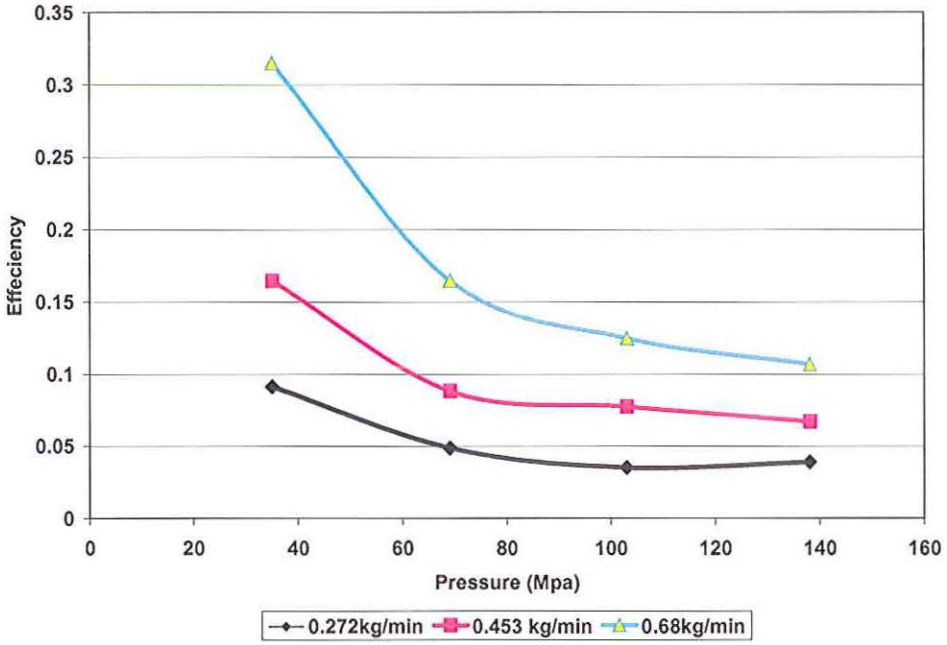

Figure 4.7. Efficiency of energy transfer for the 0.5 mm nozzle at different AFR

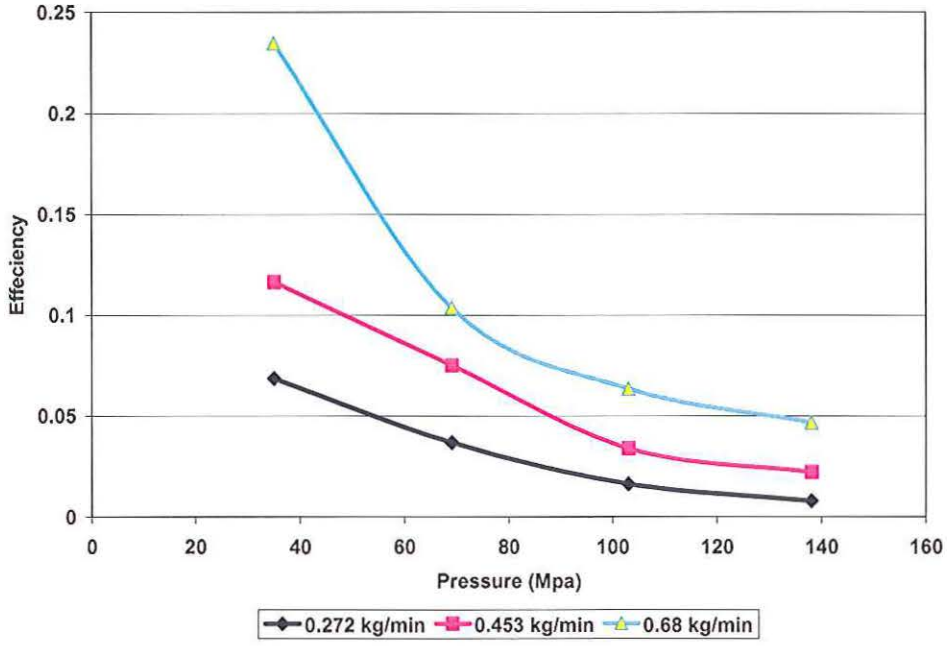

Figure 4.8. Efficiency of energy transfer for the 0.7 mm nozzle at different AFR

However, an increase in jet pressure has a negative effect on the transfer efficiency between the jet and individual particles. There appears to be a plateau in energy transfer efficiency at a critical pressure of the jet, which value is a function of nozzle diameter and thus water flow rate.

Measurement of particle velocity by distance measurement is a useful measurement tool to compare the effects of pressure, AFR and nozzle size on energy of the ASJ.

5. THEORETICAL ANALYSIS OF ABRASIVE SLURRY JETS

The key to establishing a true cutting capability equation for ASJ is in two steps. The first, involves deducing the abrasive power of the ASJ as a result of energy transfer from the fluid medium which is a fluid mechanics problem. The second involves determining the effect of this abrasive power on the material to be removed. The first step is the aim of the work in this section. This effect of abrasive power on the material is a function of probability of abrasive impact on target materials at specific angles and its properties and has to be determined experimentally.

5.1. OPERATIONAL PARAMETERS

Abrasive slurry jet cutting is a complex two-phase process involving the interaction of several system parameters. The parameters that affect the cutting capability of an ASJ system performance can be divided into four main groups

a) Cutting Parameters
   - Traverse speed
   - Cutting depth
   - Cutting width

b) Abrasive Parameters
   - Abrasive concentration
   - Abrasive size
   - Abrasive density

c) Power Parameters

- Pressure
- Nozzle size

Although the effect of each of these parameters on the cutting capability of abrasive slurry has been experimentally investigated by many researchers there has been very little effort to theoretically develop, or in detail explain, the structure of a theoretically based equation to describe cutting capability. Initial work centered on adapting abrasive water jet cutting models to describe the performance of abrasive slurry jets [Hashish, 1997]. The cutting process was divided into two modes- a cutting wear mode and a deformation wear mode. The cutting wear mode performs material removal by particle impact at shallow angles and is represented by (3)

$$h_c = \frac{(V_a / C_K) d_j}{\left(\frac{\pi \rho_a u d_j^2}{14 \dot{m}_a} \right)^{2/5} + \left(\frac{V_c}{C_k} \right)} \tag{3}$$

where

V_a is the velocity of the abrasive particles,

d_j is the diameter of the jet,

ρ_a is the density of the abrasive material,

m_a is the mass flow rate of abrasives and

V_c is the cutting threshold velocity, a property that is material dependent.

C_k is the characteristic velocity

The characteristic velocity C_K combines both work piece and abrasive material characteristics and is given by

$$C_K = \sqrt{\frac{3\sigma_f R_f^{3/5}}{\rho_a}} \tag{4}$$

In this equation, σ_f is the workpiece material flow stress and R_f is the particle roundness factor, which is the ratio of the average diameter of the abrasive particle corners to the overall diameter of the abrasive particle. The deformation mode depth of cut is given by equation (5)

$$h_d = \frac{1}{\frac{\pi d_j \sigma_j u}{2a\, m_a \left(\dot{V_a} - V_c\right)^2} + \frac{C_f}{d_j}\frac{V_a}{\left(V_a - V_c\right)}} \tag{5}$$

where C_f is the coefficient of friction of the kerf wall, a is the fraction of abrasives that actually impact the work piece surface and perform material removal.

The total cutting depth is a sum of equations (3) and (5). Although this equation is mathematically valid, there are a few problems in determining the variables used by the author. The velocity of abrasive particles is very difficult to measure experimentally and varies with nozzle geometry as well as standoff distance and a number of other system parameters. The fraction of the abrasives that actually impact the material surface and can perform material removal is a function of the traverse speed, the nozzle size, and the thickness of the target, among other parameters, and cannot be generalized. These

difficulties and confounding factors in correlating experimental data with theoretical predictions have led to considerable difficulty in application of this equation to the prediction of the cutting ability of an abrasive slurry jet.

Further research [Hashish, 1991], [Jiang, 2005] has used energy based modeling of the abrasive power of an ASJ to describe the jet power. It can be expressed as

$$P_a = \frac{1}{2} \cdot \dot{M}_a \cdot v^2 \tag{6}$$

where $\dot{M}_a$ is the mass flow rate of abrasive as it leaves a nozzle and v is the velocity of those abrasive particles. The power of the ASJ calculated by Jiang [2005], is thus given by

$$N = \frac{\pi}{4} D^2 P^{1.5} \sqrt{\frac{2}{\rho}} \frac{C}{1+C} \tag{7}$$

A significant omission from this equation is any term that describes the momentum transfer efficiency as it relates to determining the cutting capability of the jet. A momentum transfer efficiency term is needed in order to represent the losses incurred to the abrasive due to wall friction and fluid flow disturbances as the particles move through the nozzle. This equation for power was simulated using MATLAB, for a given set of parameters. The density for the slurry was developed using the equation given by [Jiang 2005]

$$\rho = \frac{1+C}{\frac{1}{\rho_w} + \frac{C}{\rho_a}} \tag{8}$$

Where:

Nozzle diameter (D) = 1mm

Pressure (P) = 100MPa and 200MPa

Abrasive density (ρ_a) = 4060 kg/m^3

Water density (ρ_w) = 1000 kg/ m^3

Concentration by weight of abrasives (C) = 0-1

The graph shown in Figure 5.1 illustrates the change in power of the jet as the abrasive concentration is increased from 0-100%. The equation clearly predicts that there is a continuous increase in energy with the increase in abrasive concentration. However, at higher concentrations the particles interact with each other, and results in consequent energy losses. During the acceleration process the particles fragment because of this impact both between particles and between the particles and the nozzle itself [Galecki, 2000]. This comminution of the particles increases with an increase in the abrasive concentration in the flow stream.

It should be borne in mind that there is only a finite amount of energy available in the fluid stream to accelerate the abrasive particles. When the concentration of the primary fluid phase decreases, then the supply of energy available also decreases. In Figure 5.1, as the concentration of primary fluid phase decreases, i.e. concentration of abrasive increases the abrasive power of the jet also increases and the power value peaks close to 100% concentration by weight of abrasive. This is physically impossible as there

is insufficient fluid to accelerate the particles at high concentrations. In the case of ASJ flow the value of concentration at which the jet has maximum abrasive power is theoretically very high as compared to AWJ. This can be seen in a comparison of Appendix A and Appendix B.

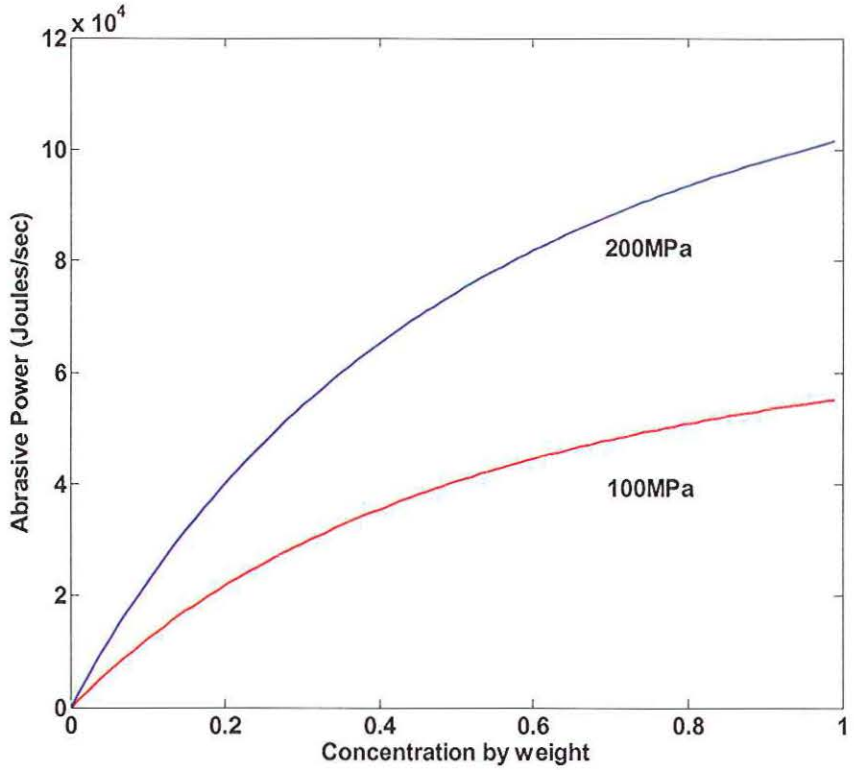

Figure 5.1. Predicted variation in abrasive power with abrasive concentration in the jet stream [Jiang, 2005]

5.2. A MODIFIED EQUATION FOR ABRASIVE POWER

High velocity Abrasive Slurry Jets (ASJ) form when premixed slurry is forced through a small nozzle by a high driving pressure. Energy based modeling of the abrasive power of an ASJ begins with the basic equation

$$P_a = \frac{1}{2} \cdot \dot{M}_a \cdot v^2 \tag{9}$$

where $\dot{M}_a$ is the mass flow rate of the abrasive and v is the velocity of the particles as they leave the nozzle. This velocity can be expressed in terms of the pressure P and density ρ_{mix} of abrasive suspension by the equation:

$$v = \mu_m \cdot \sqrt{\frac{2P}{\rho_{mix}}} \tag{10}$$

The density ρ_{mix} defined in terms of R, the loading ratio in the slurry

$$\rho_{mix} = \frac{\rho_a (1+R)}{\frac{\rho_a}{\rho_w} + R} \tag{11}$$

The loading ratio R can be expressed in terms of the concentration by weight C as

$$R = \frac{\dot{M}_a}{\dot{M}_w} = \frac{C}{1-C} \tag{12}$$

where

$$C = \frac{\dot{M}_A}{\dot{M}_A + \dot{M}_w} \tag{13}$$

$$\rho_{mix} = \frac{\rho_a\left(1+\frac{C}{1-C}\right)}{\frac{\rho_a}{\rho_w}+\frac{C}{1-C}} \tag{14}$$

The mass flow rate $\dot{M}_a$ can be expressed as

$$\dot{M}_a = \frac{\pi}{4}\cdot D^2 \cdot \sqrt{2P\rho_{miz}} \cdot \frac{C}{1+C} \tag{15}$$

where D is the nozzle diameter. Substituting (10) and (15) in (9), the abrasive power of the ASJ can be expressed as

$$P_a = \mu_m{}^2 \cdot \frac{\pi}{4} \cdot D^2 \cdot P^{1.5} \cdot \sqrt{2} \cdot \sqrt{\frac{\frac{\rho_a}{\rho_w} + \frac{C}{1-C}}{\rho_a\left(1+\frac{C}{1-C}\right)}} \frac{C}{1+C} \tag{16}$$

Using the same parameters that were used to simulate the abrasive power in Figure 5.1 leads to the results shown in Figure 5.2.

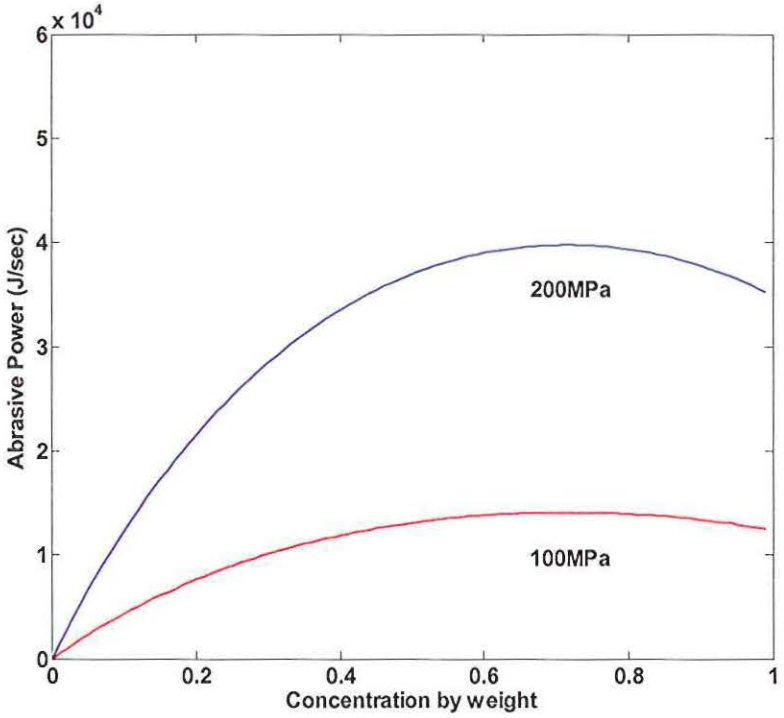

Figure 5.2. Predicted variation in abrasive power with abrasive concentration using the modified equation

The predictive model derived in Equation 16, and illustrated in Figure 5.2, has been found, in this study, to show a better agreement with experimental results derived not only here, but also elsewhere in that the curve shows the existence of an optimal abrasive concentration in an ASJ to achieve best performance. Having found the

theoretical basis to describe the presence of such a concentration, the next step in the process is to determine the factors that control this optimal concentration.

5.3. PARAMETERS AFFECTING OPTIMAL CONCENTRATION

The optimal abrasive concentration in an ASJ can be represented as the point of inflection in the curve represented by equation 16. In order to determine this optimal concentration equation 16 can be differentiated with respect to C. The steps leading up to the resulting simplified equation (Equation 17) are detailed in Appendix A.

$$\frac{\partial P_a}{\partial C} = \frac{\pi \cdot D^2 \cdot \mu_m^2 \cdot \sqrt{2} \cdot P^{3/2}}{(1+C)\cdot\sqrt{\dfrac{\rho_a\left(1+\dfrac{C}{1-C}\right)}{\dfrac{\rho_a}{\rho_w}+\dfrac{C}{1-C}}}}\cdot\left[\frac{1}{4}-\frac{C}{4\cdot(1-C)}-\frac{C}{8}\cdot\left\{\frac{\rho_a\left(\dfrac{1}{1-C}+\dfrac{C}{(1-C)^2}\right)}{\dfrac{\rho_a}{\rho_w}+\dfrac{C}{1-C}}-\frac{\rho_p\cdot\left(1+\dfrac{C}{1-C}\right)\cdot\left(\dfrac{1}{1-C}+\dfrac{C}{(1-C)^2}\right)}{\left(\dfrac{\rho_a}{\rho_w}+\dfrac{C}{1-C}\right)^2}\cdot\left\{\frac{\rho_a\left(1+\dfrac{C}{1-C}\right)}{\dfrac{\rho_a}{\rho_w}+\dfrac{C}{1-C}}\right\}\right\}\right]=0 \tag{17}$$

The first term in equation 17, outside the square brackets cannot be equal to zero unless the value of any of the parameters - pressure, diameter of nozzle, density of liquid or solid or momentum transfer coefficient- is equal to zero. Since this is not the case in a functioning system, then the second term inside the brackets which consists of concentration and density terms must be therefore equated to zero.

$$\left[\frac{1}{4}-\frac{C}{4\cdot(1+C)}-\frac{C}{8}\cdot\left\{\frac{\rho_a\left(\frac{1}{1-C}+\frac{C}{(1-C)^2}\right)}{\frac{\rho_a}{\rho_w}+\frac{C}{1-C}}-\frac{\rho_a\cdot\left(1+\frac{C}{1-C}\right)\cdot\left(\frac{1}{1-C}+\frac{C}{(1-C)^2}\right)}{\left(\frac{\rho_a}{\rho_w}+\frac{C}{1-C}\right)^2}\right\}\cdot\left\{\frac{\rho_a\left(1+\frac{C}{1-C}\right)}{\frac{\rho_a}{\rho_w}+\frac{C}{1-C}}\right\}\right]=0 \quad (18)$$

The equation is further simplified and at this stage the abrasive density parameter is converted to a value. The abrasive used in much of the cutting industry and most of the work at Missouri S&T is garnet which has a specific gravity of 4. This is therefore assumed to be a constant value as the equation evolves. Substituting in (18), the equation becomes

$$\left[\frac{1}{4\cdot(1+C)}-\frac{C}{8}\cdot\left(\frac{1-C+C}{(1-C)^2}\right)\left\{\frac{(4-1)}{\left(4+\frac{C}{1-C}\right)\cdot\left(1+\frac{C}{1-C}\right)}\right\}\right]=0 \quad (19)$$

This reduces to

$$3C^2+9C-8=0 \quad (20)$$

Solving for C we get values of -3.71 and 0.71. Since the abrasive concentration cannot be either greater than 1 or less than zero then the optimal concentration is at 71%.

It is important to note that the optimal concentration is independent of any power parameter. An important assumption in deriving Equation 16 was that the momentum transfer coefficient is independent of abrasive concentration. An increase in abrasive concentration will yield a greater number of abrasive particles in the jet stream, per unit length, and consequently more particles involved in the cutting process. An assumption commonly made is that there is no contact between individual abrasive particles during the particle passage through the nozzle, so an increase in concentration will result in an increase in abrasive power and corresponding depth of cut [Laurinat,1992], [Brandt, 1996]. This assumption is valid only for lower abrasive concentrations. At higher concentrations, particle-to-particle interactions become more common and their result must be considered in the performance prediction. There is a limited amount of kinetic energy that is available within, the liquid carried fluid, to accelerate the abrasive particles. With an increase in the number of abrasive particles per unit volume of slurry exiting the nozzle, the relative mass of liquid available to transfer energy to an individual particle drops. The momentum transfer efficiency term must therefore change with a change in the abrasive concentration. For AWJ systems this momentum transfer efficiency factor was [Hoogstrate, 2002] is defined as

$$\eta = 1 - c \cdot R \tag{21}$$

This term is introduced to account for the friction losses that occur between the jet and the inner walls of the focusing tube. In the case of an ASJ system c will represent the

quality of the accelerating section of the nozzle and must be determined experimentally. This term replaces the value μ_m in Equation 16. The modified equation thus becomes

$$P_a = (1 - a \cdot R) \cdot \frac{\pi}{4} \cdot D^2 \cdot P^{1.5} \cdot \sqrt{2} \cdot \sqrt{\frac{\frac{\rho_a}{\rho_w} + \frac{C}{1-C}}{\rho_a \left(1 + \frac{C}{1-C}\right)}} \frac{C}{1+C} \tag{22}$$

The concentration terms can then be replaced by a value R, defined as the loading ratio. From equation (10) R and C can be related:

$$C = \frac{R}{1+R} \tag{23}$$

Replacing (21) in (20)

$$P_a = (1 - a \cdot R) \cdot \frac{\pi}{4} \cdot D^2 \cdot P^{1.5} \cdot \sqrt{2} \cdot \sqrt{\frac{\frac{\rho_a}{\rho_w} + R}{\rho_a (1+R)}} \frac{R}{1+2R} \tag{24}$$

Equation 24 is then plotted using the data shown in Figure 5.1 with c = 0.1, and the resulting graph is shown in Figure 5.3.

The relative value at which the optimum concentration occurs is seen to remain the same, irrespective of the pressure at which the jet is performing. This is similar to results observed in AWJ experiments, where optimal concentrations have been experimentally determined to lie around a value of 21%.

To verify this observation in equation 24, simulation runs were made at jet operating pressures of 50MPa, 100MPa, 150MPa and 200MPa. The simulation run was halted when the abrasive power began to decrease with a further unit increase in abrasive concentration. The curves shown in Figure 5.4 illustrate that for a nozzle constant value, $c = 0.1$, that the predictive equation finds that optimal performance occurs at the same concentration of abrasive regardless of the pressure value.

It is worth noting, however, that while the optimal abrasive concentration remains the same, as the pressure increases so the volume of water flowing through the nozzle will also change, and thus the Abrasive Feed Rate (AFR) to the system must increase at an equivalent rate to the flow rate change to maintain a constant abrasive concentration.

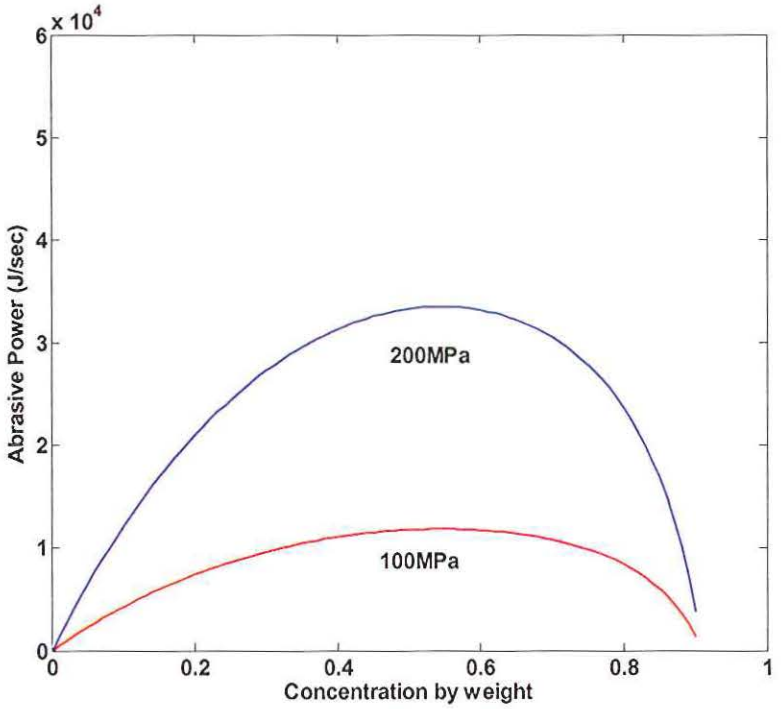

Figure 5.3. Predicted variation in abrasive power with abrasive concentration using modified equation and including a concentration dependent momentum transfer term

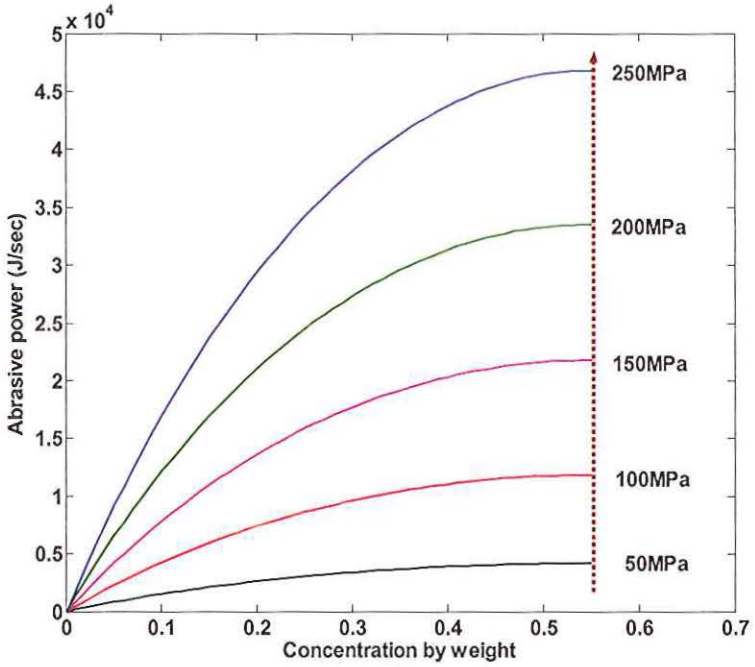

Figure 5.4. Optimal concentration non-variance with pressure changes

The term '*c*' has been used earlier to describe the quality of the nozzle. For an ideal nozzle the value for $c = 0$, i.e., there is a perfect momentum transfer between the fluid and the abrasive. The efficiency of momentum transfer reduces with a drop in the quality of the nozzles, represented with an increase in the value of *c*. This change in *c* affects the value of the optimal concentration on the curve. To determine the exact effect, the simulation prediction equation was run with $c = 0.2$, 0.4, 0.6, 0.8 and 1.0. The pressure was set at 100MPa using a 1.0mm diameter nozzle and with garnet as the abrasive. The resulting data is plotted in Figure 5.5. The optimal concentration can be seen to drop to a lower value when there is a decrease in the quality of the nozzle. The effect of this change in the value of c is not pronounced at lower concentrations i.e., from 1-20% but there a significant change in the abrasive power at higher concentrations.

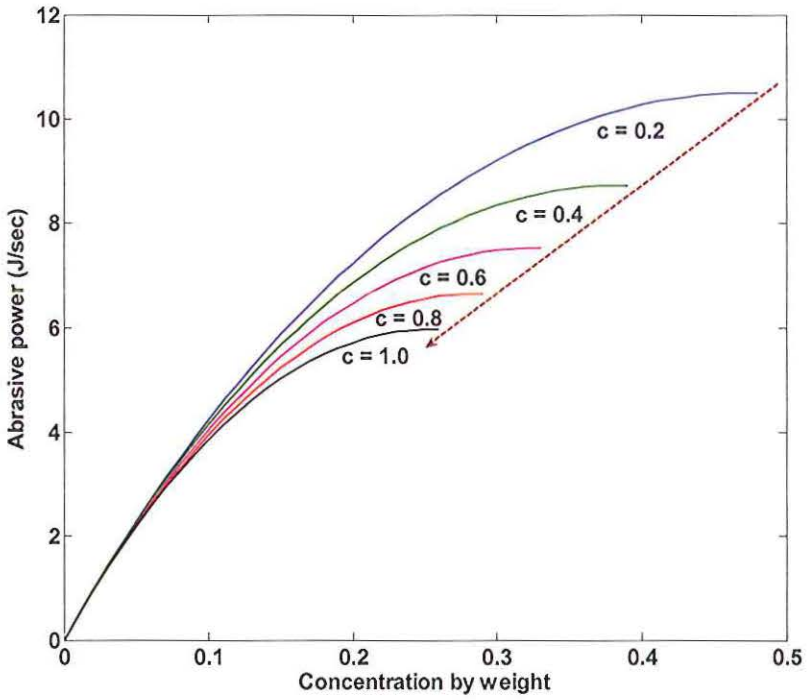

Figure 5.5. Change in the value of the optimal concentration with a change in the quality of the nozzle

5.4. DISCUSSION

The work by Jiang [2005] was the first attempt to describe the cutting capability of an ASJ in terms of the power of the abrasive that actually does the cutting. Despite the shortcomings of that initial model it provided a viable starting point from which to build the theoretical model of an ASJ described in this chapter. Data from cutting tests in the past have no provided no real baseline to include nozzle quality or design in the predictive equations for cutting performance. As a consequence, values for the optimal concentration of abrasive have been reported as varying from 15% to 40%. For a system to become optimal, it requires that a move first be made to standardize and optimize the quality of the nozzle before seeking to find the optimal concentration for best cutting

performance. The role of disintegration due to particle-particle interaction and its effect on performance has not been determined or included in this model. Relatively small degrees of fragmentation, around 15% [Galecki, 2000] have been reported for ASJ systems, in comparison with much larger percentages (up to 60%) that have been reported for more conventional AWJ systems.

Particle comminution prior to cutting impact has been found to increase at higher pressures and abrasive concentrations. Relationships have yet to be determined experimentally to show the effect of change in nozzle sizes, jet pressures, abrasive concentrations and abrasive size, and to compare the experimental results with the theoretical predictions made here.

6. DRILLING WITH ABRASIVE SLURRY JETS

6.1 INTRODUCTION

The mining industry must know what the mineral content of rock is, if it is to plan a successful mine, and the best way of knowing content is to recover a core of the rock in question. As depths grow greater recovery of that core becomes more challenging, in real time, and to speed the recovery the industry has been using continuous wire-line coring, where a central wire recovers core from within the main body of the drill, and brings it to the surface. This practice has been common for many years and provides precise knowledge of the ore in the different rock formations. Drillers have reached depths of 5000 meters in certain parts of the world with bore diameters as small as 1.75". This small diameter coring in the mining industry is termed slim-hole drilling and is used for continuously retrieving cores. The most commonly accepted definition of slim-holes is where hole diameters are less than 8.5" [Deliac, 1991]. In the oil industry this term is commonly used when the diameter drilled is smaller than that of a conventional well drilled to the same depth. This drilling technique is an attractive exploration method because of in the reduced costs of smaller holes. An alternative, more recent and more cost effective solution for exploration, monitoring and production is known as micro-hole drilling. Micro-holes are smaller in diameter than slim-holes, and are more commonly in the range below 2.5 inches in diameter, Figure 6.1.

The use of coiled tubing, Figure 6.2, which refers to a continuous reel of pipe wound on a spool in recent years has made micro-hole drilling technology more feasible and economically attractive. This spool unwinds feeding tube downhole as the drill

progresses. There is minimal pipe handing as compared to conventional which requires stopping after each section of pipe. The continuous pipe help maintain the downhole pressure with a very small rig footprint. Also the coiled tube is not rotated, thereby eliminating damage to the borehole walls. When holes this small are used for exploration to locate the best prospects for coal bed methane, it is possible to reduce drilling costs by a third [Snyder, 2005].

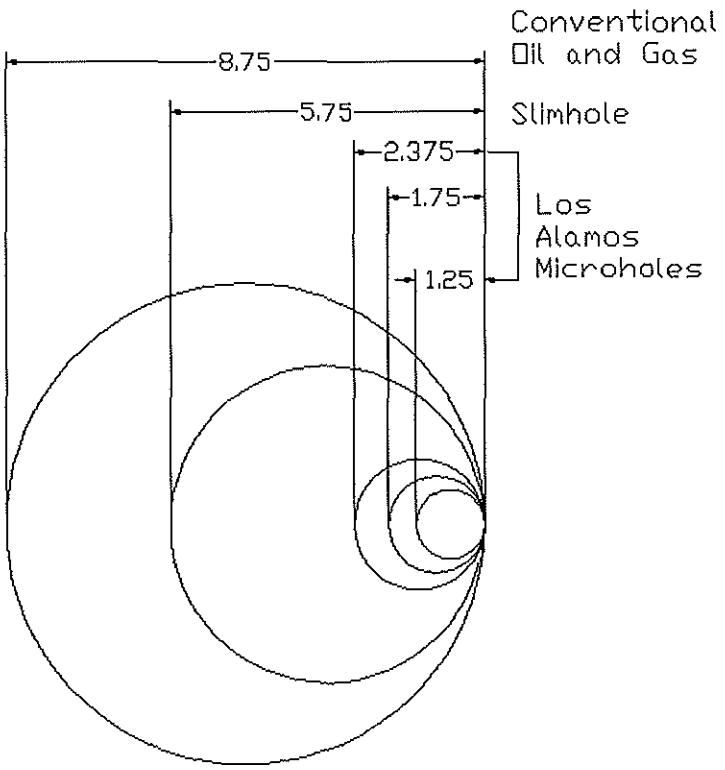

Figure 6.1 Microhole drilling systems/conventional well diameters

[http://www.fossil.energy.gov/programs/oilgas/microhole/index.html]

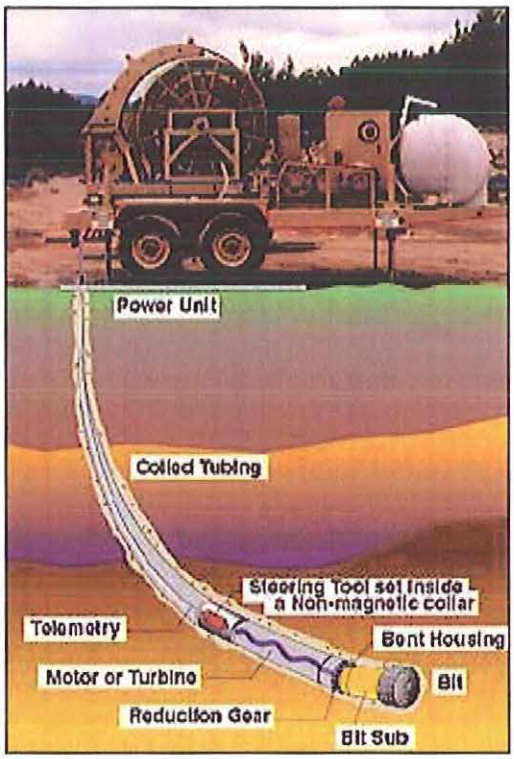

Figure 6.2 Coiled tube drill rig

[http://www.fossil.energy.gov/programs/oilgas/microhole/index.html]

Micro-hole technology would be ideal for drilling between existing wells to access oil or gas that might have been bypassed earlier, or to increase flow rate by creating lateral well extensions that increase well exposure to the formation. The Department of Energy is looking to develop and adapt alternate well completion technologies, for example, for linking wells to extract methane from multiple coal seams [DOE/NETL-2003/1193]. Under current practices, Coal Bed Methane (CBM) wells are only used to target single thick coal seams and bypass thinner seams. If several of these seams could be accessed through a single well then CBM reserves could be significantly increased, Figure 6.3.

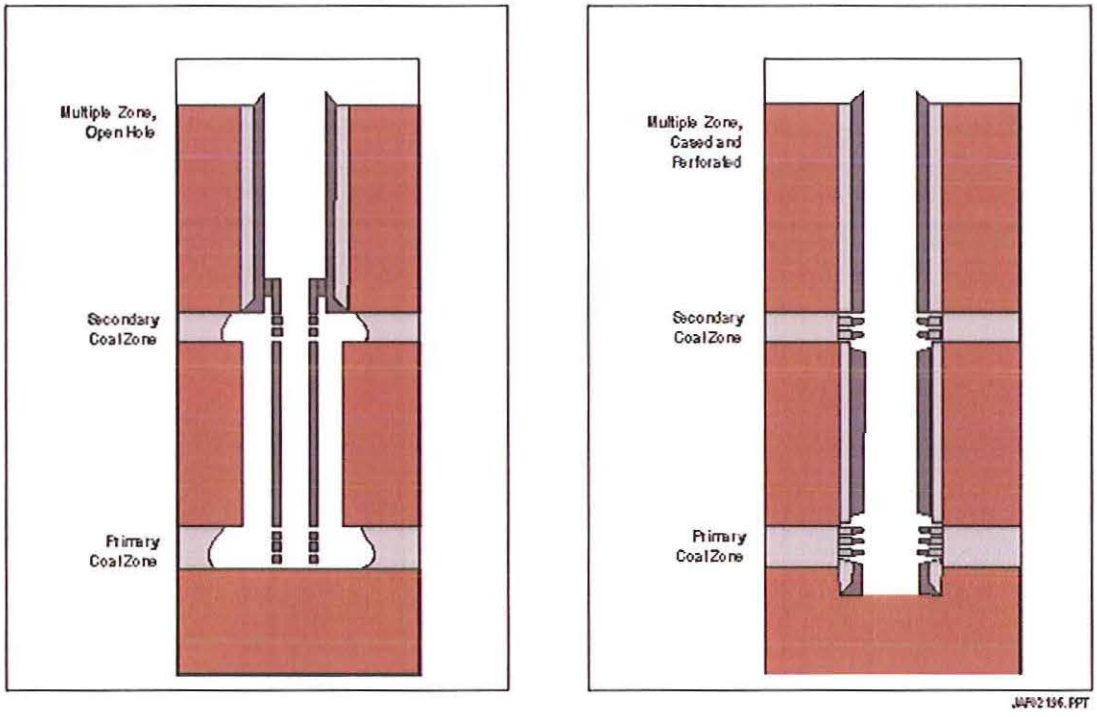

Figure 6.3. Multiseam well completion options using lateral short radius drilling

[US DOE/NETL-2003/1193]

The combination of coiled tube drilling and micro-hole technology has, thus, the potential to provide both a solution for low cost exploration and for the production of resources that would otherwise be uneconomic to extract. Reduced drilling costs and lower environmental impacts because of smaller footprints make this technology an important tool for the future. A potential roadblock to commercialization of this technology comes with the low drilling thrust that can be applied through the drill stem to the cutting tool. The micro-drilling drill rig hydraulics that provides power to the drilling head at the bottom of the tubing must be able to operate at high pressure and with low flow rates. Conventionally used polycrystalline diamond compact (PDC) bits require a high weight on bit and rotate at relatively high speed. This requires that significant power

be supplied, and this, in turn, requires more robust support tubing. To take better advantage of the more flexible coiled tubing an alternate lower thrust hard-rock drilling technology would be an advantage.

The technology that has evolved, largely based on work at Missouri University of Science & Technology (MO S&T) and which is now known as abrasive slurry jet drilling (ASJ drilling) offers the benefits of both low bit-weight and reduced torque levels. It can also be used to drill short radius laterals with small diameter coiled tubing, given the reduced needs for external power.

6.2 SMALL DIAMETER HOLE DRILLING USING ASJ

A primary requirement in drilling through long distances is that the opening created is larger than the drilling tool itself, so that the tool can advance into the hole. The concept of using abrasive slurry to drill through rock was introduced following significant research in rock drilling with plain waterjets. In order to better understand the drilling philosophy described in this section it is necessary to briefly review these early steps in development of waterjet drilling.

A high-pressure waterjet drill is a beam of energy directed down onto a target. Generally the jet will cut a diameter around 3 – 5 times that of the orifice through which the jet is formed at the end of the nozzle. For example, if the orifice size is around 1 mm, the hole diameter created by this jet would be in the range of 3-5mm. The footprint of the nozzle body and fluid supply line is significantly larger than this so that aiming a conventional jet ahead of the nozzle would not create a hole large enough to allow the nozzle to advance. If, however the jet is inclined at an angle, and rotated, then the cutting

action of the jet will cut a circular path around the axis of the nozzle movement, which under the right conditions , will make a hole large enough for the nozzle to move forward [Summers, 1968], Figure 6.4.

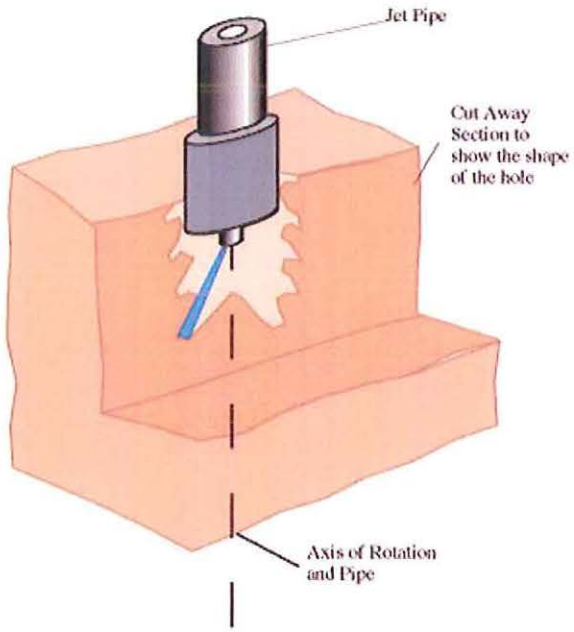

Figure 6.4. Rotating jet used to drill a hole large enough for nozzle advance

However, it was not until the early 1980's that high pressure swivels became available at a low enough cost and with sufficient reliability that a rotating waterjet drill could be commercially developed. The waterjet drill operates through water erosion of the rock ahead of the bit. Because of this lack of mechanical contact between the drill and the rock, geological effects such as encounters with steeply dipping beds, or varying geology, do not have as great an impact on drilling alignment, as can occur with a more conventional drilling assembly.

The initial designs for a high-pressure waterjet drill using just a single jet to cover the entire face were inefficient, and considerable improvement was achieved when a second orifice was added to the nozzle, axially located and directed, in order to remove the central core of rock ahead, Figure 6.5. The initial "reaming" jet was inclined out to cut a large enough diameter to allow the nozzle to advance into the rock [Summers, 1976]. Subsequent experimentation showed that an optimum angle of inclination for this jet was in the range from 20 – 25 degrees to the hole axis By placing such a jet, with a diameter half that of the main reaming jet, penetration rates were improved by two orders of magnitude.

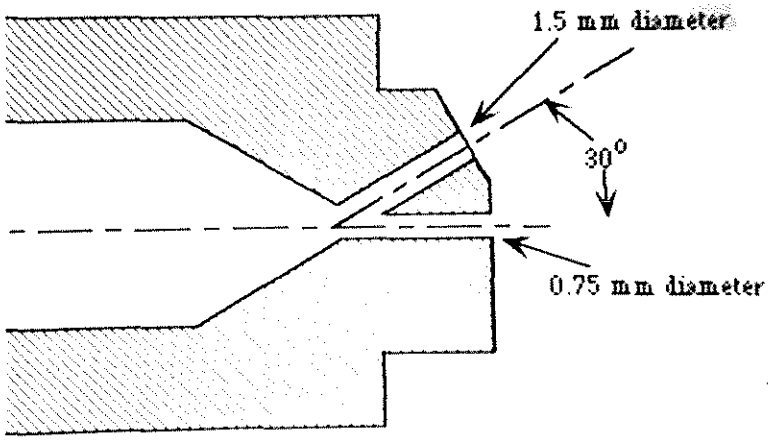

Figure 6.5. Nozzle geometry for a high pressure waterjet drilling nozzle assembly

This forward cutting action of the jet, however, carries with it a potential problem, illustrated in Figure 6.6 where a threaded hole is created because of rotation. This profile was advantageous in resin anchored rockbolts where hole roughness increased load carrying capacity of the bolts. In long hole drilling applications, where the nozzle assembly was required to enter the hole these ribs presented a challenge for advancing the

drill. The ribs must be small enough and short enough that they do not interfere with the passage of the main body of the drilling assembly and feed pipe.

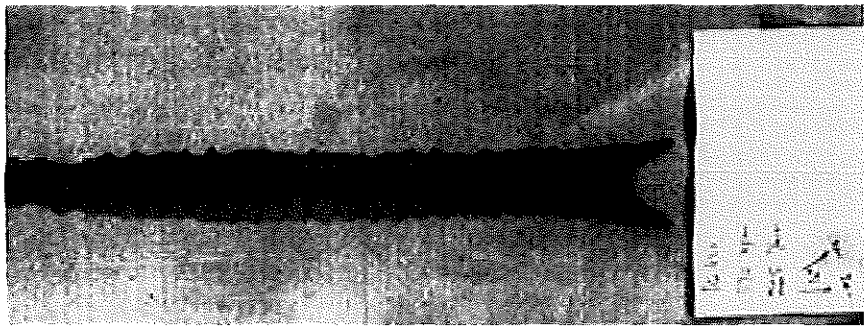

Figure 6.6. The appearance of ribs along a drilled hole

Another concern in using this tool came where there was a change of rock structure and geology. When the jet is drilling though one rock, and then reaches a second harder formation to drill, then under constant drilling parameters, the hole will reduce in diameter. This can be seen when the drilled rock changes, for example, from Berea sandstone to Indiana limestone at 69 MPa, Figure 6.7. The jet is cutting ahead of the nozzle and this change in diameter will not be noticed until the passage of the nozzle body is blocked by the walls of the smaller hole.

A gauge ring located in the plane of the desired jet contact resolved this problem. As the drill advanced into the rock, it would increase in ROP until the jet was just capable of cutting the diameter set by the ring. At that point the ring will engage the rock, and hold the advance, with the jet cutting in the plane of the obstruction, until it is removed, and the drill can then advance. It then becomes possible to consistently drill rock and obtain holes of the required size.

Figure 6.7. Change in hole geometry using a waterjet drill

This basic drill design, a central high-pressure waterjet line feeding fluid to a nozzle, with jets inclined to remove the rock ahead of the assembly, was limited in application since there are rocks that cannot effectively and economically be drilled by high-pressure water alone. For example basalt requires a higher pressure jet than is conventionally commercially available. As mentioned in Section 2, there were other logistical challenges when the AWJ system was developed in applying this technique to rock drilling, but these no longer applied after the ASJ system had been developed.

The concept of using two nozzles, one axially and the other inclined poses additional challenges when applied to an abrasive slurry jet drill. The cutting effectiveness of an abrasive particle is a function of the particle diameter, and performance has been found to significantly degrade when sand particles below 100 μm are used in the cutting stream. The orifice diameter must be roughly three times the largest particle size, to guard against the possibility of particles clogging in the nozzle and blocking further flow. With a particle size of 250 μm, this gives a minimum orifice

diameter of 750 μm, 0.75 mm. Two nozzles of this size significantly increase the volume of fluid and abrasive needed for drilling and do not allow, due to particle restrictions, the different size options available with water alone as the cutting fluid.

Rotating the entire tool can be effective in drilling small holes of limited distance it becomes an expensive option in drilling deeper holes, since the tubular steel that supports the nozzles must still be broken and remade, as with conventional drilling systems, and this detracts from some of the potential benefits of using abrasive slurry jets. These benefits include a relatively low reaction force imposed back on the drill string through the nozzle as the jet cuts, and an ability to cut forward through rock of varying geology and maintain hole alignment while doing so. These advantages, make the marriage of high-pressure drilling and coiled tubing potentially a very successful one, but requires that an alternate means for generating the larger hole size must be developed, since coiled tubing itself does not rotate.

One obvious solution to this problem is to rotate only drilling assembly that includes the cutting nozzles, and not the entire drill string. There are three main options that can be used

- Electric motor drive
- Hydraulic motor drive
- Self rotating Nozzles

6.2.1 Electric Motor Drive. These motors generally include an electromagnet coupled to a hollow shaft and an electromagnetic field is emitted by the magnet. The electromagnet is encased by a drum coupled to rotate about the axis of a hollow central shaft. The high-pressure rotary coupling that allows nozzle rotation, is mounted within

this hollow core, and connected so that the motor drives the lower section of the coupling in rotation thereby turning the nozzles mounted on the drum, Figure 6.8. The fixed part of the motor can be attached to the lower end of the coiled tubing to provide rigidity and support. These motors have been designed, and used to provide rotation in confined spaces.

While such combinations exist and have been used, in the above case to develop a tool that was used to remove high level radio-active waste, these have only been operated without abrasive in the feed fluid, and the motor sizes that are available in the sealed conditions that would be required for down-hole operation are currently larger than the anticipated space available, and thus a special motor would need to be designed. It should be noted that rotary swivels are available, in a small enough size range, with a diameter of less than an inch, which can fit within the space. Given the abrasive nature of the environment in which the motor is likely to be placed, and the need for space-demanding protection for the motor, it is considered that while this is an option, it is an expensive alternative to other possible solutions.

6.2.2. Rotation with a Hydraulic Motor. An alternative configuration would replace the electrical motor with a hydraulic motor. A variety of such tools has been developed over time for use in the oil industry, where the driving fluid can be the mud used to remove the cuttings from the drilling operation. These motors, in general, are larger than the electrical equivalent, and remain a relatively expensive option.

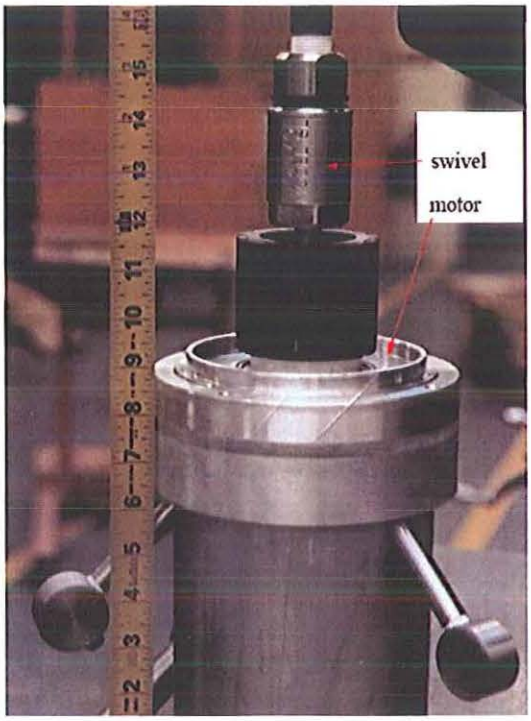

Figure 6.8. Hollow core electric motor with nozzles mounted on the drum

6.2.3 Self-Rotating Nozzle Assemblies. These nozzles use the reaction force exerted as the jet exits the nozzle, to provide the driving force that rotates the nozzle assembly around a swivel mount. This is possible if the nozzles are inclined outward from the axis of the lance and tangent to the circle of their offset position. The amount of power drawn from the jet is in the range of 75 watts if properly designed [Wolgamott, 1991]. Swivels are designed to contain some form of braking mechanism to increase jet residence times on the surface for effective operation, since otherwise the nozzle can spin at speeds of several thousand rpm, much faster than would be effective. These nozzles have been used for cleaning applications where the water jets operate without abrasive. In abrasive slurry applications, the flow of particles through the swivel has the potential to cause the bearings to seize. Although it is possible to use a special swivel design and

seal to stop abrasive from entering the bearings, such a design would need to be engineered from larger versions that have been used successfully at Missouri S&T. Because of the time constraints on the project, and the lengthy operation to retract the drill string if a swivel had to be replace, this option is currently considered time consuming and uneconomical.

6.3 NON ROTATING DISPERSED ABRASIVE SLURRY JET – (DASjet)

When drilling over long distances, it is important to be able to limit the possible sources of mechanical failure at the cutting face. If the nozzle assembly is rotating (as in the options just described) and then stops, then firstly there must be a means to sense this, then the drilling tool must be retracted from the hole in order to analyze and resolve the cause. An option to rotation is the use of dispersed abrasive slurry jet which spreads the abrasive over a large enough area ahead of the nozzle so that it drills a larger diameter hole. Traditionally, the intent of an abrasive slurry nozzle has been to focus the jet stream to achieve a consistent and deep cut. The requirement in drilling a hole is opposite that required when a jet is used in machining operations, since a large volume of rock has to be removed ahead of the nozzle assembly for the drill to advance while the aim in machining is to minimize the width of cut. This opposing intent, suggests that the shape of the abrasive laden jet should form an expanding cone when it is used for drilling.

6.3.1 Abrasive Flow Geometry. One method to increase the spread of a jet once it left the nozzle was to induce a swirl into the jet before it entered the focusing section of the nozzle. While it would be ideal to induce this swirl during jet acceleration, the abrasive nature of the jet accelerates wear of any device placed to induce this swirl as the

jet and particles move faster. For this reason it was decided to introduce a swirl inducing component just before the flow entered the inlet cone of the nozzle.

The initial configuration is shown in Figure 6.9. The component upstream of the nozzle induces a rotational component to the fluid velocity. The abrasive slurry exits the nozzle as an expanding conical shell, which distributes the eroding abrasive over the face of the rock ahead of the shell.

The nozzle was designated as a Dispersed Abrasive Slurry Jet (DASjet) with the producing nozzle consisting of three distinct component sections, a vaned inlet, a conical accelerating section and a straight section. For the first validation studies a short length of a metal drilling bit was modified, Figure 6.10, to generate a swirl in the fluid, located behind the orifice in a single-orifice nozzle holder. When a conventional ASJ system was used to feed this nozzle, it was found that the dispersed jet that resulted was able to drill a hole larger than the nozzle assembly, so that the drill could be advanced into the hole created. In these initial tests it was shown that the jet could drill through steel, concrete and rock, Figure 6.11.

While the first trials were moderately successful, and demonstrated the validity of the concept, For the tool to be effective it must drill a hole wide enough to allow nozzle passage, which required widening the jet cutting diameter without affecting the material removal rate and advance rate of the drill (which at this time as around 6 inches/minute, but with a hole diameter of less than an inch). The width of the jet is controlled by the angular velocity that is imparted to the particles as they exit the nozzle, and this is controlled by the vane angle of the insert. Material removal rates are a function of the abrasive velocity in the slurry stream at the point of impact.

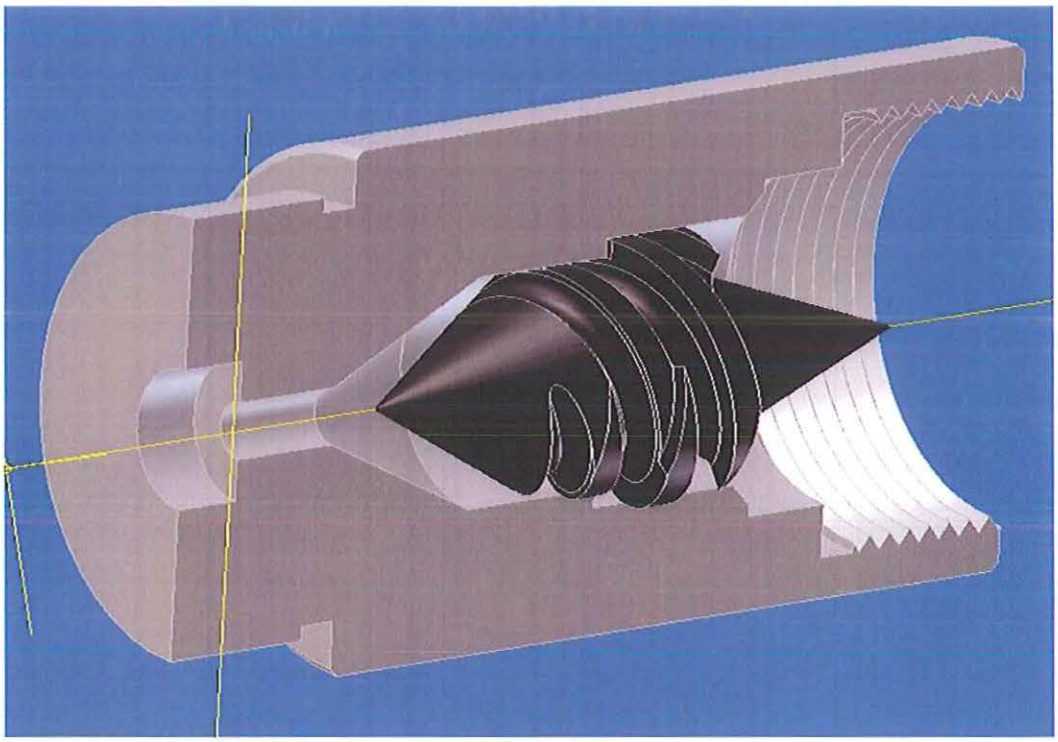

Figure 6.9. DASjet configuration with swirl inducing component

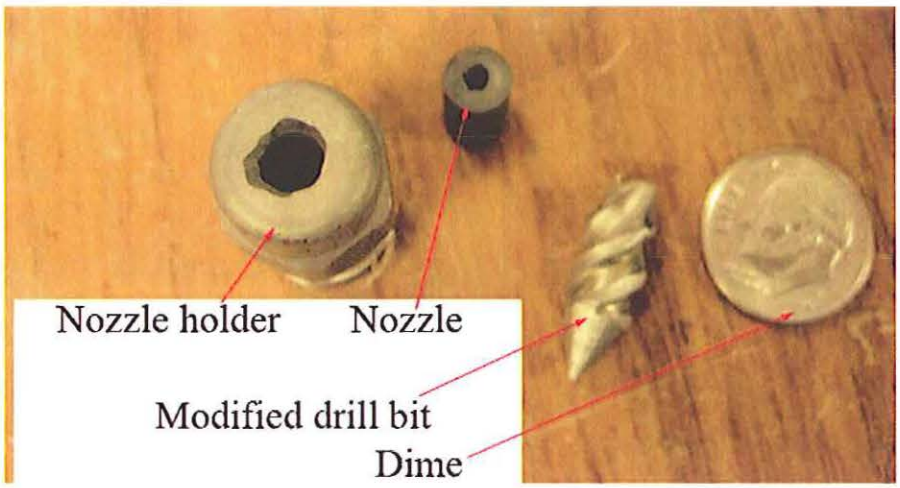

Figure 6.10. Components used to swirl the ASJ cutting stream

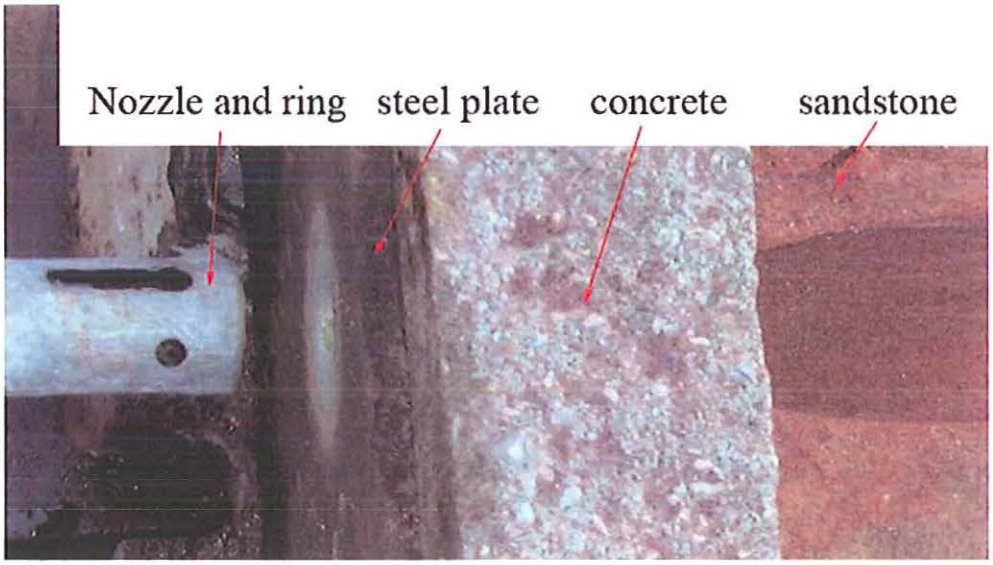

Figure 6.11. Hole drilled through steel, concrete and rock with the new jet

6.3.2 Influence of Abrasive Feed Rate. It is understood that the material removal rates increase with increase in abrasive concentration within the slurry stream. When drilling horizontally or vertically over very long distances the cuttings and used abrasives from the hole have to be removed in real time so that the drill can advance into the hole created. Abrasives flow rates of 0.453 kg/min, 0.9 kg/min and 1.36 kg/min were tested on a lime stone samples. Separate tests were run for 15, 30, 45 and 60 second durations and the material removal rates were calculated and plotted, Figure 6.12. Material removal rates at 0.9 kg/min and 1.36 kg/min are higher that 0.453 kg/min but rates at 1.36 are lower than 0.9kg/min. This suggests, for the particular combinations tested, that there is an optimal abrasive concentration within the values tested.

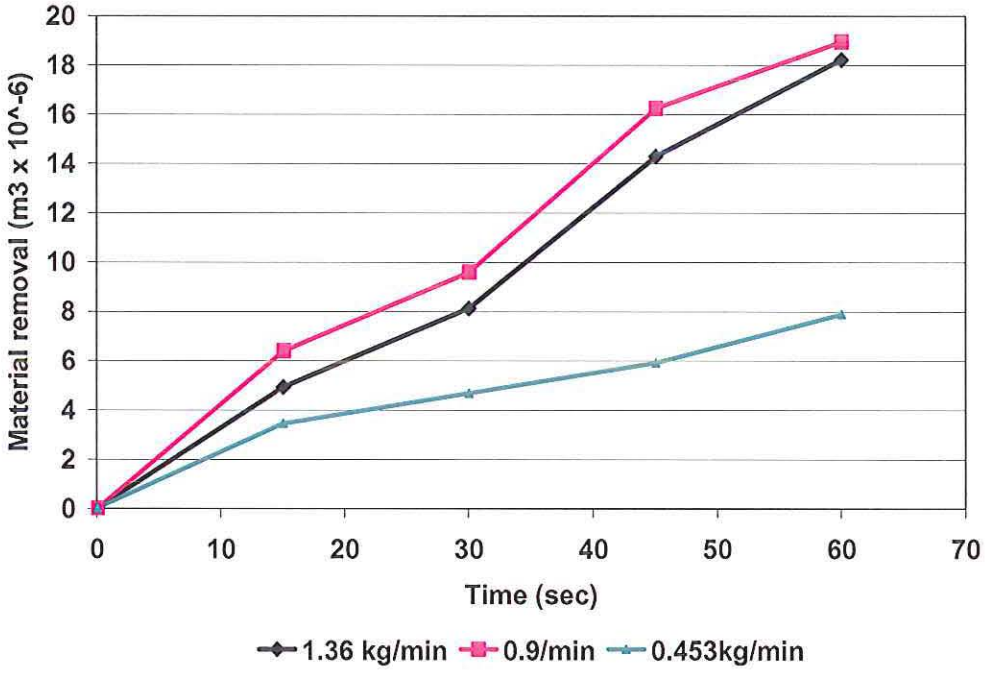

Figure 6.12. Influence of AFR on material removal

6.3.3 Influence of Vane Angle. The initial testing showed that this new concept is capable of drilling small diameter holes. To find immediate use, however, the drill must be capable of generating a well with a diameter as 50 mm (from discussions with Impact Technologies LLC, the principal funding source). The angle of the vanes inducing swirl upstream of the nozzle was identified as the parameter that would most strongly influence the hole diameter. It was initially anticipated that adding two blades in the feed section to the nozzle would be sufficient to adequately adjust the required swirling action, Figure 6.13.

Given the limitations of conventional coiled tubing, a new factorial test series was designed, with jet pressures of 21 MPa, 26 MPa and 35 MPa. The AFR range tested corresponded to the earlier tests using feeds of 0.453 kg/min, 0.9 kg/min and 1.36

kg/min. Vane angles of 45 degrees, 53 degrees and 60 degrees were used in the test matrix. Figure 6.14 shows a typical test sample showing the rock on which the tests were carried out. The dependant variable for these tests was to be the diameter of hole achieved. Further, when studies were made of the jet shape, as it flowed into a surrounding water jacket, it was seen that the resistance of the water was sufficient, in the outer edges of the jet, to absorb some of the power, cutting back on the cutting power, and thus the hole diameter that could be produced with that system. Figure 6.15 shows this phenomenon.

The results of these tests are presented in Table 6.1. From this data it is clear that a vane angle of 53 degree produced the largest diameter holes, 50 mm, the target value for this part of the program. The depth of the holes increased with the increase in AFR as expected, indicating an ability to increase the ROP. It was interesting to note that an increase in driving pressure did not give a sharp increase in either hole diameter or depth.

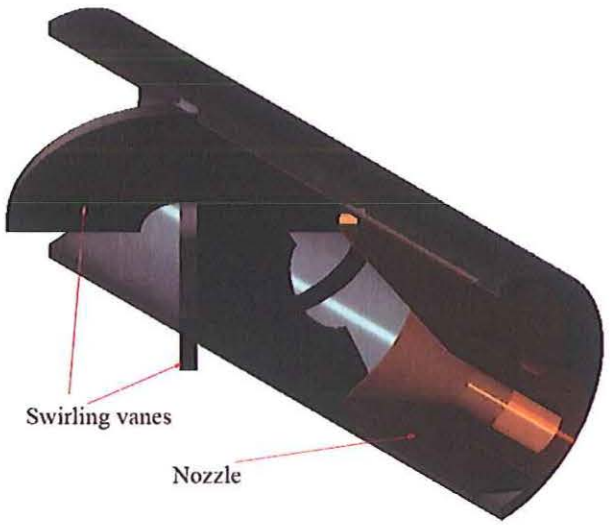

Figure 6.13. Test configuration to swirl the jet and test effect of vane angle

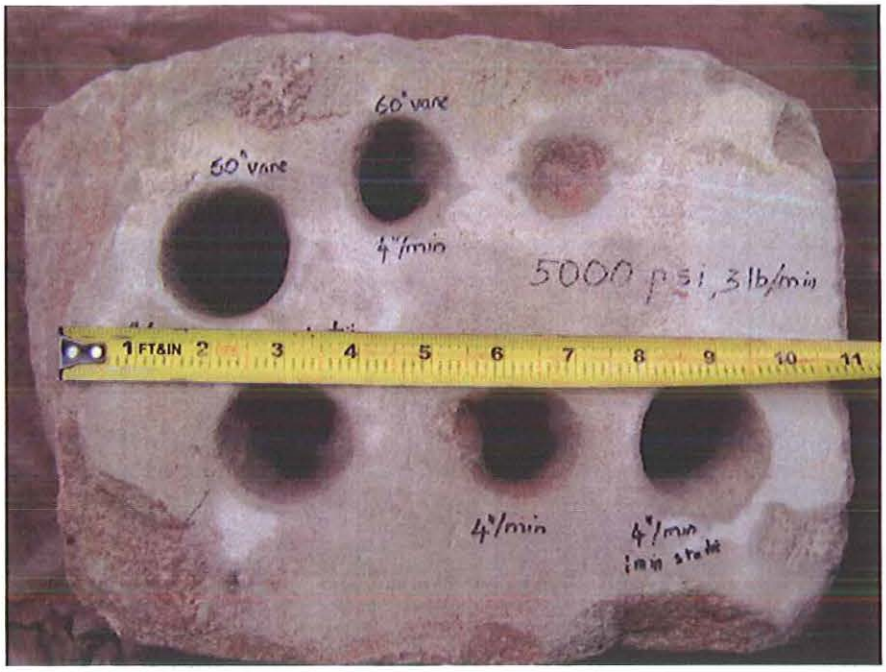

Figure 6.14. Testing influence of vane angle, AFR and pressure

Figure 6.15. Effect of water, abrasive and rock exiting the hole

Nozzle -1.1mm	45 deg vane					
Pressure (psi)	3000		4000		5000	
AFR (kg/min)	Hole diameter (mm)	Hole depth (mm)	Hole diameter (mm)	Hole depth (mm)	Hole diameter (mm)	Hole depth (mm)
0.453	25.4	25.4	31.75	25.4	28.575	28.575
0.9	31.75	31.75	34.925	34.925	31.75	34.925
1.36	31.75	38.1	34.925	50.8	28.575	44.45
Nozzle -1.1mm	53 deg vane					
AFR (kg/min)	Hole diameter (mm)	Hole depth (mm)	Hole diameter (mm)	Hole depth (mm)	Hole diameter (mm)	Hole depth (mm)
0.453	47.244	11.176	46.101	25.4	46.99	12.7
0.9	51.816	26.924	47.752	28.575	49.149	38.1
1.36	44.323	47.625	44.831	41.275	50.927	44.45
Nozzle -1.1mm	60 deg vane					
AFR (kg/min)	Hole diameter (mm)	Hole depth (mm)	Hole diameter (mm)	Hole depth (mm)	Hole diameter (mm)	Hole depth (mm)
0.453	36.957	22.225	38.354	38.1	44.704	38.1
0.9	36.449	50.8	40.64	57.15	41.529	53.975
1.36	43.307	57.15	43.18	69.85	36.068	82.55

Table 6.1. Test data for different vane angles, pressures and AFR

6.4 AIR SHROUDED DASjet

Drilling operations are typically performed with fluid inside the hole, which generates back pressure acting against the driving jet pressure. Since the drill will usually function in such conditions, it became important to assess the performance of the DASjet underwater. Initial tests showed that there was a significant reduction in the cutting range of the carrier jet and abrasive particles, particularly in the radial direction out from the axis of the jet, Figure 6.16.

Figure 6.16. The change in jet shape when the jet operates underwater

The advantage that the dispersed jet produced in having a less-concentrated stream, that was not interfered with by the material rebounding from the cut was greatly reduced when water surrounded the jet.

In order to determine the level of reduction in performance, tests were conducted with a 1.1 mm nozzle in air and underwater. The nozzle was traversed over a sample of dolomite at a standoff distance of 25.4 mm, and a speed of 400 mm/sec in each case. Two operating pressures 48MPa (Test 1) and 35MPa (Test 2) were evaluated.

The width of cut on the rock was measured as the dependant variable. Data from these tests are plotted in Figure 6.17. It can be seen that there is significant decrease of range in the radial direction when tests were run against back pressure.

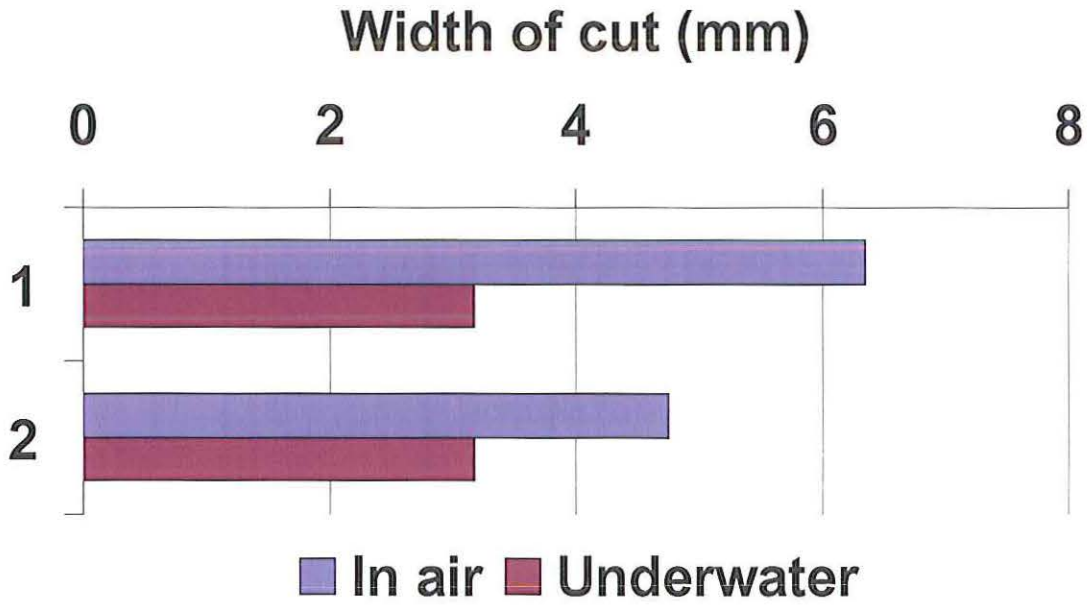

Figure 6.17. Effect of backpressure on cutting width

This reduction in diameter of cut was in the 25 – 30% range. There was a corresponding drop in the material removal rate with underwater cutting over air cutting. This reduced cutting power comes because the jet and particles must overcome the added resistance to the flow from the water.

One solution proposed to overcome this problem is shown in Figure 6.18. An air sheath was designed so that as the air exited from the nozzle it would shroud the dispersed abrasive slurry jet and remove the water from the jet path. This air sheath will surround the between the nozzle and the rock face, providing a low resistance path for the

jet. A solid gauging cone produces a guide to the flow path that would help direct the spent water and debris into the annular ring behind the nozzle, and thus out of the cutting range of the subsequent slug of water and abrasive on its way to the rock surface.

Note that the use of this cone had proved to be effective in static testing, in air, but in itself was not sufficient, when tested underwater, and when advancing the nozzle into the hole, to give a consistent improvement in performance, because of the water resistance to abrasive passage. However, the gain was sufficient to justify including the shape in the testing of air shroud. The components of this air shrouded DASjet thus become:

1. High-pressure abrasive slurry feed
2. Nozzle
3. Outer pipe to carry air forward
4. Air nozzle
5. Gauging cone

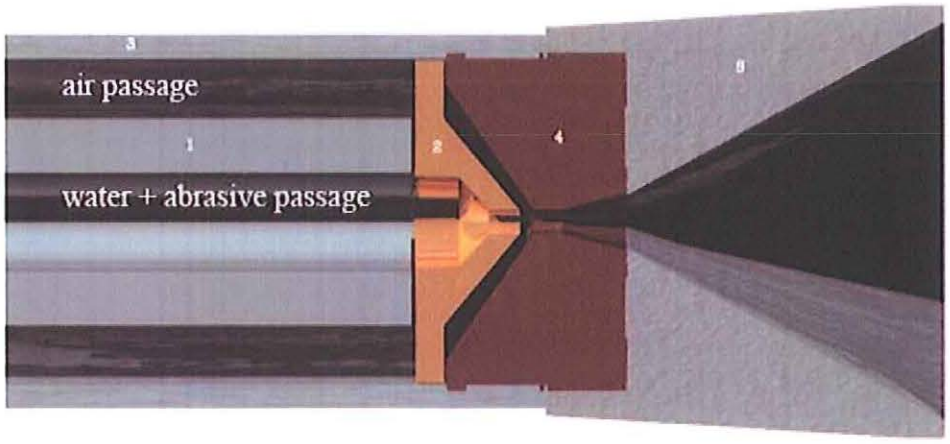

Figure 6.18. Air sheath design to surround the DASjet.

This nozzle design was machined and can be seen in Figure 6.19 with pressurized air for shrouding, though the leading edge had not been machined back (as shown in Figure 6.19 at the time that the photograph was taken). By this stage, the DASjet nozzle had transitioned from a straight defocused stream through a swirling jet to become an air shrouded swirling DASjet nozzle. A comparative study of the three nozzle configurations as they performed in air and underwater is therefore of merit. The three nozzles compared are

1. Nozzle
2. Nozzle + Spiral
3. Nozzle + Spiral + Air shroud

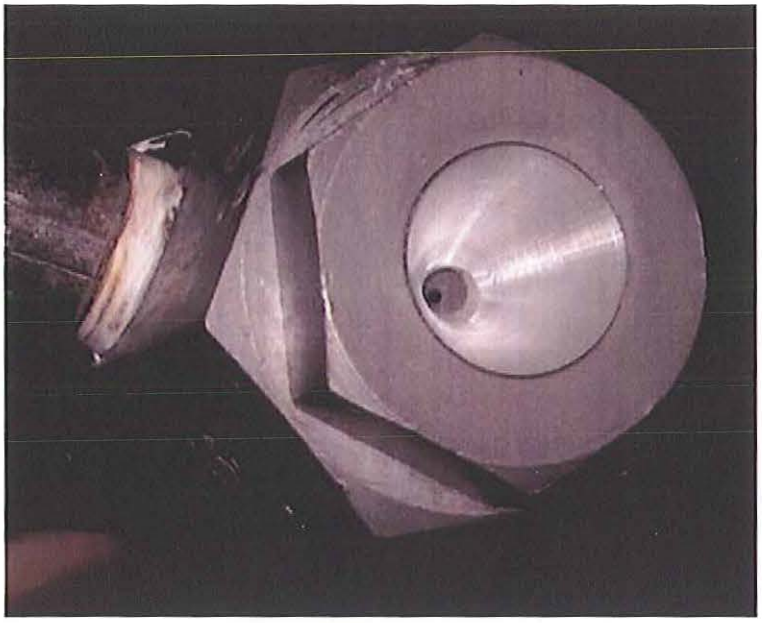

Figure 6.19. Initial nozzle assembly with gauging cone and air shroud

The tests were conducted on samples of dolomite and the comparison was made by traversing each jet at a standoff distance of 1 inch above the sample, and with the jet directed vertically downwards. The operating jet pressure for each nozzle was held constant at 48MPa and all nozzles were supplied with the same constant abrasive feed rate. The three nozzles were first tested in air and then under water. The width and depth of the slot that was created was measured. The diameter of the focusing section of the nozzle was 1.1 mm. The measurements obtained have been plotted in Figure 6.20 for width of cut and Figure 6.21 for depth of cut.

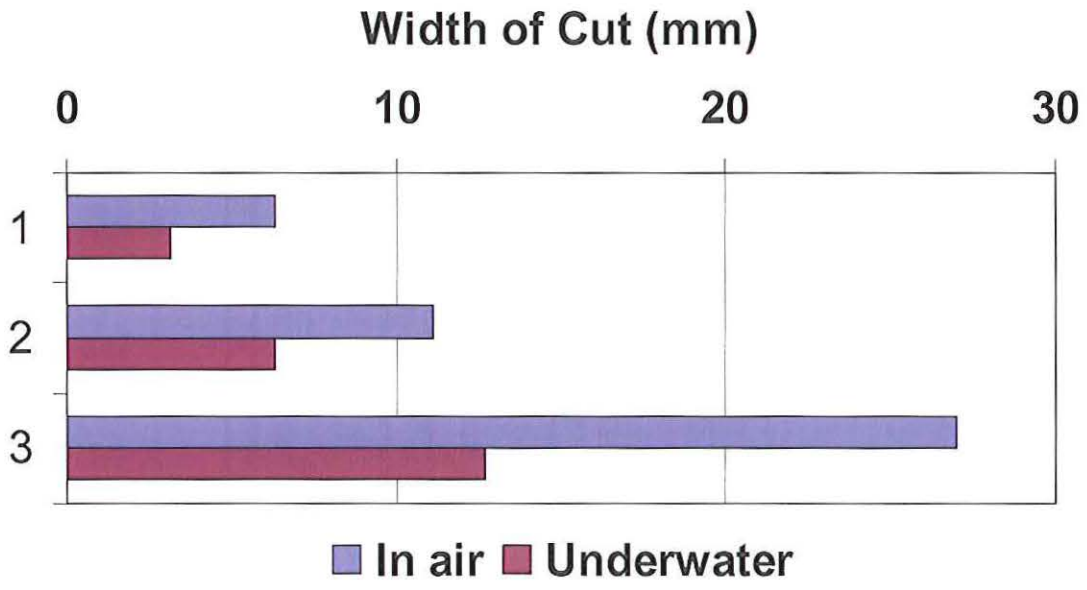

Figure 6.20. Width of cut for different nozzle configurations

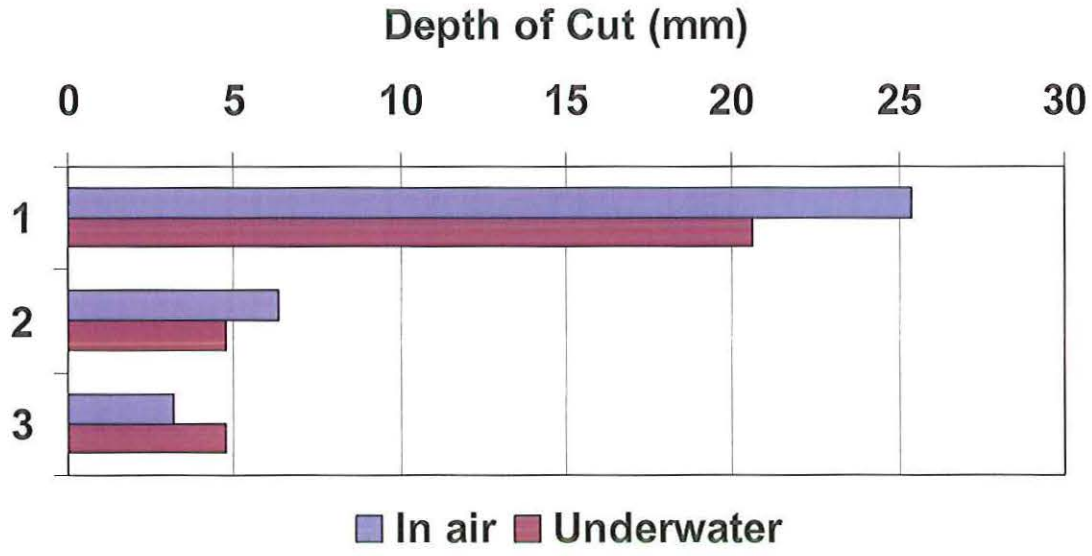

Figure 6.21. Depth of cut for different nozzle configurations

The data clearly shows that there is a decrease in cutting effectiveness of the jet underwater. It is interesting to note that configuration 3 had the widest and shallowest slot. Also this test with the addition of the air, seems to perform better underwater (for depth of cut) than in air. The width of cut increases from 1 to 3 and depth of cut decreases from 1 to 3. The results from these comparison tests indicate the effectiveness of the jet increases underwater when an air shroud is created to protect the jet. The next step in the evolution of the drill therefore is to create an air shroud around the jet without the aid of compressed air which would reduce the cost of drilling. It should be noted that a linear traversing cut such as this one does not obtain the full effect of water removal from ahead of the nozzle that would be achieved if the nozzle were advanced into the rock.

6.5 SUMMARY AND DISCUSSION

The DASjet drill concept for creating holes large enough for the drill assembly to enter without rotation has evolved from a swirling abrasive slurry jet to a air shrouded, swirling abrasive jet. The improvement in performance at each step has resulted in a final hole diameter of 50mm which was the target set at the beginning of the program. Jet pressures were shown not to have significant influence on the width of the hole achieved. Changing the vane angle was found to have most impact on the diameter, with an optimal value being found at 53 degrees. Abrasive feed rates above 0.9 kg/min were not justified, since there was no increase in hole diameter above this diameter, although the depth of cut did increase with increased abrasive concentration.

This tool coupled with coiled tubing technology has the potential to revolutionize drilling methods for small diameter holes. Low loads on tool will result in lighter drill strings and result in lower costs. The elimination of rotation of the drill string as well as the tool will reduce the risks of mechanical failure, since there are many less components prone to failure located downhole. This will result in considerable time and money savings. The next step in the evolution of the drill was to examine alternate ways of providing sufficient gas to the nozzle to clear the path to the rock face. In developing this step an alternate carrier fluid was investigated that provide the means, not only to replace water which decreases specific energy requirements but also to provide the driving power to remove the spent fluid rock and abrasive from ahead of the bit.

7. DRILLING WITH SUPERCRITICAL CO_2

Supercritical carbon dioxide ($SCCO_2$) has certain unique properties that can be usefully employed in drilling activities. Initial work where $SCCO_2$ was used for jet-assisted coiled tube drilling was reported to show the ability to increase rate of penetration (ROP) in drilling deep oil and gas wells, a place where rocks is often harder to drill with conventional drill bits [Kolle, 2000]. Such a gain is an attractive option when drilling small diameter holes because the hydraulic power that can be supplied through the fluid, is greater than the mechanical power that can be delivered to the bit from small diameter motors. Initial experiments indicate that $SCCO_2$ was able to cut hard shale, marble and granite at much lower operating pressures than would be required were water used as the drilling fluid. The ROP in Mancos shale with $SCCO_2$ was 3.5 times greater than with water [Kolle, 2000]. This initial test data identified $SCCO_2$ as an ideal candidate for replacing water as a carrier fluid in the DASjet drilling tool.

7.1 PROPERTIES OF SUPERCRITICAL CO_2

Any substance that is held in a condition that is above its critical temperature and pressure is considered to be in supercritical state. The critical point represents the highest pressure and temperature at which the fluid and vapor stage of a substance exist in equilibrium, Figure 7.1. Above this point the substance can only exists in a fluid state. Figure 7.2 is a phase diagram with triple point and critical points shown where carbon dioxide is that substance.

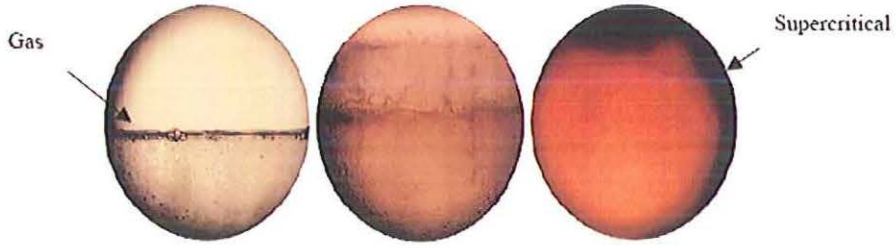

Figure 7.1. Phase change of CO_2 to supercritical state

[www.firstscience.com]

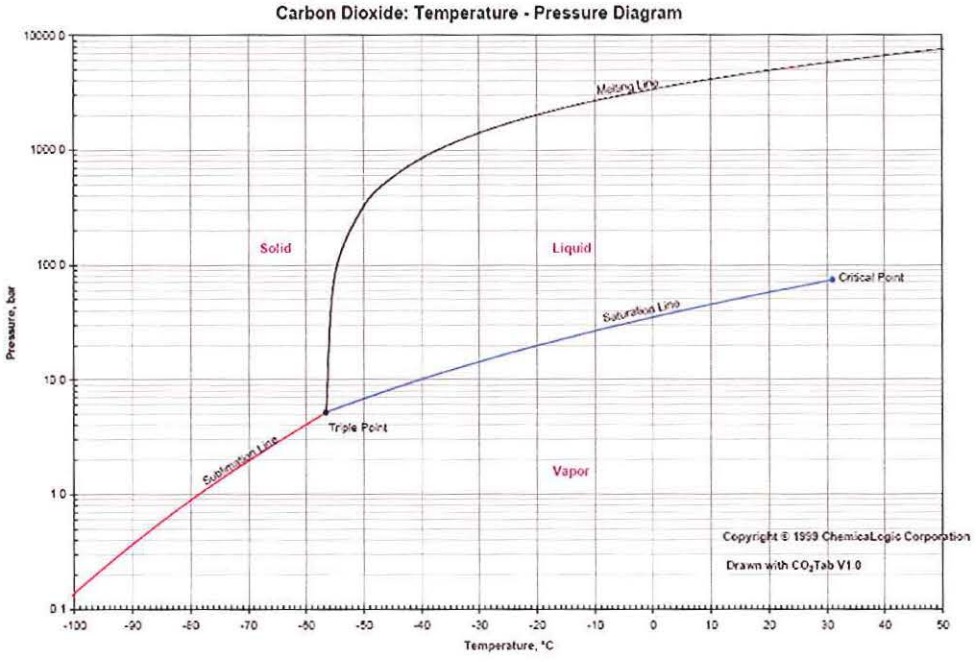

Figure 7.2. Carbon-dioxide phase diagram

[www.chemicalogic.com/co2tab/downloads.htm]

Liquid CO_2 is relatively incompressible and can be pumped with a positive displacement pump [Kolle, 2000]. Figure 7.3 shows the equation of state properties for CO_2 near the critical point. Jet erosion occurs when the cutting fluid from the jet penetrates between the grains of the target rock and propagates cracks that intersect and liberate material. Erosion rates are proportional to viscosity and density of the fluid [Kolle, 2000]. Figure 7.4 shows the variation of fluid viscosity with an increase in fluid pressure.

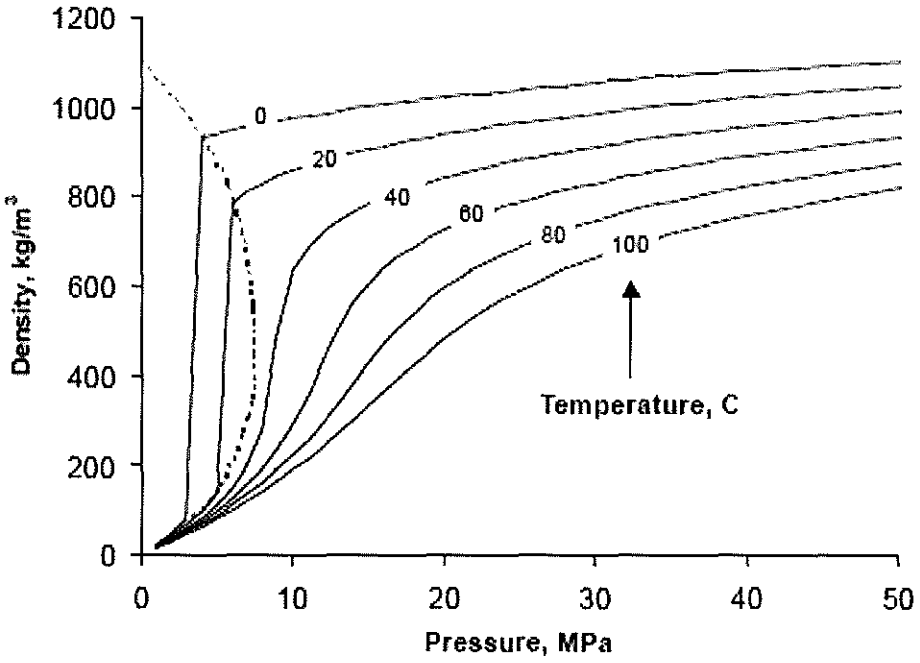

Figure 7.3. Equation of state data for CO_2 near critical point [Lemmon, 1998]

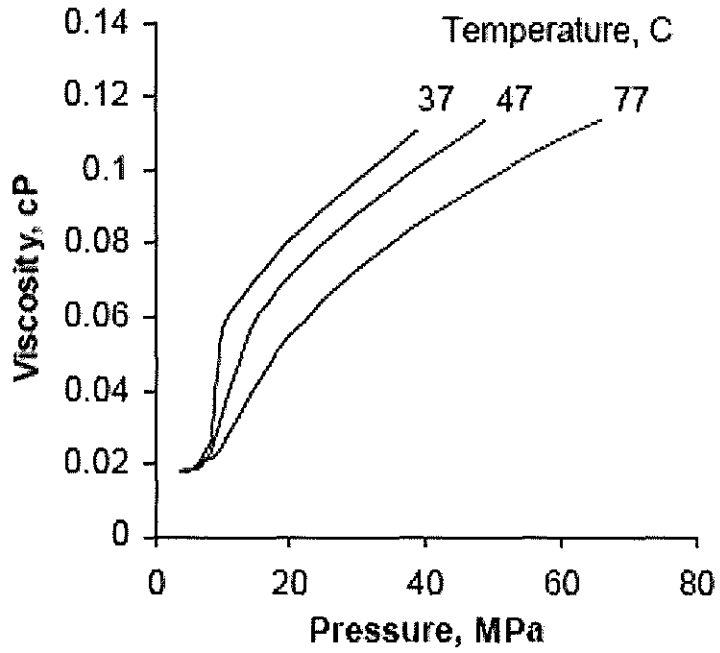

Figure 7.4. Viscosity of $SCCO_2$ [McHugh, 1994]

7.2 SUPERCRITICAL CARBON-DIOXIDE ABRASIVE CUTTING [SCAC]

Tests carried out with the DASjet with water as the carrier fluid demonstrated a limit to the ROP attainable, due to limits on the particle velocity achieved through energy transfer from the carrier fluid and the need to distribute the abrasive over the rock face ahead of the drill. The effects of these constraints are magnified when cutting underwater because of back pressure in the hole ahead of the bit reduces the effectiveness of both conditions. Adding an air shroud around the jet was shown to mitigate these constraints and to improve ROP underwater.

The function of the carrier fluid is to accelerate the abrasive particles to their maximum velocity which should be reached as they exit the nozzle orifice. Beyond this point the presence of the fluid becomes detrimental to the drilling process. This is

because down hole the fluid generates a back pressure in the hole due to the overlying column of fluid between the bit and the surface. If, however, the carrier medium was liquid at higher pressures but converted to a gas phase as it underwent the pressure drop across the nozzle, the back pressure due to the fluid column would drop to an insignificant value.

Supercritical CO_2 satisfies this criterion at operating pressures that are being considered for use with DASjet drilling. As the supercritical fluid exits the nozzle it will initially expand and vaporize as the confining pressure drops below the critical value. This change in state also increases the volume of the fluid, further accelerating the contained particles of abrasive. As the stream leaves the confinement of the nozzle throat the jet also expands laterally with gas expansion, so that the abrasive is distributed over a larger area on the surface of the underlying rock. Figure 7.5 shows the resulting post-supercritical CO_2 stream carrying the abrasive and cutting into Roubideaux sandstone.

Figure 7.5. Supercritical CO_2 jet carrying abrasive cutting into Roubideaux sandstone

The orifice diameter was 1.1 mm, and the test was carried out at a jet pressure of 21MPa. The hole diameter created was 22mm at a depth of 70mm in four seconds. (The test was carried out using the apparatus described below).

7.3 DESIGN OF EQUIPMENT AND EXPERIMENTAL PROCEDURE

A special chamber was developed to contain the supercritical carbon dioxide, Figure 7.6. For the actual test the CO_2 in this chamber had to be liquid, however, to facilitate testing, pellets of solid carbon dioxide were first placed in the cylinder, and a small amount of abrasive (8 oz) located in a feed section just behind the discharge nozzle. A mixing chamber was designed and inserted into the chamber, Figure 7.7 and Figure 7.8. The rest of cylinder was then filled with liquid carbon dioxide, prior to test. A high pressure pump was then connected to the upstream size of the floating piston.

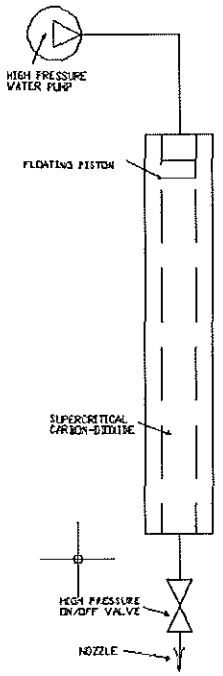

Figure 7.6. Component part diagram for SCAC

The system was left for eight hours to stabilize, and the pressurizing high pressure waterjet pump brought up to pressure. This pressure was transmitted through the cylinder piston to the liquid carbon-dioxide, and served to hold it at operating pressure during the time of discharge. The nozzle was then located over a target rock, and the high pressure valve (between the cylinder and the nozzle) opened wide enough so that the narrowest point in the flow channel was the converging section of the discharge nozzle.

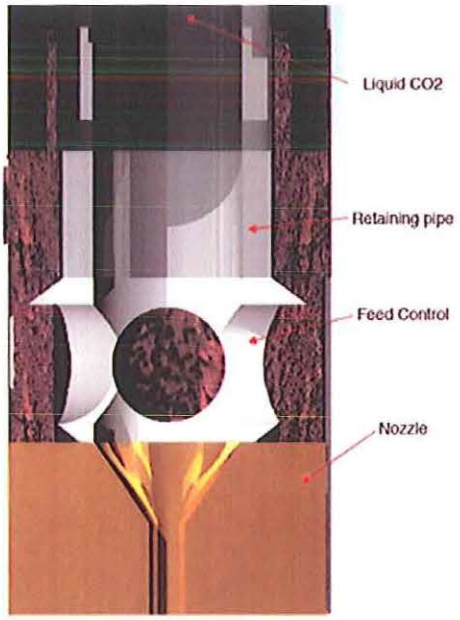

Figure 7.7. Design for abrasive injection into carbon-dioxide flow

In a typical test, the abrasive flow lasted on the order of 3 seconds, following which time the subsequent exhaustion of the cylinder produced no additional cutting. Tests with this system showed that the jet worked effectively to transfer energy to the abrasive particles, and that the holes could be drilled quite efficiently. This simple preliminary test equipment restricted any more extensive and comprehensive testing beyond that level.

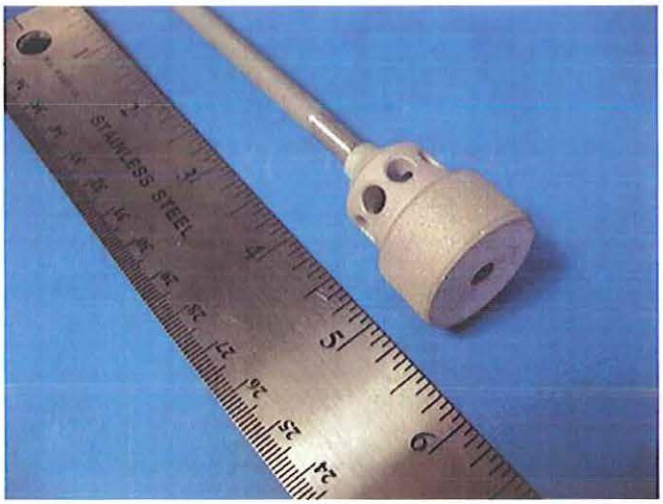

Figure 7.8. Constructed abrasive feed for carbon-dioxide cylinder

7.4 TESTING THE SCAC CONCEPT

The performance of Supercritical CO_2 as a replacement for water in DASjet needed to establish for different rock types. In order to evaluate this performance a special protocol was designed. The nozzle was locates so that the resulting jet would cut down the side of the sample of rock rather than through drilling through solid material. The abrasive laden jet could then be observed, as it was penetrating through the rock. An advantage of this process was that it allowed an assessment of the ROP during drilling. This would otherwise have been difficult, since the small quantity of abrasive in the cutting fluid meant that the actual length of time the jet was drilling was limited and not easy to assess from normal observation. However, by following the rebound of the jet as it sprayed out into the free space beside the bottom of the hole, it was possible to estimate at any given time, what the depth of the hole was. The tests were recorded using a standard digital camera that records images at a rate of 30 images per second (ips). Thus the inter-frame time was 0.033 seconds by noting the position of the lateral spray at

increments and scaling the distance against this record of time, point ROP's down the hole could be established. Figure 7.9 show a test with the jet rebounding at the bottom of the instantaneous hole at two different points in time. The depth of the hole is measured at the end of the cut and scaled, relative to the hole shown in the video. The hole depth could then be determined at various points during drilling, and the number of frames that it took to reach that position counted. This provided a measure therefore of distance traveled and time, from which the ROP at different points along the hole length could be calculated. This information also allowed calculation of the specific energy of drilling with SCAC through the various types of rock.

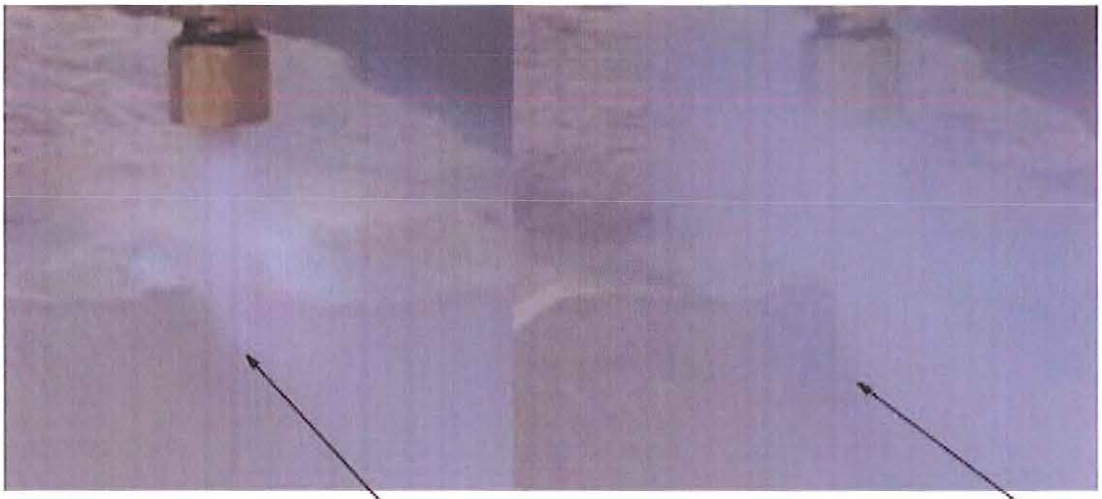

Figure 7.9. Two frames of video of an SCAC jet drilling in limestone

Observation of the video record showed that the ROP was not consistent through out any test. This was a result of the inadequate abrasive mixing process that was used inside the pressure chamber. The rate of penetration was measured at several intervals during each test, using this video technique. The data compiled in Table 7.1 shows the

maximum and minimum ROP as well as the specific energy for each test. Specific energy is defined as the energy required to remove a unit volume of material.

The properties of the rock samples on which SCAC was tested

- Roubideaux sandstone- UCS of 3,700 psi.
- Joachim limestone- UCS of 2,000 psi.
- Indiana limestone (Bedford limestone) -UCS in the range from 8-10,000 psi.
- Missouri dolomite –UCS 17,000 to 19,000 psi UCS.
- Basalt -- UCS values above 30,000 psi are reported.

7.5 THE EFFECT OF NOZZLE DESIGN ON HOLE GEOMETRY

The initial tests in Section 7.4 were carried out using a conventional waterjet converging nozzle with a straight throat and no secondary expansion cone beyond the narrow throat. The jet thus was free to expand out under the ambient conditions and cut an unconstrained hole in each rock. With this design the fluid, and thereby abrasive, velocity is strongly controlled by nozzle design. To evaluate how much of a role this factor played, four nozzles with a converging portion connected at the neck to an expanding channel were designed.

The aim of these nozzles was to control the expansion of the supercritical fluid within the expansion section of the nozzle and thereby control the spread of the abrasives in the SCAC. The nozzles were designed with exit half angles of 2.5, 5 and 7.5 degrees, Figure 7.10. The nozzles were tested on samples of Joachim limestone, and Missouri dolomite and the results showed that there was a controllable increase in hole depth and diameter with an increase in the divergent cone angle.

Table 7.1. Performance of SCAC in different rocks

Rock	Jet	Nozzle	ROP	ROP	Specific Energy		Hole
	Pressure (psi)	Dia. (in)	Max (ft/min)	Min (ft/min)	Minimum (j/cc)	Max (j/cc)	Dia. (in)
Roubideaux	3,000	0.044	11.2	2.1	150	810	0.875
Roubideaux	2,500	0.044	17		75		1.00
Roubideaux	3,500	0.044	15.9	3.8	133	560	1.00
Jouchim lls	4,500	0.044	8.9	4.4	350	701	1.00
Joachim lls	4,000	0.039	8.9	8.9	360	360	0.80
Joachim lls	4,000	0.039	11.8	2.5	334	1560	0.71
Joachim lls	4,000	0.039	8.9	1.4	641	4090	0.60
Indiana lls	4,000	0.039	8.9	1.7	360	1890	0.80
Indiana lls	4,000	0.039	9.8	3.9	207	519	1.00
Indiana lls	4,000	0.039	8.9	0.9	230	2,250	1.00
Missouri do	4,000	0.039	14.8	2.1	216	1,488	0.80
Missouri do	4,000	0.039	14.8	3.2	216	992	0.80
Joachim lls	4,000	0.039	15.7	2.0	560	4,510	0.50
Missouri do	4,000	0.039	8.9	2.0	736	2,210	0.55
Missouri do	4,000	0.039	7.4	3.0	277	692	1.00
Joachim lls	4,000	0.039	13.8	3.9	410	1,443	0.6
Missouri do	4,000	0.039	17.7	2.0	721	6,490	0.40
Missouri do	4,000	0.039	9.8	5.9	320	540	0.80
Basalt	4,000	0.039	3	-	3,000	-	0.5

Figure 7.11 shows the comparison between a test run at 2.5 degrees on the left and 7.5 degrees on the right. This illustrative result demonstrates the potential for of changing the drilled diameter of the hole, and ROP, by changing nozzle geometry.

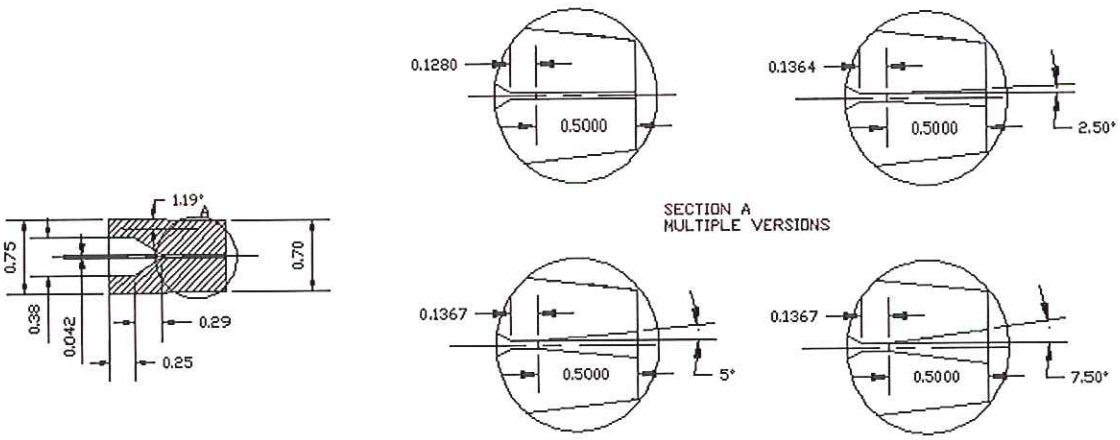

Figure 7.10. Converging diverging nozzle geometries for SCAC

Figure 7.11. Hole geometries created with 2.5 degree and 7.5 degree nozzles

7.6 DISCUSSION

The evolution of a drill that creates a hole, large enough for the following drill assembly to enter, without the need for rotation, has been documented in previous sections. The potential of a supercritical CO2 system to provide such a hole was demonstrated in the tests described in this section. The limited amount of flow available with the carbon dioxide system did not allow a full definition of the performance achievable with the system. Rather it is necessary to assume that some of the results obtained with continuous flow from water driven dispersed jet will yield an equivalent result when run with carbon dioxide as the cutting fluid. The data presented, however, has shown that the carbon dioxide system is much superior in cutting ability to the water-based system, and thus the performance parameters that are designated in recommending the design should be more than ample for the need.

8. CONCLUSIONS AND RECOMMENDATIONS

This research work has concentrated on the development of a non-rotating Dispersed-Abrasive-Slurry jet (DASjet) drilling tool for use in creating long holes of small diameter. The task was split into three basic parts

1. Design of Equipment
2. Optimization of DASjet parameters
3. Theoretical and experimental understanding of the process

The equipment that had to be created needed to resolve several issues that could be separated to relate to the two components of the DASjet drill. The first component is the abrasive slurry jet feed system, while the second is the abrasive delivery and the design of the DASjet nozzle.

8.1. ABRASIVE FEED SYSTEM

Two requirements were placed on the feed system, the first that it provide for an easy and effective start/stop for intermittent cutting operations and, the second that there be a steady, controllable and stable abrasive feed. These requirements led to the design of a new system that eliminated the drawbacks of existing designs. The abrasive mixing and control circuitry were redesigned to provide flow through the chamber from the bottom to the top, with abrasive outlet from the top, with fluid control through valves that only operated on clean water components of the system. This eliminated high-wear components from the system.

By controlling abrasive output, using a separate valve that controlled the replacement volume of water fed into the supply tank, it was possible to eliminate the dependence in abrasive concentration on supply pressure that had been a weakness of previous designs. The validity and stability in performance of this new design was proven experimentally, initially using existing measurement techniques. A new experimental technique was introduced that increased both the accuracy and reliability of this testing.

The new abrasive injection system has been adopted and has been operational in the HPWL at Missouri S&T for the past two years. Operational use within that time frame has further validated the reliability of the new system that was evolved.

- **Recommendation 1.** The next step in automating the new ASJ feed system design should be to create a real time concentration measurement tool. Previous attempts have been unsuccessful in this regard and further research is still required to provide a simple, reliable, inexpensive, and easy to use procedure. This tool combined with computer controlled valving on the system will simplify the operation of the feed system.

  The real time concentration tool must measure the concentration of abrasive in the stream that exits the nozzle. Depending on the abrasive concentration setting the computer controlled valving must adjust the main flow rate and bypass flow rates to achieve this value. With pressure inputs from the pumping source it will be possible to adjust the AFR values corresponding to optimal concentration for different pressures. This entire process can be controlled by a computer with minimal manual input.

8.2. NOZZLE DESIGN

The requirement that the DASjet nozzle should meet was to demonstrate the capability of drilling holes of at least two-inches in diameter through rock without rotating the nozzle. This required evolution of a section in the feed line that would spin the fluid before it entered the focusing section of the nozzle. Such a design was built and tested. In the course of this test program it was found, for the design recommended, that a change in jet pressure would not influence the hole diameter but rather affected the rate of penetration and therefore higher pressures result in faster drill operation. Given the need for a hole of relatively constant diameter, this is advantageous.

A modification to the original nozzle design was developed that would remove the constraint on diameter imposed as back pressure in the fluid contained within the drillhole increases. This modified design included means to form an air shroud around the jet as it exited into the fluid-filled borehole. The resulting air stream had sufficient power to displace the fluid from the path of the cutting jet, so that the abrasive particles were able to reach the rock face with sufficient energy that they could cut the rock, thus the shroud significantly improved performance by maintaining the desired hole diameter against the presence of fluid in the hole. Because the air was delivered at a lower pressure than that of the fluid in the cutting jet, results showed that the air shrouded jet, while yielding wider cuts both in air and underwater, caused a drop in the depth of cut achieved. Since it is critical to maintain hole diameter, this loss in performance was initially considered acceptable.

Adding an air shroud to the simple flow path of a coiled tube system, with its single conduit to the nozzle, would add complexity to the drill. Thus, the study expanded

to consider alternate methods of supplying a gas to the system, beyond the nozzle orifice. The solution derived was to change the cutting fluid from water to liquefied and thus supercritical, carbon dioxide (CO_2). This change created the possibility of achieving an even greater cutting potential than was possible with the use of water alone as the ASJ fluid. This is because the drop in pressure across the orifice of the nozzle not only accelerated the fluid (and thereby also abrasive) to a higher velocity, but the concurrent expansion of the CO_2 as it transformed into a gas added additional velocity to the fluid stream, and a consequent increase in velocity and momentum were added to the abrasive. In order to test this new concept it was not practical to develop a complete circuit that would allow continuous CO_2 delivery. Instead a simple test apparatus was constructed that allowed a very short period (< 10 seconds) of abrasive delivery in a CO_2 stream. Results from the tests with this equipment validated this concept and concurrently allowed estimations of the ROP that such a system might produce. These rates were considerably higher than the initial target of 6 inches/minute, and ranged to values that were more than ten times this fast. Because the energy stored in the supercritical phase of the fluid is released with the drop in pressure there is a significant decrease in the apparent specific energy required for material removal which the system shows.

- **Recommendation 2.** The limited amount of flow available with the carbon dioxide system used in these preliminary experiments meant that it was necessary to assume that some of the results obtained with continuous flow from water driven dispersed jet could be repeated with carbon dioxide as the cutting fluid. The data presented, however, showed that the carbon dioxide system gave a much superior cutting performance than the equivalent water-based system.

The results from these preliminary tests should be extended to greater pressures and flow volumes. Tests should be carried out with a continuous delivery system, rather than the very short duration tests that were the upper limit of possible experimentation in this work.

- **Recommendation 3**. In particular, the pressure should be increased so that, at the point supercritical CO_2 accelerates the abrasive, the fluid travels above sonic speeds at the throat of a converging diverging nozzle. Once this is achieved, then the diverging cone of the nozzle must be also modified to ensure that this supersonic flow persists through the cone. Under such circumstances, the vapor will continue to expand and accelerate over the cone, adding additional energy to the particles, and further improving both the ROP and the efficiency of the cutting process. This should to the basis of the next set of tests with this technology.

8.3. THEORETICAL UNDERPINNING TO THE WORK

The theoretical modeling of abrasive slurry jets has not, historically, been greatly developed, partly because of the perceived limitations in commercial application of this new tool, imposed by the earlier feed system designs that have been used. The improvements that have been made in the system with this work make it significantly more likely that the technology will now find further commercial use. During testing with this new MS&T abrasive feed system, the importance that abrasive concentration played in the cutting performance was noted. Experimental work in the field to this point has concentrated on the influence of AFR on the abrasive cutting power of the jet. While this controls the abrasive concentration, it is, in fact, a different parameter. Previous models

were analyzed and found to be unable to properly describe the role that concentration of abrasive plays in the cutting capability of the ASJ. An existing model, was therefore, suitably modified to recognize that it is concentration, not AFR, that is the valid parameter and the model results have been presented. A term has also been introduced into the model to standardize the quality of the nozzle performance. Previous experimental work has failed to recognize any influence that different characteristics of the nozzle might impose on the performance of the system, other than the flow change incurred with a change in orifice diameter.

The results of the model study revealed not only that abrasive concentration in the stream is a superior predictor of performance compared with AFR, but also showed that for any particular nozzle, that the optimal concentration was constant over a range of jet pressures. Because this optimal value varied with nozzle quality, (as evident by changes in the transfer efficiency of moving energy from the fluid to abrasive particles) the use of a nozzle design coefficient was validated.

- **Recommendation 4**. The factors that control the value to be assigned to the nozzle design coefficient should be established.
- **Recommendation 5.** At present, the model assumes that the abrasive particles retain their shape and size as they move through the process. It has been found, experimentally, that this is not the case. Accordingly the model should be modified to include the energy lost from comminution of abrasive particles through the acceleration process. This is a function of the pressure, nozzle

diameter and concentration of abrasives in the slurry. Experiments should also be designed to determine this relation and to provide results that can then guide the theoretical development that includes this in the model.

APPENDIX A.

OPTIMAL CONCENTRATION CALCULATION FOR ASJ

OPTIMAL CONCENTRATION CALCULATION FOR ASJ

High velocity Abrasive Slurry Jets (ASJ) is as a result of a premixed slurry forced through a nozzle by high pressures. Previous works by Hashish (), Jiang () have relied on energy based modeling of the abrasive power of an ASJ. It can be expressed as

$$P_a = \frac{1}{2} \cdot \dot{M}_a \cdot v^2 \tag{1}$$

where $\dot{M}_a$ is the mass flow rate of abrasive out of a nozzle and v is the velocity of abrasive particles exiting the nozzle. The velocity of the exiting abrasive particles can be expressed in terms of the pressure P and density ρ_{mix} of abrasive suspension.

$$v = \mu_m \cdot \sqrt{\frac{2P}{\rho_{mix}}} \tag{2}$$

The density ρ_{mix} defined in terms of R, the loading ratio in the slurry

$$\rho_{mix} = \frac{\rho_a (1+R)}{\frac{\rho_a}{\rho_w} + R} \tag{3}$$

The loading ratio R can be expressed in terms of the concentration by weight C as

$$R = \frac{\dot{M}_a}{\dot{M}_w} = \frac{C}{1-C} \tag{4}$$

where

$$C = \frac{\dot{M}_A}{\dot{M}_A + \dot{M}_w} \tag{5}$$

$$\rho_{mix} = \frac{\rho_a\left(1+\frac{C}{1-C}\right)}{\frac{\rho_a}{\rho_w}+\frac{C}{1-C}} \tag{6}$$

The mass flow rate $\dot{M}_a$ can be expressed as

$$\dot{M}_a = \frac{\pi}{4}\cdot D^2 \cdot \sqrt{2P\rho_{miz}} \cdot \frac{C}{1+C} \tag{7}$$

where D is the nozzle diameter. Substituting (2) and (6) in (1) we get the abrasive power of the ASJ as

$$P_a = \mu_m \cdot \frac{\pi}{4}\cdot D^2 \cdot P^{1.5} \cdot \sqrt{2} \cdot \sqrt{\frac{\frac{\rho_a}{\rho_w}+\frac{C}{1-C}}{\rho_a\left(1+\frac{C}{1-C}\right)}}\frac{C}{1+C} \tag{8}$$

Differentiating (8) with respect to concentration C it is possible to find the optimal concentration when the abrasive power of an ASJ is maximum.

$$\frac{\partial P_a}{\partial C} = \frac{\pi \cdot D^2 \cdot \mu_m^2 \cdot \sqrt{2} \cdot P^{3/2}}{(1+C) \cdot \sqrt{\dfrac{\rho_a\left(1+\dfrac{C}{1-C}\right)}{\dfrac{\rho_a}{\rho_w}+\dfrac{C}{1-C}}}} \cdot \left[\frac{1}{4} - \frac{C}{4\cdot(1-C)} - \frac{C}{8} \cdot \left\{ \frac{\dfrac{\rho_a\left(\dfrac{1}{1-C}+\dfrac{C}{(1-C)^2}\right)}{\dfrac{\rho_a}{\rho_w}+\dfrac{C}{1-C}} - \dfrac{\rho_p \cdot \left(1+\dfrac{C}{1-C}\right)\cdot\left(\dfrac{1}{1-C}+\dfrac{C}{(1-C)^2}\right)}{\left(\dfrac{\rho_a}{\rho_w}+\dfrac{C}{1-C}\right)^2}}{\cdot\left\{\dfrac{\rho_a\left(1+\dfrac{C}{1-C}\right)}{\dfrac{\rho_a}{\rho_w}+\dfrac{C}{1-C}}\right\}} \right\} \right] = 0 \quad (9)$$

The first term in (9) cannot be equal to zero, equating the second to zero we get

$$\left[\frac{1}{4} - \frac{C}{4\cdot(1+C)} - \frac{C}{8} \cdot \left\{ \frac{\dfrac{\rho_a\left(\dfrac{1}{1-C}+\dfrac{C}{(1-C)^2}\right)}{\dfrac{\rho_a}{\rho_w}+\dfrac{C}{1-C}} - \dfrac{\rho_p \cdot \left(1+\dfrac{C}{1-C}\right)\cdot\left(\dfrac{1}{1-C}+\dfrac{C}{(1-C)^2}\right)}{\left(\dfrac{\rho_a}{\rho_w}+\dfrac{C}{1-C}\right)^2}}{\cdot\left\{\dfrac{\rho_a\left(1+\dfrac{C}{1-C}\right)}{\dfrac{\rho_a}{\rho_w}+\dfrac{C}{1-C}}\right\}} \right\} \right] = 0 \quad (10)$$

Simplifying further we get

$$\left[\frac{1}{4\cdot(1+C)}-\frac{C}{8}\cdot\left(\frac{1}{1-C}+\frac{C}{(1-C)^2}\right)\left\{\frac{\dfrac{\rho_a}{1}-\dfrac{\rho_a\cdot\left(1+\dfrac{C}{1-C}\right)}{\left(\dfrac{\rho_a}{\rho_w}+\dfrac{C}{1-C}\right)}}{\cdot\dfrac{\rho_a\left(1+\dfrac{C}{1-C}\right)}{1}}\right\}\right]=0 \qquad (11)$$

$$\left[\frac{1}{4\cdot(1+C)}-\frac{C}{8}\cdot\left(\frac{1}{1-C}+\frac{C}{(1-C)^2}\right)\left\{\frac{\dfrac{\rho_a\cdot\left(\dfrac{\rho_a}{\rho_w}+\dfrac{C}{1-C}\right)-\rho_a\cdot\left(1+\dfrac{C}{1-C}\right)}{\left(\dfrac{\rho_a}{\rho_w}+\dfrac{C}{1-C}\right)}}{\cdot\dfrac{\rho_a\left(1+\dfrac{C}{1-C}\right)}{1}}\right\}\right]=0 \qquad (12)$$

$$\left[\frac{1}{4\cdot(1+C)}-\frac{C}{8}\cdot\left(\frac{1}{1-C}+\frac{C}{(1-C)^2}\right)\left\{\frac{\left(\dfrac{\rho_a^2}{\rho_w}+\dfrac{\rho_a\cdot C}{1-C}\right)-\left(\rho_a+\dfrac{\rho_a\cdot C}{1-C}\right)}{\left(\dfrac{\rho_a}{\rho_w}+\dfrac{C}{1-C}\right)\cdot\rho_a\left(1+\dfrac{C}{1-C}\right)}{1}\right\}\right]=0 \qquad (13)$$

$$\left[\frac{1}{4\cdot(1+C)}-\frac{C}{8}\cdot\left(\frac{1}{1-C}+\frac{C}{(1-C)^2}\right)\left\{\frac{\left(\frac{\rho_a^2}{\rho_w}\right)-(\rho_a)}{\left(\frac{\rho_a}{\rho_w}+\frac{C}{1-C}\right)\cdot\rho_a\left(1+\frac{C}{1-C}\right)}\right\}\right]=0 \qquad (14)$$

$$\left[\frac{1}{4\cdot(1+C)}-\frac{C}{8}\cdot\left(\frac{1}{1-C}+\frac{C}{(1-C)^2}\right)\left\{\frac{\rho_a\cdot\left(\frac{\rho_a}{\rho_w}-1\right)}{\left(\frac{\rho_a}{\rho_w}+\frac{C}{1-C}\right)\cdot\rho_a\left(1+\frac{C}{1-C}\right)}\right\}\right]=0 \qquad (15)$$

$$\left[\frac{1}{4\cdot(1+C)}-\frac{C}{8}\cdot\left(\frac{1}{1-C}+\frac{C}{(1-C)^2}\right)\left\{\frac{\left(\frac{\rho_a}{\rho_w}-1\right)}{\left(\frac{\rho_a}{\rho_w}+\frac{C}{1-C}\right)\cdot\left(1+\frac{C}{1-C}\right)}\right\}\right]=0 \qquad (16)$$

At this stage the abrasive used is assumed to be granet which has a specific gravity of 4.

Substituting in (16) we get

$$\left[\frac{1}{4\cdot(1+C)}-\frac{C}{8}\cdot\left(\frac{1-C+C}{(1-C)^2}\right)\left\{\frac{(4-1)}{\left(4+\frac{C}{1-C}\right)\cdot\left(1+\frac{C}{1-C}\right)}\right\}\right]=0 \qquad (17)$$

$$\left[\frac{1}{4\cdot(1+C)}-\frac{C}{8}\cdot\left(\frac{1}{(1-C)^2}\right)\left\{\frac{(3)}{\left(\frac{4-4C+C}{1-C}\right)\cdot\left(\frac{1}{1-C}\right)}\right\}\right]=0 \tag{18}$$

$$\left[\frac{1}{4\cdot(1+C)}-\frac{C}{8}\cdot\left(\frac{1}{(1-C)^2}\right)\left\{\frac{(3)\cdot(1-C)^2}{\left(\frac{4-4C+C}{1}\right)\cdot}\right\}\right]=0 \tag{19}$$

$$\left[\frac{1}{4\cdot(1+C)}-\frac{C}{8}\cdot\left\{\frac{(3)}{4-4C+C}\right\}\right]=0 \tag{20}$$

$$\frac{C}{8}\cdot\left\{\frac{(3)}{4-4C+C}\right\}=\frac{1}{4\cdot(1+C)} \tag{21}$$

$$\frac{1}{2}\cdot\left\{\frac{C\cdot 3}{4-3C}\right\}=\frac{1}{(1+C)} \tag{22}$$

$$3C\cdot(1+C)=2\cdot(4-3C) \tag{23}$$

$$3C+3C^2=8-6C \tag{24}$$

$$3C^2+9C-8=0 \tag{25}$$

Solving for C we get values of -3.71 and 0.71. Since the value of concentration cannot be greater than 1 or negative the optimal concentration is 71%.

Nomenclature

a_3 - Constant

C - Mass concentration of abrasive

D - Nozzle diameter

E_i - Input energy

$\dot{M}_A$ - Abrasive mass flow rate

$\dot{M}_w$ - Water mass flow rate

P - Pressure

Q - Total flow rate

R - Loading ratio

v - Abrasive slurry velocity

η_t -Momentum transfer coefficient

μ_m - Momentum transfer parameter

ρ_a - Density of abrasive

ρ_w - Density of water

APPENDIX B.

OPTIMAL CONCENTRATION CALCULATION FOR AWJ

OPTIMAL CONCENTRATION FOR AWJ

Using Bernoulli's law we get

$$P_{at} + \frac{\rho_w}{2} \cdot V_{0th}^2 + \rho_w \cdot g \cdot h_1 = P + \frac{\rho_{w1}}{2} \cdot V^2 + \rho_{w1} \cdot g \cdot h_2 \tag{1}$$

Since $P_{at} << P$ and $V_{0th} >> V_1$ and $h_1 = h_2$ the above equation reduces to

$$V_{0th} = \sqrt{\frac{2P}{\rho_w}} \tag{2}$$

Considering momentum losses the above equation can be written as

$$V_0 = \mu \cdot \sqrt{\frac{2P}{\rho_w}} \tag{3}$$

Design of the mixing tube in a AWJ cutting head transfers the energy of the waterjet from the jewel to the abrasive particles which are introduced into the mixing chamber. There is considerable air that acts as a carrier so a significant part of the energy goes into accelerating this volume of air too but the corresponding mass is negligible. Using the concept of balancing the impulse in the mixing chamber we get

$$m_A \cdot V_{P0} + m_w \cdot V_0 + m_L \cdot V_L = (m_A + m_w) \cdot V_{pth} \tag{4}$$

At this stage it is assumed that V_{P0} and V_L are negligible compared to V_{Pth} so they do not contribute enough energy to the LHS of the equation to be significant. The mass of air will be taken into consideration because as mentioned earlier a significant amount of energy is utilized in accelerating this mass of air.

The above equation reduces to

$$m_w \cdot V_0 = (m_A + m_w) \cdot V_{pth} \tag{5}$$

At this stage the concentration term is introduced with is mathematically given by

$$c = \frac{m_A}{m_A + m_w} \tag{6}$$

Dividing (5) by $m_A + m_w$ we get

$$\frac{m_w \cdot V_0}{m_A + m_w} = \frac{(m_A + m_w)}{m_A + m_w} \cdot V_{pth} \tag{7}$$

$$\frac{m_w \cdot V_0}{m_A + m_w} = V_{pth} \tag{8}$$

Using (6) in (8) we get

$$(1-c)\cdot V_0 = V_{pth} \tag{9}$$

$$V_{pth} = (1-c)\cdot V \tag{10}$$

Using a momentum transfer coefficient η_t we get

$$V_p = \eta_t \cdot (1-c)\cdot V_0 \tag{11}$$

From (11) the theoretical energy of the abrasive particles can be calculated as

$$E_{th} = \frac{1}{2}\cdot m_A V_p^2 = \frac{1}{2}\cdot m_A \cdot (\eta_t \cdot (1-c)\cdot V)^2 \tag{12}$$

Substituting for m_A from (6) we get

$$E_{th} = \frac{1}{2}\cdot m_w \cdot \frac{c}{1-c}\cdot (\eta_t \cdot (1-c)\cdot V_0)^2 \tag{13}$$

The momentum transfer coefficient from [Hoogstrate, 2002] can be expressed as

$$\eta_t = a_1 - a_2 \cdot R \tag{14}$$

The loading ratio R can be expressed in terms of concentration as

$$R = \frac{c}{1-c} \tag{15}$$

Substituting (15) in (14)

$$\eta_t = a_1 - a_2 \cdot \frac{c}{1-c} \tag{16}$$

(13) then becomes

$$E_{th} = \frac{1}{2} \cdot m_w \cdot \frac{c}{1-c} \cdot \left((a_1 - a_2 \cdot \frac{c}{1-c_t}) \cdot (1-c) \cdot V_0 \right)^2 \tag{17}$$

Optimum concentration can be calculated by differentiating (13) with respect to concentration

$$\frac{\partial E_{th}}{\partial c} = \left(a_1 - a_2 \frac{c}{1-c} \right) \cdot m_w \cdot V_0^2 \cdot \left[\frac{1}{2} \cdot (1-c) \cdot \left(a_1 - a_2 \frac{c}{1-c} \right) - \frac{1}{2} \cdot c \cdot \left(a_1 - a_2 \frac{c}{1-c} \right) + c \cdot (1-c) \cdot \left(\frac{-a_2}{1-c} - \frac{a_2 c}{(1-c)^2} \right) \right] = 0 \tag{17}$$

Simplifying further we get

$$\left[\frac{1}{2} \cdot (1-c) \cdot \left(a_1 - a_2 \frac{c}{1-c} \right) - \frac{1}{2} \cdot c \cdot \left(a_1 - a_2 \frac{c}{1-c} \right) + c \cdot (1-c) \cdot \left(\frac{-a_2}{1-c} - \frac{a_2 c}{(1-c)^2} \right) \right] = 0 \tag{18}$$

$$\frac{1}{2}\cdot(1-c)\cdot\left(a_1-a_2\frac{c}{1-c}\right)-\frac{1}{2}\cdot c\cdot\left(a_1-a_2\frac{c}{1-c}\right)-c\cdot\left(\frac{a_2}{1}+\frac{a_2c}{(1-c)}\right)=0 \tag{19}$$

$$\frac{1}{2}\cdot(1-c)\cdot\left(a_1-a_2\frac{c}{1-c}\right)-\frac{1}{2}\cdot ca_1+\frac{1}{2}\cdot a_2\frac{c^2}{1-c}-\frac{ca_2}{1}-\frac{c^2a_2}{(1-c)}=0 \tag{20}$$

$$\frac{1}{2}\cdot\left(a_1-a_1c-a_2\frac{c}{1-c}+a_2\frac{c^2}{1-c}\right)-\frac{1}{2}\cdot ca_1-\frac{1}{2}\cdot a_2\frac{c^2}{1-c}-ca_2=0 \tag{21}$$

$$\frac{1}{2}a_1-\cdot ca_1-ca_2\cdot\left(\frac{1}{2\cdot(1-c)}+1\right)=0 \tag{22}$$

$$\frac{1}{2}a_1-\cdot ca_1-\frac{ca_2}{2\cdot(1-c)}-ca_2=0 \tag{23}$$

$$a_1\left(\frac{1}{2}-c\right)-a_2\cdot\left(\frac{c}{2\cdot(1-c)}-c\right)=0 \tag{24}$$

Ideally $a_1=1$ i.e. no momentum loss because there is no abrasive involved before the mixing chamber and $a_2=0$ i.e. momentum transfer efficiency is independent of the concentration the optimal concentration is 50% from (24). It can then be safely assumed that the optimal concentration for a given configuration of the cutting head is dependent on the two constants a_1 and $a2$

Nomenclature

a_3 - Constant

c - Mass concentration of abrasive

d_0 - Orifice diameter

E_{th} - Theoretical abrasive energy

h_1 - Height at exit of nozzle

h_2 - Height of water before entering the orifice

m_A - Abrasive mass flow rate

m_L - Air mass flow rate

m_w - Water mass flow rate

P - Pressure before exiting the jewel orifice

P_{at} - Atmospheric pressure

Q_L -Volumetric flow rate of air

V_0 - Actual water jet velocity

V_{0th} - Theoretical water jet velocity

V_1 - Water velocity before exiting the jewel orifice

V_L - Air velocity before entering the mixing chamber

V_P - Actual abrasive velocity after exiting the mixing chamber

V_{P0} - Initial velocity of abrasive before entering the mixing chamber

V_{Pth} - Theoretical abrasive velocity after exiting the mixing chamber

η_t -Momentum transfer coefficient

μ - Efficiency of jewel orifice

ρ_L - Density of air

ρ_w - Density of water

APPENDIX C.

EXPERIMENTAL DATA FOR DEPTH OF CUT

Depth of Cut test with 1mm nozzle at 69MPa for different AFR and traverse speeds

AFR (lb/min)	Speed (mm/min)	Depth of cut (mm)
0.5	38.1	20.9042
0.8	38.1	30.4546
1.2	38.1	37.0205
1.5	38.1	41.6179
0.5	101.6	9.2964
0.8	101.6	13.6906
1.2	101.6	18.1356
0.5	152.4	6.2738
0.8	152.4	9.4488
1.2	152.4	12.6238
0.5	203.2	4.9403
0.8	203.2	7.3787
1.2	203.2	10.0076

APPENDIX D.

ASJ JET PUMP EXPERIMENTAL DATA

JET PUMP TEST DATA

PRESSURE (MPa)	NOZZLE DIAMETER (mm)			
	1.651	1.143	0.889	0.635
	PRESSURE DROP (MPa)			
0	0.006058626	0.004633006	0.00483667	0.00478575
3.45	0.065120019			
6.9	0.079070728	0.079121643		
10.35	0.087726277	0.085689677		
13.8	0.091595816	0.088540916	0.08309301	
17.25	0.093174181	0.090119281	0.08762445	
20.7	0.094243396	0.091188496	0.08930464	
24.15	0.095618101	0.092257711	0.09042477	
27.6	0.096127251	0.093530586	0.0911885	0.09169765
31.05	0.096483656	0.094039736	0.09149399	0.09210497
34.5	0.096789146	0.094294311	0.09210497	0.09261412
37.95	0.097043721	0.094701631	0.09261412	0.09291961
41.4	0.09724738	0.095108951	0.09297052	0.09332693
44.85	0.09734921	0.095210781	0.0932251	0.0935815
48.3		0.095159866	0.09347967	0.09383608
51.75		0.094905291	0.09378516	0.09409065
55.2		0.094854376	0.09393791	0.09439614
58.65		0.095058036	0.09419248	0.09490529
62.1		0.095261696	0.0942434	0.09521078
65.55		0.095363526	0.09434523	0.09541444
69		0.095363526	0.09439614	0.09546536

APPENDIX E.

FLOWMETER CALIBRATION DATA

Flowmeter Calibration Data

Number	Flow (l/min)	Pressure (Mpa)	AFR (kg/min)
Trial 1	0.4	20.7	0.903
Trial 1	0.4	20.7	1.006
Trial 1	0.4	20.7	1.006
Trial 2	0.4	20.7	1.196
Trial 2	0.4	20.7	0.993
Trial 2	0.4	20.7	1.011
Trial 3	0.4	20.7	0.856
Trial 3	0.4	20.7	0.942
Trial 3	0.4	20.7	1.054
Trial 1	0.7	20.7	1.891
Trial 1	0.7	20.7	1.970
Trial 1	0.7	20.7	1.970
Trial 2	0.7	20.7	1.858
Trial 2	0.7	20.7	1.897
Trial 2	0.7	20.7	1.961
Trial 3	0.7	20.7	1.968
Trial 3	0.7	20.7	1.905
Trial 3	0.7	20.7	1.990
Trial 1	1	20.7	2.777
Trial 1	1	20.7	2.931
Trial 1	1	20.7	2.984
Trial 2	1	20.7	2.909
Trial 2	1	20.7	2.869
Trial 2	1	20.7	2.853
Trial 3	1	20.7	2.724

Number	Flow (l/min)	Pressure (Mpa)	AFR (kg/min)
Trial 3	1	20.7	3.015
Trial 3	1	20.7	2.997
Trial 1	0.4	27.6	1.009432
Trial 1	0.4	27.6	1.03588
Trial 1	0.4	27.6	1.009432
Trial 2	0.4	27.6	1.143929756
Trial 2	0.4	27.6	1.049319024
Trial 2	0.4	27.6	1.032117073
Trial 3	0.4	27.6	1.12404
Trial 3	0.4	27.6	0.9918
Trial 3	0.4	27.6	1.022656
Trial 1	0.7	27.6	1.908664
Trial 1	0.7	27.6	1.952744
Trial 1	0.7	27.6	1.952744
Trial 2	0.7	27.6	1.973045634
Trial 2	0.7	27.6	1.960007887
Trial 2	0.7	27.6	1.990429296
Trial 3	0.7	27.6	1.860176
Trial 3	0.7	27.6	1.921888
Trial 3	0.7	27.6	1.988008
Trial 1	1	27.6	2.968653061
Trial 1	1	27.6	2.883191837
Trial 1	1	27.6	3.063110204
Trial 2	1	27.6	2.854900935
Trial 2	1	27.6	2.949652336
Trial 2	1	27.6	2.933173832

Number	Flow (l/min)	Pressure (Mpa)	AFR (kg/min)
Trial 3	1	27.6	2.957768
Trial 3	1	27.6	2.9754
Trial 3	1	27.6	2.922504
Trial 1	0.4	34.5	1.251872
Trial 1	0.4	34.5	1.03588
Trial 1	0.4	34.5	1.044696
Trial 2	0.4	34.5	1.049104
Trial 2	0.4	34.5	1.07996
Trial 2	0.4	34.5	1.097592
Trial 3	0.4	34.5	1.150488
Trial 3	0.4	34.5	1.05792
Trial 3	0.4	34.5	1.040288
Trial 1	0.7	34.5	1.85136
Trial 1	0.7	34.5	1.585656
Trial 1	0.7	34.5	0.977107
Trial 2	0.7	34.5	1.864584
Trial 2	0.7	34.5	1.957152
Trial 2	0.7	34.5	1.96156
Trial 3	0.7	34.5	1.793226
Trial 3	0.7	34.5	1.913966
Trial 3	0.7	34.5	1.936326
Trial 1	1	34.5	2.71092
Trial 1	1	34.5	2.768224
Trial 1	1	34.5	2.79908
Trial 2	1	34.5	2.66684
Trial 2	1	34.5	2.851976

Number	Flow (l/min)	Pressure (Mpa)	AFR (kg/min)
Trial 2	1	34.5	2.812304
Trial 3	1	34.5	2.361429
Trial 3	1	34.5	2.752751
Trial 3	1	34.5	2.698776

APPENDIX F.

EXPERIMENTAL DATA FOR ABRASIVE POWER OF ASJ

0.5mm nozzle with AFR 0.6 lb/min at 35MPa test data

Dish no	Abrasive wt (g)	Velocity (m/s)	V^2 $(m/s)^2$	Energy(J)
2	0.28	3.788688626	14.3541615	0.00201
3	0.9	5.68303294	32.2968634	0.014534
4	2.04	7.577377253	57.416646	0.058565
5	4.26	9.471721566	89.7135094	0.19109
6	5.34	11.36606588	129.187454	0.344931
7	8.34	13.26041019	175.838478	0.733246
8	9.46	15.15475451	229.666584	1.086323
9	12.4	17.04909882	290.671771	1.802165
10	13.64	18.94344313	358.854038	2.447385
11	16.22	20.83778745	434.213386	3.521471
12	15.92	22.73213176	516.749814	4.113329
13	17.96	24.62647607	606.463324	5.446041
14	19.52	26.52082039	703.353914	6.864734
15	20.16	28.4151647	807.421585	8.13881
16	18.2	30.30950901	918.666337	8.359864
17	17.14	32.20385333	1037.08817	8.887846
18	15.92	34.09819764	1162.68708	9.254989
19	13.56	35.99254195	1295.46308	8.78324
20	13.62	37.88688626	1435.41615	9.775184
21	12	39.78123058	1582.54631	9.495278
22	11.34	41.67557489	1736.85354	9.84796
23	8.88	43.5699192	1898.33786	8.42862
24	8.36	45.46426352	2066.99926	8.640057
25	7.5	47.35860783	2242.83774	8.410642
26	4.94	49.25295214	2425.85329	5.991858

27	4.42	51.14729646	2616.04593	5.781462
28	3.32	53.04164077	2813.41566	4.67027
29	2.4	54.93598508	3017.96246	3.621555
30	1.62	56.8303294	3229.68634	2.616046
31	1.12	58.72467371	3448.5873	1.931209
32	0.74	60.61901802	3674.66535	1.359626
33	0.58	62.51336234	3907.92047	1.133297
34	0.36	64.40770665	4148.35268	0.746703
35	0.24	66.30205096	4395.96196	0.527515
36	0.22	68.19639528	4650.74833	0.511582
37	0.12	70.09073959	4912.71178	0.294763

0.5mm nozzle with AFR 1.0lb/min at 35MPa test data

Dish no	Abrasive wt (g)	Velocity (m/s)	V^2 $(m/s)^2$	Energy(J)
2	0.4	3.788688626	14.35416	0.002871
3	1.52	5.68303294	32.29686	0.024546
4	3.32	7.577377253	57.41665	0.095312
5	5.7	9.471721566	89.71351	0.255684
6	10.62	11.36606588	129.1875	0.685985
7	14.62	13.26041019	175.8385	1.285379
8	15.96	15.15475451	229.6666	1.832739
9	20.62	17.04909882	290.6718	2.996826
10	24.06	18.94344313	358.854	4.317014
11	27.76	20.83778745	434.2134	6.026882
12	27.46	22.73213176	516.7498	7.094975
13	32.4	24.62647607	606.4633	9.824706
14	35.12	26.52082039	703.3539	12.35089
15	34.96	28.4151647	807.4216	14.11373
16	32.24	30.30950901	918.6663	14.8089
17	30.44	32.20385333	1037.088	15.78448
18	25.96	34.09819764	1162.687	15.09168
19	23.66	35.99254195	1295.463	15.32533
20	21.86	37.88688626	1435.416	15.6891
21	19.3	39.78123058	1582.546	15.27157
22	17.28	41.67557489	1736.854	15.00641
23	13.56	43.5699192	1898.338	12.87073
24	13.02	45.46426352	2066.999	13.45617
25	11.24	47.35860783	2242.838	12.60475
26	7.7	49.25295214	2425.853	9.339535

27	5.46	51.14729646	2616.046	7.141805
28	7.5	53.04164077	2813.416	10.55031
29	3.62	54.93598508	3017.962	5.462512
30	2.64	56.8303294	3229.686	4.263186
31	1.76	58.72467371	3448.587	3.034757
32	1.34	60.61901802	3674.665	2.462026
33	0.98	62.51336234	3907.92	1.914881
34	0.68	64.40770665	4148.353	1.41044
35	0.44	66.30205096	4395.962	0.967112
36	0.34	68.19639528	4650.748	0.790627
37	0.2	70.09073959	4912.712	0.491271
38	0.26	71.9850839	5181.852	0.673641
39	0.12	73.87942822	5458.17	0.32749

Dish no	Abrasive wt (g)	Velocity (m/s)	V^2 $(m/s)^2$	Energy(J)
2	0.32	3.788688626	14.35416	0.002297
3	1.62	5.68303294	32.29686	0.02616
4	3.5	7.577377253	57.41665	0.100479
5	6.16	9.471721566	89.71351	0.276318
6	10.14	11.36606588	129.1875	0.65498
7	15.2	13.26041019	175.8385	1.336372
8	17.76	15.15475451	229.6666	2.039439
9	24.12	17.04909882	290.6718	3.505502
10	32.06	18.94344313	358.854	5.75243
11	38.16	20.83778745	434.2134	8.284791
12	39.36	22.73213176	516.7498	10.16964
13	49.28	24.62647607	606.4633	14.94326
14	52.6	26.52082039	703.3539	18.49821
15	59.42	28.4151647	807.4216	23.9885
16	53.36	30.30950901	918.6663	24.51002
17	49.94	32.20385333	1037.088	25.89609
18	50.24	34.09819764	1162.687	29.2067
19	44.94	35.99254195	1295.463	29.10906
20	43.24	37.88688626	1435.416	31.0337
21	39.28	39.78123058	1582.546	31.08121
22	37.7	41.67557489	1736.854	32.73969
23	26.76	43.5699192	1898.338	25.39976
24	26.86	45.46426352	2066.999	27.7598
25	22.12	47.35860783	2242.838	24.80579
26	16.6	49.25295214	2425.853	20.13458

27	14.7	51.14729646	2616.046	19.22794
28	10.46	53.04164077	2813.416	14.71416
29	7.92	54.93598508	3017.962	11.95113
30	5.42	56.8303294	3229.686	8.75245
31	3.64	58.72467371	3448.587	6.276429
32	2.44	60.61901802	3674.665	4.483092
33	1.8	62.51336234	3907.92	3.517128
34	1.12	64.40770665	4148.353	2.323077
35	0.82	66.30205096	4395.962	1.802344
36	0.28	68.19639528	4650.748	0.651105
37	0.26	70.09073959	4912.712	0.638653
38	0.5	71.9850839	5181.852	1.295463
39	0.06	73.87942822	5458.17	0.163745
40	0.06	75.77377253	5741.665	0.17225

0.5mm nozzle with AFR 0.6lb/min at 69MPa test data

Dish no	Abrasive wt (g)	Velocity (m/s)	V^2 $(m/s)^2$	Energy(J)
2	0.2	3.788688626	14.35416	0.001435
3	0.62	5.68303294	32.29686	0.010012
4	1.7	7.577377253	57.41665	0.048804
5	3.28	9.471721566	89.71351	0.14713
6	5.7	11.36606588	129.1875	0.368184
7	6.82	13.26041019	175.8385	0.599609
8	7.16	15.15475451	229.6666	0.822206
9	7.32	17.04909882	290.6718	1.063859
10	8.58	18.94344313	358.854	1.539484
11	10.32	20.83778745	434.2134	2.240541
12	10.16	22.73213176	516.7498	2.625089
13	14.78	24.62647607	606.4633	4.481764
14	15.48	26.52082039	703.3539	5.443959
15	18.48	28.4151647	807.4216	7.460575
16	16.72	30.30950901	918.6663	7.680051
17	17.04	32.20385333	1037.088	8.835991
18	17.92	34.09819764	1162.687	10.41768
19	16.42	35.99254195	1295.463	10.63575
20	17.2	37.88688626	1435.416	12.34458
21	16.62	39.78123058	1582.546	13.15096
22	16.34	41.67557489	1736.854	14.19009
23	13.78	43.5699192	1898.338	13.07955
24	15.36	45.46426352	2066.999	15.87455
25	16.46	47.35860783	2242.838	18.45855

26	11.24	49.25295214	2425.853	13.6333
27	12.34	51.14729646	2616.046	16.141
28	10.76	53.04164077	2813.416	15.13618
29	9	54.93598508	3017.962	13.58083
30	7.1	56.8303294	3229.686	11.46539
31	6.04	58.72467371	3448.587	10.41473
32	4.98	60.61901802	3674.665	9.149917
33	4.62	62.51336234	3907.92	9.027296
34	3.5	64.40770665	4148.353	7.259617
35	3.1	66.30205096	4395.962	6.813741
36	2.54	68.19639528	4650.748	5.90645
37	1.96	70.09073959	4912.712	4.814458
38	1.78	71.9850839	5181.852	4.611849
39	0.92	73.87942822	5458.17	2.510758
40	0.92	75.77377253	5741.665	2.641166
41	0.7	77.66811684	6032.336	2.111318
42	0.56	79.56246116	6330.185	1.772452
43	0.42	81.45680547	6635.211	1.393394
44	0.36	83.35114978	6947.414	1.250535
45	0.28	85.2454941	7266.794	1.017351
46	0.24	87.13983841	7593.351	0.911202
47	0.2	89.03418272	7927.086	0.792709
48	0.14	90.92852704	8267.997	0.57876
49	0.12	92.82287135	8616.085	0.516965
50	0.08	94.71721566	8971.351	0.358854

0.5mm nozzle with AFR 1.0lb/min at 69MPa test data

Dish no	Abrasive wt (g)	Velocity (m/s)	V^2 $(m/s)^2$	Energy(J)
2	0.14	3.788688626	14.35416	0.001005
3	1.58	5.68303294	32.29686	0.025515
4	0.62	7.577377253	57.41665	0.017799
5	2.68	9.471721566	89.71351	0.120216
6	4.92	11.36606588	129.1875	0.317801
7	5.94	13.26041019	175.8385	0.52224
8	6.72	15.15475451	229.6666	0.77168
9	8.02	17.04909882	290.6718	1.165594
10	9	18.94344313	358.854	1.614843
11	10.84	20.83778745	434.2134	2.353437
12	11.22	22.73213176	516.7498	2.898966
13	14.86	24.62647607	606.4633	4.506022
14	16.28	26.52082039	703.3539	5.725301
15	19.04	28.4151647	807.4216	7.686653
16	17.08	30.30950901	918.6663	7.845411
17	18.92	32.20385333	1037.088	9.810854
18	16.74	34.09819764	1162.687	9.731691
19	16.42	35.99254195	1295.463	10.63575
20	17.5	37.88688626	1435.416	12.55989
21	15.18	39.78123058	1582.546	12.01153
22	16.8	41.67557489	1736.854	14.58957
23	13.14	43.5699192	1898.338	12.47208
24	15.92	45.46426352	2066.999	16.45331
25	14.3	47.35860783	2242.838	16.03629

26	12.08	49.25295214	2425.853	14.65215
27	12.74	51.14729646	2616.046	16.66421
28	10.76	53.04164077	2813.416	15.13618
29	9.62	54.93598508	3017.962	14.5164
30	8.2	56.8303294	3229.686	13.24171
31	6.74	58.72467371	3448.587	11.62174
32	5.22	60.61901802	3674.665	9.590877
33	4.84	62.51336234	3907.92	9.457168
34	3.78	64.40770665	4148.353	7.840387
35	2.98	66.30205096	4395.962	6.549983
36	5.02	68.19639528	4650.748	11.67338
37	2.3	70.09073959	4912.712	5.649619
38	1.42	71.9850839	5181.852	3.679115
39	1.02	73.87942822	5458.17	2.783667
40	0.84	75.77377253	5741.665	2.411499
41	0.56	77.66811684	6032.336	1.689054
42	0.5	79.56246116	6330.185	1.582546
43	0.44	81.45680547	6635.211	1.459746
44	0.38	83.35114978	6947.414	1.320009
45	0.24	85.2454941	7266.794	0.872015
46	0.28	87.13983841	7593.351	1.063069
47	0.18	89.03418272	7927.086	0.713438
48	0.12	90.92852704	8267.997	0.49608
49	0.02	92.82287135	8616.085	0.086161
50	0.08	94.71721566	8971.351	0.358854

0.5mm nozzle with AFR 1.5lb/min at 69MPa test data

Dish no	Abrasive wt (g)	Velocity (m/s)	V^2 $(m/s)^2$	Energy(J)
2	0	3.788688626	14.35416	0
3	0.8	5.68303294	32.29686	0.012919
4	3.08	7.577377253	57.41665	0.088422
5	4.56	9.471721566	89.71351	0.204547
6	6.02	11.36606588	129.1875	0.388854
7	7.82	13.26041019	175.8385	0.687528
8	8.78	15.15475451	229.6666	1.008236
9	9.88	17.04909882	290.6718	1.435919
10	10.86	18.94344313	358.854	1.948577
11	14.76	20.83778745	434.2134	3.204495
12	14.68	22.73213176	516.7498	3.792944
13	21.9	24.62647607	606.4633	6.640773
14	23.42	26.52082039	703.3539	8.236274
15	30.18	28.4151647	807.4216	12.18399
16	25.84	30.30950901	918.6663	11.86917
17	27.32	32.20385333	1037.088	14.16662
18	20.52	34.09819764	1162.687	11.92917
19	28.68	35.99254195	1295.463	18.57694
20	25.68	37.88688626	1435.416	18.43074
21	29.44	39.78123058	1582.546	23.29508
22	29.6	41.67557489	1736.854	25.70543
23	24.76	43.5699192	1898.338	23.50142
24	29.98	45.46426352	2066.999	30.98432
25	31.88	47.35860783	2242.838	35.75083

26	24.58	49.25295214	2425.853	29.81374
27	25.88	51.14729646	2616.046	33.85163
28	24.4	53.04164077	2813.416	34.32367
29	23.08	54.93598508	3017.962	34.82729
30	18.08	56.8303294	3229.686	29.19636
31	14.88	58.72467371	3448.587	25.65749
32	12.48	60.61901802	3674.665	22.92991
33	11.34	62.51336234	3907.92	22.15791
34	9.3	64.40770665	4148.353	19.28984
35	8.06	66.30205096	4395.962	17.71573
36	6.88	68.19639528	4650.748	15.99857
37	5.68	70.09073959	4912.712	13.9521
38	3.56	71.9850839	5181.852	9.223697
39	2.52	73.87942822	5458.17	6.877294
40	2.82	75.77377253	5741.665	8.095747
41	1.92	77.66811684	6032.336	5.791043
42	1.34	79.56246116	6330.185	4.241224
43	1.02	81.45680547	6635.211	3.383958
44	0.76	83.35114978	6947.414	2.640017
45	0.62	85.2454941	7266.794	2.252706
46	0.56	87.13983841	7593.351	2.126138
47	0.48	89.03418272	7927.086	1.902501
48	0.4	90.92852704	8267.997	1.653599
49	0.28	92.82287135	8616.085	1.206252
50	0.22	94.71721566	8971.351	0.986849

0.5mm nozzle with AFR 0.6lb/min at 103MPa test data

Dish no	Abrasive wt (g)	Velocity (m/s)	V^2 $(m/s)^2$	Energy(J)
2	0.28	3.788688626	14.35416	0.00201
3	0.42	5.68303294	32.29686	0.006782
4	0.74	7.577377253	57.41665	0.021244
5	1.6	9.471721566	89.71351	0.071771
6	2.4	11.36606588	129.1875	0.155025
7	3.72	13.26041019	175.8385	0.32706
8	3.94	15.15475451	229.6666	0.452443
9	4.9	17.04909882	290.6718	0.712146
10	5.02	18.94344313	358.854	0.900724
11	5.98	20.83778745	434.2134	1.298298
12	5.44	22.73213176	516.7498	1.405559
13	7.32	24.62647607	606.4633	2.219656
14	7.02	26.52082039	703.3539	2.468772
15	8.08	28.4151647	807.4216	3.261983
16	7.38	30.30950901	918.6663	3.389879
17	8.14	32.20385333	1037.088	4.220949
18	7.6	34.09819764	1162.687	4.418211
19	7.54	35.99254195	1295.463	4.883896
20	6.9	37.88688626	1435.416	4.952186
21	7.1	39.78123058	1582.546	5.618039
22	7.2	41.67557489	1736.854	6.252673
23	6.34	43.5699192	1898.338	6.017731
24	7.48	45.46426352	2066.999	7.730577
25	6.64	47.35860783	2242.838	7.446221

26	6.68	49.25295214	2425.853	8.10235
27	7.82	51.14729646	2616.046	10.22874
28	7.16	53.04164077	2813.416	10.07203
29	6.76	54.93598508	3017.962	10.20071
30	6.02	56.8303294	3229.686	9.721356
31	5.42	58.72467371	3448.587	9.345672
32	4.78	60.61901802	3674.665	8.78245
33	3.88	62.51336234	3907.92	7.581366
34	4.06	64.40770665	4148.353	8.421156
35	5.06	66.30205096	4395.962	11.12178
36	3.78	68.19639528	4650.748	8.789914
37	3.06	70.09073959	4912.712	7.516449
38	2.8	71.9850839	5181.852	7.254593
39	1.62	73.87942822	5458.17	4.421118
40	1.86	75.77377253	5741.665	5.339748
41	1.36	77.66811684	6032.336	4.101989
42	1.24	79.56246116	6330.185	3.924715
43	1.06	81.45680547	6635.211	3.516662
44	0.82	83.35114978	6947.414	2.84844
45	0.76	85.2454941	7266.794	2.761382
46	0.78	87.13983841	7593.351	2.961407
47	0.62	89.03418272	7927.086	2.457397
48	0.54	90.92852704	8267.997	2.232359
49	0.4	92.82287135	8616.085	1.723217
50	0.4	94.71721566	8971.351	1.79427
51	0.56	96.61155998	9333.794	2.613462
52	0.52	98.50590429	9703.413	2.522887

53	0.48	100.4002486	10080.21	2.41925
54	0.42	102.2945929	10464.18	2.197479

0.5mm nozzle with AFR 1.0lb/min at 103MPa test data

Dish no	Abrasive wt (g)	Velocity (m/s)	V^2 $(m/s)^2$	Energy(J)
2	0	3.788688626	14.35416	0
3	0.34	5.68303294	32.29686	0.00549
4	0.64	7.577377253	57.41665	0.018373
5	1.32	9.471721566	89.71351	0.059211
6	2.32	11.36606588	129.1875	0.149857
7	3.14	13.26041019	175.8385	0.276066
8	3.18	15.15475451	229.6666	0.36517
9	3.84	17.04909882	290.6718	0.55809
10	6.42	18.94344313	358.854	1.151921
11	7.52	20.83778745	434.2134	1.632642
12	6.94	22.73213176	516.7498	1.793122
13	9.66	24.62647607	606.4633	2.929218
14	9.3	26.52082039	703.3539	3.270596
15	12.02	28.4151647	807.4216	4.852604
16	10.74	30.30950901	918.6663	4.933238
17	13.22	32.20385333	1037.088	6.855153
18	13.44	34.09819764	1162.687	7.813257
19	13.08	35.99254195	1295.463	8.472329
20	11.5	37.88688626	1435.416	8.253643
21	11.34	39.78123058	1582.546	8.973038
22	10.86	41.67557489	1736.854	9.431115
23	9.32	43.5699192	1898.338	8.846254
24	10.58	45.46426352	2066.999	10.93443
25	12.16	47.35860783	2242.838	13.63645
26	7.22	49.25295214	2425.853	8.75733

27	11.34	51.14729646	2616.046	14.83298
28	10.64	53.04164077	2813.416	14.96737
29	13.48	54.93598508	3017.962	20.34107
30	12.72	56.8303294	3229.686	20.54081
31	11.98	58.72467371	3448.587	20.65704
32	11.48	60.61901802	3674.665	21.09258
33	12.68	62.51336234	3907.92	24.77622
34	11.1	64.40770665	4148.353	23.02336
35	10.8	66.30205096	4395.962	23.73819
36	10.48	68.19639528	4650.748	24.36992
37	9.6	70.09073959	4912.712	23.58102
38	7.3	71.9850839	5181.852	18.91376
39	5.74	73.87942822	5458.17	15.66495
40	6.72	75.77377253	5741.665	19.29199
41	4.62	77.66811684	6032.336	13.9347
42	4.68	79.56246116	6330.185	14.81263
43	3.82	81.45680547	6635.211	12.67325
44	2.96	83.35114978	6947.414	10.28217
45	2.48	85.2454941	7266.794	9.010825
46	1.8	87.13983841	7593.351	6.834016
47	1.68	89.03418272	7927.086	6.658752
48	1.24	90.92852704	8267.997	5.126158
49	1.3	92.82287135	8616.085	5.600456
50	0.98	94.71721566	8971.351	4.395962
51	0.74	96.61155998	9333.794	3.453504
52	0.54	98.50590429	9703.413	2.619922
53	0.52	100.4002486	10080.21	2.620855

54	0.44	102.2945929	10464.18	2.30212
55	0.46	104.1889372	10855.33	2.496727
56	0.3	106.0832815	11253.66	1.688049
57	0.22	107.9776259	11659.17	1.282508
58	0.16	109.8719702	12071.85	0.965748
59	0.16	111.7663145	12491.71	0.999337
60	0.08	113.6606588	12918.75	0.51675
61	0	115.5550031	13352.96	0
62	0.06	117.4493474	13794.35	0.41383

0.5mm nozzle with AFR 1.5lb/min at 103MPa test data

Dish no	Abrasive wt (g)	Velocity (m/s)	V^2 $(m/s)^2$	Energy(J)
2	0.88	3.788688626	14.35416	0.006316
3	0.74	5.68303294	32.29686	0.01195
4	1.26	7.577377253	57.41665	0.036172
5	3	9.471721566	89.71351	0.13457
6	5.08	11.36606588	129.1875	0.328136
7	7.3	13.26041019	175.8385	0.64181
8	6.18	15.15475451	229.6666	0.70967
9	6.78	17.04909882	290.6718	0.985377
10	8	18.94344313	358.854	1.435416
11	10.84	20.83778745	434.2134	2.353437
12	11.58	22.73213176	516.7498	2.991981
13	17.84	24.62647607	606.4633	5.409653
14	16.46	26.52082039	703.3539	5.788603
15	21.96	28.4151647	807.4216	8.865489
16	19.92	30.30950901	918.6663	9.149917
17	24.66	32.20385333	1037.088	12.7873
18	26.68	34.09819764	1162.687	15.51025
19	26.04	35.99254195	1295.463	16.86693
20	22.34	37.88688626	1435.416	16.0336
21	22.78	39.78123058	1582.546	18.0252
22	20.34	41.67557489	1736.854	17.6638
23	18.04	43.5699192	1898.338	17.12301
24	21.24	45.46426352	2066.999	21.95153
25	24.8	47.35860783	2242.838	27.81119
26	14.46	49.25295214	2425.853	17.53892

27	21.52	51.14729646	2616.046	28.14865
28	22.9	53.04164077	2813.416	32.21361
29	24.72	54.93598508	3017.962	37.30202
30	23.86	56.8303294	3229.686	38.53016
31	21.98	58.72467371	3448.587	37.89997
32	20.36	60.61901802	3674.665	37.40809
33	22.2	62.51336234	3907.92	43.37792
34	21.74	64.40770665	4148.353	45.09259
35	19.04	66.30205096	4395.962	41.84956
36	18.56	68.19639528	4650.748	43.15894
37	17.24	70.09073959	4912.712	42.34758
38	15.62	71.9850839	5181.852	40.47027
39	11.84	73.87942822	5458.17	32.31237
40	12.58	75.77377253	5741.665	36.11507
41	9.86	77.66811684	6032.336	29.73942
42	8.32	79.56246116	6330.185	26.33357
43	6.44	81.45680547	6635.211	21.36538
44	5.26	83.35114978	6947.414	18.2717
45	4.12	85.2454941	7266.794	14.9696
46	3.92	87.13983841	7593.351	14.88297
47	3.14	89.03418272	7927.086	12.44552
48	2.8	90.92852704	8267.997	11.5752
49	2.32	92.82287135	8616.085	9.994659
50	1.68	94.71721566	8971.351	7.535935
51	1.6	96.61155998	9333.794	7.467035
52	1.12	98.50590429	9703.413	5.433911
53	1	100.4002486	10080.21	5.040105

54	0.8	102.2945929	10464.18	4.185673
55	0.76	104.1889372	10855.33	4.125027
56	0.6	106.0832815	11253.66	3.376099
57	0.32	107.9776259	11659.17	1.865467
58	0.28	109.8719702	12071.85	1.690059
59	0.26	111.7663145	12491.71	1.623922
60	0.18	113.6606588	12918.75	1.162687
61	0.2	115.5550031	13352.96	1.335296
62	0.1	117.4493474	13794.35	0.689717

0.5mm nozzle with AFR 0.6lb/min at 138MPa test data

Dish no	Abrasive wt (g)	Velocity (m/s)	V^2 $(m/s)^2$	Energy(J)
2	0	3.788688626	14.354162	0
3	0.18	5.68303294	32.296863	0.002907
4	0.18	7.577377253	57.416646	0.005167
5	0.46	9.471721566	89.713509	0.020634
6	0.78	11.36606588	129.18745	0.050383
7	1.02	13.26041019	175.83848	0.089678
8	1.28	15.15475451	229.66658	0.146987
9	1.1	17.04909882	290.67177	0.159869
10	1.88	18.94344313	358.85404	0.337323
11	1.9	20.83778745	434.21339	0.412503
12	2.92	22.73213176	516.74981	0.754455
13	4.04	24.62647607	606.46332	1.225056
14	2.28	26.52082039	703.35391	0.801823
15	2.82	28.4151647	807.42158	1.138464
16	2.42	30.30950901	918.66634	1.111586
17	3.24	32.20385333	1037.0882	1.680083
18	3.32	34.09819764	1162.6871	1.930061
19	3.08	35.99254195	1295.4631	1.995013
20	3.04	37.88688626	1435.4162	2.181833
21	3.16	39.78123058	1582.5463	2.500423
22	2.78	41.67557489	1736.8535	2.414226
23	2.68	43.5699192	1898.3379	2.543773
24	3.08	45.46426352	2066.9993	3.183179
25	4.04	47.35860783	2242.8377	4.530532
26	2.1	49.25295214	2425.8533	2.547146

27	2.7	51.14729646	2616.0459	3.531662
28	3.12	53.04164077	2813.4157	4.388928
29	3.36	54.93598508	3017.9625	5.070177
30	3.22	56.8303294	3229.6863	5.199795
31	3.32	58.72467371	3448.5873	5.724655
32	2.92	60.61901802	3674.6653	5.365011
33	3.58	62.51336234	3907.9205	6.995178
34	3.52	64.40770665	4148.3527	7.301101
35	2.72	66.30205096	4395.962	5.978508
36	3.84	68.19639528	4650.7483	8.929437
37	3.64	70.09073959	4912.7118	8.941135
38	3.74	71.9850839	5181.8523	9.690064
39	1.84	73.87942822	5458.1699	5.021516
40	3.48	75.77377253	5741.6646	9.990496
41	2.42	77.66811684	6032.3364	7.299127
42	2.8	79.56246116	6330.1852	8.862259
43	2.9	81.45680547	6635.2112	9.621056
44	2.22	83.35114978	6947.4142	7.71163
45	2.1	85.2454941	7266.7943	7.630134
46	1.9	87.13983841	7593.3514	7.213684
47	2.1	89.03418272	7927.0857	8.32344
48	1.66	90.92852704	8267.997	6.862438
49	1.5	92.82287135	8616.0854	6.462064
50	1.36	94.71721566	8971.3509	6.100519
51	1.24	96.61155998	9333.7935	5.786952
52	0.56	98.50590429	9703.4132	2.716956
53	0.86	100.4002486	10080.21	4.33449

54	0.86	102.2945929	10464.184	4.499599
55	0.74	104.1889372	10855.335	4.016474
56	0.66	106.0832815	11253.663	3.713709
57	0.52	107.9776259	11659.168	3.031384
58	0.52	109.8719702	12071.85	3.138681
59	0.42	111.7663145	12491.709	2.623259
60	0.38	113.6606588	12918.745	2.454562
61	0.42	115.5550031	13352.959	2.804121
62	0.26	117.4493474	13794.349	1.793265
63	0.36	119.3436917	14242.917	2.563725

0.5mm nozzle with AFR 1.0lb/min at 138MPa test data

Dish no	Abrasive wt (g)	Velocity (m/s)	V^2 $(m/s)^2$	Energy(J)
2	0	3.788688626	14.35416	0
3	0.5	5.68303294	32.29686	0.008074
4	0.5	7.577377253	57.41665	0.014354
5	0.98	9.471721566	89.71351	0.04396
6	1.7	11.36606588	129.1875	0.109809
7	1.8	13.26041019	175.8385	0.158255
8	2.44	15.15475451	229.6666	0.280193
9	2.2	17.04909882	290.6718	0.319739
10	3.4	18.94344313	358.854	0.610052
11	3.82	20.83778745	434.2134	0.829348
12	4.72	22.73213176	516.7498	1.21953
13	7.76	24.62647607	606.4633	2.353078
14	5.8	26.52082039	703.3539	2.039726
15	7.98	28.4151647	807.4216	3.221612
16	7.08	30.30950901	918.6663	3.252079
17	9.56	32.20385333	1037.088	4.957281
18	9.94	34.09819764	1162.687	5.778555
19	9.38	35.99254195	1295.463	6.075722
20	8.88	37.88688626	1435.416	6.373248
21	9.24	39.78123058	1582.546	7.311364
22	8.08	41.67557489	1736.854	7.016888
23	7.66	43.5699192	1898.338	7.270634
24	8.86	45.46426352	2066.999	9.156807
25	9.76	47.35860783	2242.838	10.94505
26	6.34	49.25295214	2425.853	7.689955

27	8.38	51.14729646	2616.046	10.96123
28	8.46	53.04164077	2813.416	11.90075
29	9.7	54.93598508	3017.962	14.63712
30	9.12	56.8303294	3229.686	14.72737
31	9.04	58.72467371	3448.587	15.58761
32	8.76	60.61901802	3674.665	16.09503
33	10.76	62.51336234	3907.92	21.02461
34	9.58	64.40770665	4148.353	19.87061
35	10.16	66.30205096	4395.962	22.33149
36	10.66	68.19639528	4650.748	24.78849
37	9.5	70.09073959	4912.712	23.33538
38	9.32	71.9850839	5181.852	24.14743
39	6.44	73.87942822	5458.17	17.57531
40	9.46	75.77377253	5741.665	27.15807
41	7.4	77.66811684	6032.336	22.31964
42	8.7	79.56246116	6330.185	27.53631
43	7.9	81.45680547	6635.211	26.20908
44	5.4	83.35114978	6947.414	18.75802
45	6	85.2454941	7266.794	21.80038
46	6	87.13983841	7593.351	22.78005
47	5.08	89.03418272	7927.086	20.1348
48	4.62	90.92852704	8267.997	19.09907
49	4	92.82287135	8616.085	17.23217
50	3.12	94.71721566	8971.351	13.99531
51	2.78	96.61155998	9333.794	12.97397
52	2.16	98.50590429	9703.413	10.47969
53	1.78	100.4002486	10080.21	8.971387

54	1.76	102.2945929	10464.18	9.208482
55	1.62	104.1889372	10855.33	8.792821
56	1.44	106.0832815	11253.66	8.102637
57	1.1	107.9776259	11659.17	6.412542
58	0.78	109.8719702	12071.85	4.708021
59	0.76	111.7663145	12491.71	4.746849
60	0.56	113.6606588	12918.75	3.617249
61	0.48	115.5550031	13352.96	3.20471
62	0.42	117.4493474	13794.35	2.896813
63	0	119.3436917	14242.92	0

0.5mm nozzle with AFR 1.5lb/min at 138MPa test data

Dish no	Abrasive wt (g)	Velocity (m/s)	V^2 $(m/s)^2$	Energy(J)
2	0.36	3.788688626	14.35416	0.002584
3	1.2	5.68303294	32.29686	0.019378
4	1.56	7.577377253	57.41665	0.044785
5	2.52	9.471721566	89.71351	0.113039
6	3.62	11.36606588	129.1875	0.233829
7	4.08	13.26041019	175.8385	0.35871
8	4.8	15.15475451	229.6666	0.5512
9	3.98	17.04909882	290.6718	0.578437
10	6.16	18.94344313	358.854	1.10527
11	6.48	20.83778745	434.2134	1.406851
12	6.28	22.73213176	516.7498	1.622594
13	12.62	24.62647607	606.4633	3.826784
14	10.82	26.52082039	703.3539	3.805145
15	13.98	28.4151647	807.4216	5.643877
16	12.42	30.30950901	918.6663	5.704918
17	17.08	32.20385333	1037.088	8.856733
18	19.5	34.09819764	1162.687	11.3362
19	19.54	35.99254195	1295.463	12.65667
20	17.76	37.88688626	1435.416	12.7465
21	18.72	39.78123058	1582.546	14.81263
22	18.32	41.67557489	1736.854	15.90958
23	15.16	43.5699192	1898.338	14.3894
24	19.74	45.46426352	2066.999	20.40128
25	21.36	47.35860783	2242.838	23.95351

26	13.7	49.25295214	2425.853	16.6171
27	18.58	51.14729646	2616.046	24.30307
28	19.1	53.04164077	2813.416	26.86812
29	22.42	54.93598508	3017.962	33.83136
30	16.54	56.8303294	3229.686	26.70951
31	15.64	58.72467371	3448.587	26.96795
32	18.12	60.61901802	3674.665	33.29247
33	15.52	62.51336234	3907.92	30.32546
34	20.02	64.40770665	4148.353	41.52501
35	16.02	66.30205096	4395.962	35.21166
36	21.36	68.19639528	4650.748	49.66999
37	21.2	70.09073959	4912.712	52.07474
38	20.42	71.9850839	5181.852	52.90671
39	11.6	73.87942822	5458.17	31.65739
40	17.84	75.77377253	5741.665	51.21565
41	14.96	77.66811684	6032.336	45.12188
42	15.02	79.56246116	6330.185	47.53969
43	14.44	81.45680547	6635.211	47.90622
44	12.3	83.35114978	6947.414	42.7266
45	11.68	85.2454941	7266.794	42.43808
46	10.7	87.13983841	7593.351	40.62443
47	9.18	89.03418272	7927.086	36.38532
48	7.74	90.92852704	8267.997	31.99715
49	6.9	92.82287135	8616.085	29.72549
50	5.7	94.71721566	8971.351	25.56835
51	4.76	96.61155998	9333.794	22.21443
52	2.98	98.50590429	9703.413	14.45809

53	3.44	100.4002486	10080.21	17.33796
54	2.86	102.2945929	10464.18	14.96378
55	2.36	104.1889372	10855.33	12.80929
56	1.96	106.0832815	11253.66	11.02859
57	1.5	107.9776259	11659.17	8.744376
58	1.24	109.8719702	12071.85	7.484547
59	0.88	111.7663145	12491.71	5.496352
60	0.74	113.6606588	12918.75	4.779936
61	0.54	115.5550031	13352.96	3.605299
62	0.46	117.4493474	13794.35	3.1727
63	0.36	119.3436917	14242.92	2.563725

0.7mm nozzle with AFR 0.6 lb/min at 35MPa test data

Dish no	Abrasive wt (g)	Velocity (m/s)	V^2 $(m/s)^2$	Energy(J)
2	0.06	3.788688626	14.35416	0.000431
3	0.5	5.68303294	32.29686	0.008074
4	1.24	7.577377253	57.41665	0.035598
5	2.68	9.471721566	89.71351	0.120216
6	4.12	11.36606588	129.1875	0.266126
7	5.64	13.26041019	175.8385	0.495865
8	5.44	15.15475451	229.6666	0.624693
9	7.56	17.04909882	290.6718	1.098739
10	7.62	18.94344313	358.854	1.367234
11	9.48	20.83778745	434.2134	2.058171
12	9.08	22.73213176	516.7498	2.346044
13	9.64	24.62647607	606.4633	2.923153
14	11.64	26.52082039	703.3539	4.09352
15	13.08	28.4151647	807.4216	5.280537
16	13.34	30.30950901	918.6663	6.127504
17	13.92	32.20385333	1037.088	7.218134
18	13.1	34.09819764	1162.687	7.6156
19	12.06	35.99254195	1295.463	7.811642
20	12.16	37.88688626	1435.416	8.72733
21	11.9	39.78123058	1582.546	9.416151
22	10.92	41.67557489	1736.854	9.48322
23	11.34	43.5699192	1898.338	10.76358
24	9.66	45.46426352	2066.999	9.983606
25	11.1	47.35860783	2242.838	12.44775
26	9.16	49.25295214	2425.853	11.11041

27	10.3	51.14729646	2616.046	13.47264
28	9.18	53.04164077	2813.416	12.91358
29	8.48	54.93598508	3017.962	12.79616
30	6.62	56.8303294	3229.686	10.69026
31	5.42	58.72467371	3448.587	9.345672
32	4.3	60.61901802	3674.665	7.90053
33	3.66	62.51336234	3907.92	7.151494
34	2.7	64.40770665	4148.353	5.600276
35	1.34	66.30205096	4395.962	2.945295
36	1.6	68.19639528	4650.748	3.720599
37	1.12	70.09073959	4912.712	2.751119
38	0.62	71.9850839	5181.852	1.606374
39	0.54	73.87942822	5458.17	1.473706
40	0.54	75.77377253	5741.665	1.550249
41	0.46	77.66811684	6032.336	1.387437
42	0.34	79.56246116	6330.185	1.076131
43	0.42	81.45680547	6635.211	1.393394
44	0.28	83.35114978	6947.414	0.972638
45	0.18	85.2454941	7266.794	0.654011
46	0.24	87.13983841	7593.351	0.911202
47	0.34	89.03418272	7927.086	1.347605
48	0.22	90.92852704	8267.997	0.90948
49	0.18	92.82287135	8616.085	0.775448
50	0.18	94.71721566	8971.351	0.807422

0.7mm nozzle with AFR 1.0 lb/min at 35MPa test data

Dish no	Abrasive wt (g)	Velocity (m/s)	V^2 $(m/s)^2$	Energy(J)
2	0.24	3.788688626	14.35416	0.001722
3	1.08	5.68303294	32.29686	0.01744
4	2.62	7.577377253	57.41665	0.075216
5	4.86	9.471721566	89.71351	0.218004
6	7.16	11.36606588	129.1875	0.462491
7	8.6	13.26041019	175.8385	0.756105
8	8.8	15.15475451	229.6666	1.010533
9	11.62	17.04909882	290.6718	1.688803
10	11.92	18.94344313	358.854	2.13877
11	14.2	20.83778745	434.2134	3.082915
12	12.12	22.73213176	516.7498	3.131504
13	15.72	24.62647607	606.4633	4.766802
14	18.88	26.52082039	703.3539	6.639661
15	22	28.4151647	807.4216	8.881637
16	19.78	30.30950901	918.6663	9.08561
17	21.82	32.20385333	1037.088	11.31463
18	23.72	34.09819764	1162.687	13.78947
19	20.1	35.99254195	1295.463	13.0194
20	20.5	37.88688626	1435.416	14.71302
21	19.7	39.78123058	1582.546	15.58808
22	19.82	41.67557489	1736.854	17.21222
23	15.64	43.5699192	1898.338	14.845
24	17.84	45.46426352	2066.999	18.43763
25	17.74	47.35860783	2242.838	19.89397
26	14.92	49.25295214	2425.853	18.09687

27	16.9	51.14729646	2616.046	22.10559
28	14.62	53.04164077	2813.416	20.56607
29	13.02	54.93598508	3017.962	19.64694
30	11.04	56.8303294	3229.686	17.82787
31	8.28	58.72467371	3448.587	14.27715
32	6.82	60.61901802	3674.665	12.53061
33	5.68	62.51336234	3907.92	11.09849
34	4.4	64.40770665	4148.353	9.126376
35	3.66	66.30205096	4395.962	8.04461
36	2.78	68.19639528	4650.748	6.46454
37	2.14	70.09073959	4912.712	5.256602
38	1.3	71.9850839	5181.852	3.368204
39	1	73.87942822	5458.17	2.729085
40	0.74	75.77377253	5741.665	2.124416
41	0.7	77.66811684	6032.336	2.111318
42	0.46	79.56246116	6330.185	1.455943
43	0.38	81.45680547	6635.211	1.26069
44	0.32	83.35114978	6947.414	1.111586
45	0.26	85.2454941	7266.794	0.944683
46	0.16	87.13983841	7593.351	0.607468
47	0.12	89.03418272	7927.086	0.475625
48	0.08	90.92852704	8267.997	0.33072
49	0.1	92.82287135	8616.085	0.430804
50	0.04	94.71721566	8971.351	0.179427

0.7mm nozzle with AFR 1.5 lb/min at 35MPa test data

Dish no	Abrasive wt (g)	Velocity (m/s)	V^2 $(m/s)^2$	Energy(J)
2	0.68	3.788688626	14.35416	0.00488
3	4.16	5.68303294	32.29686	0.067177
4	4.88	7.577377253	57.41665	0.140097
5	9.32	9.471721566	89.71351	0.418065
6	13.68	11.36606588	129.1875	0.883642
7	16.54	13.26041019	175.8385	1.454184
8	16.48	15.15475451	229.6666	1.892453
9	20.8	17.04909882	290.6718	3.022986
10	22.38	18.94344313	358.854	4.015577
11	27.78	20.83778745	434.2134	6.031224
12	25.5	22.73213176	516.7498	6.58856
13	31.28	24.62647607	606.4633	9.485086
14	34.56	26.52082039	703.3539	12.15396
15	43.56	28.4151647	807.4216	17.58564
16	40.36	30.30950901	918.6663	18.53869
17	43.84	32.20385333	1037.088	22.73297
18	41.3	34.09819764	1162.687	24.00949
19	39.08	35.99254195	1295.463	25.31335
20	40.74	37.88688626	1435.416	29.23943
21	38.34	39.78123058	1582.546	30.33741
22	35.32	41.67557489	1736.854	30.67283
23	32.12	43.5699192	1898.338	30.48731
24	34.66	45.46426352	2066.999	35.8211
25	36.1	47.35860783	2242.838	40.48322
26	25.78	49.25295214	2425.853	31.26925

27	29.4	51.14729646	2616.046	38.45588
28	26.1	53.04164077	2813.416	36.71507
29	25.17	54.93598508	3017.962	37.98106
30	24.14	56.8303294	3229.686	38.98231
31	14.88	58.72467371	3448.587	25.65749
32	12.52	60.61901802	3674.665	23.00341
33	10.96	62.51336234	3907.92	21.4154
34	8.16	64.40770665	4148.353	16.92528
35	6.38	66.30205096	4395.962	14.02312
36	3.8	68.19639528	4650.748	8.836422
37	2.68	70.09073959	4912.712	6.583034
38	5	71.9850839	5181.852	12.95463
39	1.46	73.87942822	5458.17	3.984464
40	1.54	75.77377253	5741.665	4.421082
41	1.26	77.66811684	6032.336	3.800372
42	0.92	79.56246116	6330.185	2.911885
43	0.7	81.45680547	6635.211	2.322324
44	0.5	83.35114978	6947.414	1.736854
45	0.38	85.2454941	7266.794	1.380691
46	0.3	87.13983841	7593.351	1.139003
47	0.24	89.03418272	7927.086	0.95125
48	0.2	90.92852704	8267.997	0.8268
49	0.14	92.82287135	8616.085	0.603126
50	0.06	94.71721566	8971.351	0.269141

0.7mm nozzle with AFR 0.6lb/min at 69MPa test data

Dish no	Abrasive wt (g)	Velocity (m/s)	V^2 $(m/s)^2$	Energy(J)
2	0.08	3.788688626	14.35416	0.000574
3	0.5	5.68303294	32.29686	0.008074
4	1.02	7.577377253	57.41665	0.029282
5	2.04	9.471721566	89.71351	0.091508
6	3.74	11.36606588	129.1875	0.241581
7	5.44	13.26041019	175.8385	0.478281
8	6.36	15.15475451	229.6666	0.73034
9	8.74	17.04909882	290.6718	1.270236
10	6.64	18.94344313	358.854	1.191395
11	7.12	20.83778745	434.2134	1.5458
12	6.22	22.73213176	516.7498	1.607092
13	8.06	24.62647607	606.4633	2.444047
14	7.42	26.52082039	703.3539	2.609443
15	5.36	28.4151647	807.4216	2.16389
16	7.68	30.30950901	918.6663	3.527679
17	8.8	32.20385333	1037.088	4.563188
18	9.5	34.09819764	1162.687	5.522764
19	9.36	35.99254195	1295.463	6.062767
20	8.68	37.88688626	1435.416	6.229706
21	8.18	39.78123058	1582.546	6.472614
22	5.66	41.67557489	1736.854	4.915296
23	7.2	43.5699192	1898.338	6.834016
24	7.96	45.46426352	2066.999	8.226657
25	8.92	47.35860783	2242.838	10.00306
26	7.18	49.25295214	2425.853	8.708813

27	9.16	51.14729646	2616.046	11.98149
28	9.08	53.04164077	2813.416	12.77291
29	10.02	54.93598508	3017.962	15.11999
30	9.94	56.8303294	3229.686	16.05154
31	9.5	58.72467371	3448.587	16.38079
32	7.74	60.61901802	3674.665	14.22095
33	8.3	62.51336234	3907.92	16.21787
34	6.56	64.40770665	4148.353	13.6066
35	6.8	66.30205096	4395.962	14.94627
36	5.94	68.19639528	4650.748	13.81272
37	5.48	70.09073959	4912.712	13.46083
38	4.02	71.9850839	5181.852	10.41552
39	3.76	73.87942822	5458.17	10.26136
40	4.28	75.77377253	5741.665	12.28716
41	3.46	77.66811684	6032.336	10.43594
42	2.88	79.56246116	6330.185	9.115467
43	2.34	81.45680547	6635.211	7.763197
44	1.86	83.35114978	6947.414	6.461095
45	1.48	85.2454941	7266.794	5.377428
46	1.34	87.13983841	7593.351	5.087545
47	1.1	89.03418272	7927.086	4.359897
48	0.78	90.92852704	8267.997	3.224519
49	0.64	92.82287135	8616.085	2.757147
50	0.42	94.71721566	8971.351	1.883984
51	0.44	96.61155998	9333.794	2.053435
52	0.42	98.50590429	9703.413	2.037717
53	0.36	100.4002486	10080.21	1.814438

54	0.28	102.2945929	10464.18	1.464986
55	0.24	104.1889372	10855.33	1.30264
56	0.22	106.0832815	11253.66	1.237903
57	0.18	107.9776259	11659.17	1.049325
58	0.12	109.8719702	12071.85	0.724311
59	0.1	111.7663145	12491.71	0.624585
60	0.06	113.6606588	12918.75	0.387562
61	0.06	115.5550031	13352.96	0.400589
62	0.04	117.4493474	13794.35	0.275887
63	0	119.3436917	14242.92	0

0.7mm nozzle with AFR 1.0lb/min at 69MPa test data

Dish no	Abrasive wt (g)	Velocity (m/s)	V^2 $(m/s)^2$	Energy(J)
2	0.06	3.788688626	14.35416	0.000431
3	0.56	5.68303294	32.29686	0.009043
4	1.48	7.577377253	57.41665	0.042488
5	2.78	9.471721566	89.71351	0.124702
6	4.38	11.36606588	129.1875	0.282921
7	5.42	13.26041019	175.8385	0.476522
8	5.98	15.15475451	229.6666	0.686703
9	7.36	17.04909882	290.6718	1.069672
10	7.52	18.94344313	358.854	1.349291
11	8.48	20.83778745	434.2134	1.841065
12	8.14	22.73213176	516.7498	2.103172
13	11.92	24.62647607	606.4633	3.614521
14	11.34	26.52082039	703.3539	3.988017
15	14.34	28.4151647	807.4216	5.789213
16	13.58	30.30950901	918.6663	6.237744
17	15.56	32.20385333	1037.088	8.068546
18	16.52	34.09819764	1162.687	9.603795
19	15.34	35.99254195	1295.463	9.936202
20	15.72	37.88688626	1435.416	11.28237
21	16.84	39.78123058	1582.546	13.32504
22	12.46	41.67557489	1736.854	10.8206
23	12.38	43.5699192	1898.338	11.75071
24	15.14	45.46426352	2066.999	15.64718
25	16.38	47.35860783	2242.838	18.36884
26	13.82	49.25295214	2425.853	16.76265

27	18.46	51.14729646	2616.046	24.1461
28	18.14	53.04164077	2813.416	25.51768
29	21.48	54.93598508	3017.962	32.41292
30	18.8	56.8303294	3229.686	30.35905
31	16.32	58.72467371	3448.587	28.14047
32	14.96	60.61901802	3674.665	27.4865
33	17.02	62.51336234	3907.92	33.2564
34	12.62	64.40770665	4148.353	26.17611
35	12.52	66.30205096	4395.962	27.51872
36	11.04	68.19639528	4650.748	25.67213
37	10.06	70.09073959	4912.712	24.71094
38	8.1	71.9850839	5181.852	20.9865
39	7.76	73.87942822	5458.17	21.1777
40	8.14	75.77377253	5741.665	23.36857
41	6.98	77.66811684	6032.336	21.05285
42	5.9	79.56246116	6330.185	18.67405
43	5.16	81.45680547	6635.211	17.11884
44	3.8	83.35114978	6947.414	13.20009
45	3.24	85.2454941	7266.794	11.77221
46	2.82	87.13983841	7593.351	10.70663
47	2.44	89.03418272	7927.086	9.671045
48	2.06	90.92852704	8267.997	8.516037
49	1.42	92.82287135	8616.085	6.117421
50	1.1	94.71721566	8971.351	4.934243
51	0.92	96.61155998	9333.794	4.293545
52	1	98.50590429	9703.413	4.851707
53	0.88	100.4002486	10080.21	4.435292

54	0.74	102.2945929	10464.18	3.871748
55	0.68	104.1889372	10855.33	3.690814
56	0.6	106.0832815	11253.66	3.376099
57	0.44	107.9776259	11659.17	2.565017
58	0.4	109.8719702	12071.85	2.41437
59	0.36	111.7663145	12491.71	2.248508
60	0.36	113.6606588	12918.75	2.325374
61	0.18	115.5550031	13352.96	1.201766
62	0.2	117.4493474	13794.35	1.379435
63	0.2	119.3436917	14242.92	1.424292

0.7mm nozzle with AFR 1.5lb/min at 69MPa test data

Dish no	Abrasive wt (g)	Velocity (m/s)	V^2 $(m/s)^2$	Energy(J)
2	0.2	3.788688626	14.35416	0.001435
3	1.52	5.68303294	32.29686	0.024546
4	4.24	7.577377253	57.41665	0.121723
5	7	9.471721566	89.71351	0.313997
6	10.96	11.36606588	129.1875	0.707947
7	16.18	13.26041019	175.8385	1.422533
8	17.08	15.15475451	229.6666	1.961353
9	21.28	17.04909882	290.6718	3.092748
10	19.94	18.94344313	358.854	3.577775
11	19.22	20.83778745	434.2134	4.172791
12	17.98	22.73213176	516.7498	4.645581
13	19.06	24.62647607	606.4633	5.779595
14	21.1	26.52082039	703.3539	7.420384
15	25.94	28.4151647	807.4216	10.47226
16	23.5	30.30950901	918.6663	10.79433
17	29.64	32.20385333	1037.088	15.36965
18	30.9	34.09819764	1162.687	17.96352
19	28.74	35.99254195	1295.463	18.6158
20	27.9	37.88688626	1435.416	20.02406
21	27.3	39.78123058	1582.546	21.60176
22	24.58	41.67557489	1736.854	21.34593
23	22.54	43.5699192	1898.338	21.39427
24	26.12	45.46426352	2066.999	26.99501
25	30.06	47.35860783	2242.838	33.70985
26	23.48	49.25295214	2425.853	28.47952

27	28.3	51.14729646	2616.046	37.01705
28	28.24	53.04164077	2813.416	39.72543
29	30.9	54.93598508	3017.962	46.62752
30	25.9	56.8303294	3229.686	41.82444
31	22.94	58.72467371	3448.587	39.5553
32	20.76	60.61901802	3674.665	38.14303
33	20.92	62.51336234	3907.92	40.87685
34	17.68	64.40770665	4148.353	36.67144
35	15.92	66.30205096	4395.962	34.99186
36	13.74	68.19639528	4650.748	31.95064
37	12.38	70.09073959	4912.712	30.40969
38	9.5	71.9850839	5181.852	24.6138
39	8.56	73.87942822	5458.17	23.36097
40	8.4	75.77377253	5741.665	24.11499
41	7.28	77.66811684	6032.336	21.9577
42	5.78	79.56246116	6330.185	18.29424
43	4.9	81.45680547	6635.211	16.25627
44	4.02	83.35114978	6947.414	13.9643
45	3.02	85.2454941	7266.794	10.97286
46	2.48	87.13983841	7593.351	9.415756
47	1.98	89.03418272	7927.086	7.847815
48	1.58	90.92852704	8267.997	6.531718
49	1.24	92.82287135	8616.085	5.341973
50	0.94	94.71721566	8971.351	4.216535
51	0.8	96.61155998	9333.794	3.733517
52	0.7	98.50590429	9703.413	3.396195
53	0.56	100.4002486	10080.21	2.822459

54	0.6	102.2945929	10464.18	3.139255
55	0.38	104.1889372	10855.33	2.062514
56	0.26	106.0832815	11253.66	1.462976
57	0.2	107.9776259	11659.17	1.165917
58	0.16	109.8719702	12071.85	0.965748
59	0.12	111.7663145	12491.71	0.749503
60	0.06	113.6606588	12918.75	0.387562
61	0.04	115.5550031	13352.96	0.267059
62	0.06	117.4493474	13794.35	0.41383
63	0.04	119.3436917	14242.92	0.284858

0.7mm nozzle with AFR 0.6lb/min at 103MPa test data

Dish no	Abrasive wt (g)	Velocity (m/s)	V^2 $(m/s)^2$	Energy(J)
2	0.06	3.788688626	14.35416	0.000431
3	0.2	5.68303294	32.29686	0.00323
4	0.4	7.577377253	57.41665	0.011483
5	0.9	9.471721566	89.71351	0.040371
6	2.18	11.36606588	129.1875	0.140814
7	3.04	13.26041019	175.8385	0.267274
8	0.98	15.15475451	229.6666	0.112537
9	3.72	17.04909882	290.6718	0.540649
10	3.72	18.94344313	358.854	0.667469
11	4.48	20.83778745	434.2134	0.972638
12	3.88	22.73213176	516.7498	1.002495
13	7.06	24.62647607	606.4633	2.140816
14	4.94	26.52082039	703.3539	1.737284
15	5.8	28.4151647	807.4216	2.341523
16	4.86	30.30950901	918.6663	2.232359
17	5.6	32.20385333	1037.088	2.903847
18	5.56	34.09819764	1162.687	3.23227
19	5.28	35.99254195	1295.463	3.420023
20	4.86	37.88688626	1435.416	3.488061
21	4.92	39.78123058	1582.546	3.893064
22	4.78	41.67557489	1736.854	4.15108
23	4.36	43.5699192	1898.338	4.138377
24	4.9	45.46426352	2066.999	5.064148
25	6.5	47.35860783	2242.838	7.289223

26	5.9	49.25295214	2425.853	7.156267
27	5.24	51.14729646	2616.046	6.85404
28	4.86	53.04164077	2813.416	6.8366
29	5.32	54.93598508	3017.962	8.02778
30	5.18	56.8303294	3229.686	8.364888
31	5.46	58.72467371	3448.587	9.414643
32	5.06	60.61901802	3674.665	9.296903
33	6.9	62.51336234	3907.92	13.48233
34	5.28	64.40770665	4148.353	10.95165
35	5.4	66.30205096	4395.962	11.8691
36	5.7	68.19639528	4650.748	13.25463
37	5.58	70.09073959	4912.712	13.70647
38	4.58	71.9850839	5181.852	11.86644
39	4.1	73.87942822	5458.17	11.18925
40	4.22	75.77377253	5741.665	12.11491
41	3.68	77.66811684	6032.336	11.0995
42	3	79.56246116	6330.185	9.495278
43	2.64	81.45680547	6635.211	8.758479
44	2.02	83.35114978	6947.414	7.016888
45	1.66	85.2454941	7266.794	6.031439
46	1.46	87.13983841	7593.351	5.543147
47	1.22	89.03418272	7927.086	4.835522
48	1.08	90.92852704	8267.997	4.464718
49	0.82	92.82287135	8616.085	3.532595
50	0.7	94.71721566	8971.351	3.139973
51	0.62	96.61155998	9333.794	2.893476
52	0.48	98.50590429	9703.413	2.328819

53	0.48	100.4002486	10080.21	2.41925
54	0.36	102.2945929	10464.18	1.883553
55	0.32	104.1889372	10855.33	1.736854
56	0.56	106.0832815	11253.66	3.151026
57	0.18	107.9776259	11659.17	1.049325
58	0.12	109.8719702	12071.85	0.724311
59	0.08	111.7663145	12491.71	0.499668

0.7mm nozzle with AFR 1.0lb/min at 103MPa test data

Dish no	Abrasive wt (g)	Velocity (m/s)	V^2 $(m/s)^2$	Energy(J)
2	0.14	3.788688626	14.35416	0.001005
3	0.48	5.68303294	32.29686	0.007751
4	1.26	7.577377253	57.41665	0.036172
5	1.74	9.471721566	89.71351	0.078051
6	4	11.36606588	129.1875	0.258375
7	6.26	13.26041019	175.8385	0.550374
8	4.78	15.15475451	229.6666	0.548903
9	6.38	17.04909882	290.6718	0.927243
10	6.56	18.94344313	358.854	1.177041
11	7.3	20.83778745	434.2134	1.584879
12	7.82	22.73213176	516.7498	2.020492
13	12.8	24.62647607	606.4633	3.881365
14	8.76	26.52082039	703.3539	3.08069
15	10.62	28.4151647	807.4216	4.287409
16	9.56	30.30950901	918.6663	4.391225
17	10.56	32.20385333	1037.088	5.475826
18	10.76	34.09819764	1162.687	6.255257
19	10.72	35.99254195	1295.463	6.943682
20	9.76	37.88688626	1435.416	7.004831
21	10.36	39.78123058	1582.546	8.19759
22	8.88	41.67557489	1736.854	7.71163
23	9.72	43.5699192	1898.338	9.225922
24	10.96	45.46426352	2066.999	11.32716
25	12.98	47.35860783	2242.838	14.55602
26	9.36	49.25295214	2425.853	11.35299

27	11.7	51.14729646	2616.046	15.30387
28	11.64	53.04164077	2813.416	16.37408
29	13.04	54.93598508	3017.962	19.67712
30	10.44	56.8303294	3229.686	16.85896
31	10.78	58.72467371	3448.587	18.58789
32	9.3	60.61901802	3674.665	17.08719
33	10.84	62.51336234	3907.92	21.18093
34	9.72	64.40770665	4148.353	20.16099
35	9.96	66.30205096	4395.962	21.89189
36	10.4	68.19639528	4650.748	24.18389
37	10.2	70.09073959	4912.712	25.05483
38	8.7	71.9850839	5181.852	22.54106
39	8.08	73.87942822	5458.17	22.05101
40	8.46	75.77377253	5741.665	24.28724
41	7.42	77.66811684	6032.336	22.37997
42	6.5	79.56246116	6330.185	20.5731
43	5.36	81.45680547	6635.211	17.78237
44	4.44	83.35114978	6947.414	15.42326
45	3.8	85.2454941	7266.794	13.80691
46	3.16	87.13983841	7593.351	11.9975
47	2.76	89.03418272	7927.086	10.93938
48	2.32	90.92852704	8267.997	9.590877
49	1.8	92.82287135	8616.085	7.754477
50	1.42	94.71721566	8971.351	6.369659
51	1.16	96.61155998	9333.794	5.4136
52	1.12	98.50590429	9703.413	5.433911
53	1.08	100.4002486	10080.21	5.443313

54	0.9	102.2945929	10464.18	4.708883
55	0.86	104.1889372	10855.33	4.667794
56	0.72	106.0832815	11253.66	4.051319
57	0.56	107.9776259	11659.17	3.264567
58	0.46	109.8719702	12071.85	2.776525
59	0.38	111.7663145	12491.71	2.373425
60	0.3	113.6606588	12918.75	1.937812
61	0.24	115.5550031	13352.96	1.602355
62	0.16	117.4493474	13794.35	1.103548
63	0.22	119.3436917	14242.92	1.566721

0.7mm nozzle with AFR 1.5lb/min at 103MPa test data

Dish no	Abrasive wt (g)	Velocity (m/s)	V^2 $(m/s)^2$	Energy(J)
2	0.28	3.788688626	14.35416	0.00201
3	3.02	5.68303294	32.29686	0.048768
4	0.78	7.577377253	57.41665	0.022392
5	1.54	9.471721566	89.71351	0.069079
6	6.28	11.36606588	129.1875	0.405649
7	9.88	13.26041019	175.8385	0.868642
8	8.42	15.15475451	229.6666	0.966896
9	9.48	17.04909882	290.6718	1.377784
10	9.46	18.94344313	358.854	1.69738
11	12.1	20.83778745	434.2134	2.626991
12	12.46	22.73213176	516.7498	3.219351
13	21.9	24.62647607	606.4633	6.640773
14	17.38	26.52082039	703.3539	6.112146
15	20.58	28.4151647	807.4216	8.308368
16	17.58	30.30950901	918.6663	8.075077
17	19.9	32.20385333	1037.088	10.31903
18	20.54	34.09819764	1162.687	11.9408
19	18.6	35.99254195	1295.463	12.04781
20	17.06	37.88688626	1435.416	12.2441
21	17.7	39.78123058	1582.546	14.00553
22	16.92	41.67557489	1736.854	14.69378
23	15.24	43.5699192	1898.338	14.46533
24	17.98	45.46426352	2066.999	18.58232
25	22.02	47.35860783	2242.838	24.69364
26	14.5	49.25295214	2425.853	17.58744

27	18.34	51.14729646	2616.046	23.98914
28	18.38	53.04164077	2813.416	25.85529
29	20.62	54.93598508	3017.962	31.11519
30	19.08	56.8303294	3229.686	30.81121
31	19.7	58.72467371	3448.587	33.96858
32	18.42	60.61901802	3674.665	33.84367
33	24.32	62.51336234	3907.92	47.52031
34	20.52	64.40770665	4148.353	42.5621
35	21.88	66.30205096	4395.962	48.09182
36	20.8	68.19639528	4650.748	48.36778
37	20.74	70.09073959	4912.712	50.94482
38	16.76	71.9850839	5181.852	43.42392
39	15.02	73.87942822	5458.17	40.99086
40	17.16	75.77377253	5741.665	49.26348
41	14.14	77.66811684	6032.336	42.64862
42	11.44	79.56246116	6330.185	36.20866
43	9.72	81.45680547	6635.211	32.24713
44	7.6	83.35114978	6947.414	26.40017
45	6.28	85.2454941	7266.794	22.81773
46	5.28	87.13983841	7593.351	20.04645
47	4.44	89.03418272	7927.086	17.59813
48	3.62	90.92852704	8267.997	14.96507
49	3.11	92.82287135	8616.085	13.39801
50	2.86	94.71721566	8971.351	12.82903
51	1.9	96.61155998	9333.794	8.867104
52	1.7	98.50590429	9703.413	8.247901
53	1.64	100.4002486	10080.21	8.265772

54	1.24	102.2945929	10464.18	6.487794
55	1.16	104.1889372	10855.33	6.296094
56	1	106.0832815	11253.66	5.626831
57	0.74	107.9776259	11659.17	4.313892
58	0.68	109.8719702	12071.85	4.104429
59	0.5	111.7663145	12491.71	3.122927
60	0.3	113.6606588	12918.75	1.937812
61	0.24	115.5550031	13352.96	1.602355
62	0.42	117.4493474	13794.35	2.896813
63	0.34	119.3436917	14242.92	2.421296

0.7mm nozzle with AFR 0.6lb/min at 138MPa test data

Dish no	Abrasive wt (g)	Velocity (m/s)	V^2 $(m/s)^2$	Energy(J)
2	0.02	3.788688626	14.35416	0.000144
3	0.08	5.68303294	32.29686	0.001292
4	0.18	7.577377253	57.41665	0.005167
5	0.36	9.471721566	89.71351	0.016148
6	0.84	11.36606588	129.1875	0.054259
7	1.58	13.26041019	175.8385	0.138912
8	1.44	15.15475451	229.6666	0.16536
9	1.84	17.04909882	290.6718	0.267418
10	2.22	18.94344313	358.854	0.398328
11	2.72	20.83778745	434.2134	0.59053
12	2.44	22.73213176	516.7498	0.630435
13	4.28	24.62647607	606.4633	1.297832
14	2.58	26.52082039	703.3539	0.907327
15	3	28.4151647	807.4216	1.211132
16	2.48	30.30950901	918.6663	1.139146
17	2.8	32.20385333	1037.088	1.451923
18	2.72	34.09819764	1162.687	1.581254
19	2.54	35.99254195	1295.463	1.645238
20	2.32	37.88688626	1435.416	1.665083
21	2.44	39.78123058	1582.546	1.930706
22	2.36	41.67557489	1736.854	2.049487
23	2.44	43.5699192	1898.338	2.315972
24	2.72	45.46426352	2066.999	2.811119
25	3.68	47.35860783	2242.838	4.126821
26	1.88	49.25295214	2425.853	2.280302

27	2.4	51.14729646	2616.046	3.139255
28	2.38	53.04164077	2813.416	3.347965
29	2.74	54.93598508	3017.962	4.134609
30	2.72	56.8303294	3229.686	4.392373
31	2.72	58.72467371	3448.587	4.690079
32	2.5	60.61901802	3674.665	4.593332
33	3.02	62.51336234	3907.92	5.90096
34	2.78	64.40770665	4148.353	5.76621
35	2.76	66.30205096	4395.962	6.066428
36	3.3	68.19639528	4650.748	7.673735
37	3.24	70.09073959	4912.712	7.958593
38	3.88	71.9850839	5181.852	10.05279
39	2.52	73.87942822	5458.17	6.877294
40	2.98	75.77377253	5741.665	8.55508
41	2.98	77.66811684	6032.336	8.988181
42	2.46	79.56246116	6330.185	7.786128
43	2.38	81.45680547	6635.211	7.895901
44	1.94	83.35114978	6947.414	6.738992
45	1.82	85.2454941	7266.794	6.612783
46	1.72	87.13983841	7593.351	6.530282
47	1.46	89.03418272	7927.086	5.786773
48	1.36	90.92852704	8267.997	5.622238
49	1.04	92.82287135	8616.085	4.480364
50	1.06	94.71721566	8971.351	4.754816
51	0.9	96.61155998	9333.794	4.200207
52	0.8	98.50590429	9703.413	3.881365
53	0.78	100.4002486	10080.21	3.931282

54	0.72	102.2945929	10464.18	3.767106
55	0.6	104.1889372	10855.33	3.2566
56	0.54	106.0832815	11253.66	3.038489
57	0.56	107.9776259	11659.17	3.264567
58	0.4	109.8719702	12071.85	2.41437
59	0.32	111.7663145	12491.71	1.998673
60	0.32	113.6606588	12918.75	2.066999
61	0.24	115.5550031	13352.96	1.602355
62	0.2	117.4493474	13794.35	1.379435
63	0.2	119.3436917	14242.92	1.424292

0.7mm nozzle with AFR 1.0lb/min at 138MPa test data

Dish no	Abrasive wt (g)	Velocity (m/s)	V^2 $(m/s)^2$	Energy(J)
2	0.16	3.788688626	14.35416	0.001148
3	0.2	5.68303294	32.29686	0.00323
4	0.56	7.577377253	57.41665	0.016077
5	1.4	9.471721566	89.71351	0.062799
6	2.64	11.36606588	129.1875	0.170527
7	4.48	13.26041019	175.8385	0.393878
8	3.52	15.15475451	229.6666	0.404213
9	4.94	17.04909882	290.6718	0.717959
10	5.32	18.94344313	358.854	0.954552
11	6.56	20.83778745	434.2134	1.42422
12	9.86	22.73213176	516.7498	2.547577
13	6.28	24.62647607	606.4633	1.904295
14	7.6	26.52082039	703.3539	2.672745
15	6.2	28.4151647	807.4216	2.503007
16	7.78	30.30950901	918.6663	3.573612
17	7.18	32.20385333	1037.088	3.723147
18	6.54	34.09819764	1162.687	3.801987
19	6.64	35.99254195	1295.463	4.300937
20	7.02	37.88688626	1435.416	5.038311
21	6.04	39.78123058	1582.546	4.77929
22	6.02	41.67557489	1736.854	5.227929
23	7.1	43.5699192	1898.338	6.739099
24	5.68	45.46426352	2066.999	5.870278
25	9.4	47.35860783	2242.838	10.54134
26	5.38	49.25295214	2425.853	6.525545

27	6.3	51.14729646	2616.046	8.240545
28	6.08	53.04164077	2813.416	8.552784
29	7.24	54.93598508	3017.962	10.92502
30	7.14	56.8303294	3229.686	11.52998
31	7.12	58.72467371	3448.587	12.27697
32	6.72	60.61901802	3674.665	12.34688
33	7.66	62.51336234	3907.92	14.96734
34	8.8	64.40770665	4148.353	18.25275
35	8.04	66.30205096	4395.962	17.67177
36	8.96	68.19639528	4650.748	20.83535
37	10.34	70.09073959	4912.712	25.39872
38	9.1	71.9850839	5181.852	23.57743
39	8.54	73.87942822	5458.17	23.30639
40	9.44	75.77377253	5741.665	27.10066
41	9.18	77.66811684	6032.336	27.68842
42	8.76	79.56246116	6330.185	27.72621
43	7.68	81.45680547	6635.211	25.47921
44	6.2	83.35114978	6947.414	21.53698
45	5.74	85.2454941	7266.794	20.8557
46	5.08	87.13983841	7593.351	19.28711
47	4.34	89.03418272	7927.086	17.20178
48	3.7	90.92852704	8267.997	15.29579
49	2.9	92.82287135	8616.085	12.49332
50	2.34	94.71721566	8971.351	10.49648
51	1.94	96.61155998	9333.794	9.05378
52	1.9	98.50590429	9703.413	9.218243
53	1.76	100.4002486	10080.21	8.870585
54	1.58	102.2945929	10464.18	8.266705

55	1.38	104.1889372	10855.33	7.490181
56	1.34	106.0832815	11253.66	7.539954
57	1	107.9776259	11659.17	5.829584
58	0.88	109.8719702	12071.85	5.311614
59	0.74	111.7663145	12491.71	4.621932
60	0.54	113.6606588	12918.75	3.488061
61	0.38	115.5550031	13352.96	2.537062
62	0.3	117.4493474	13794.35	2.069152
63	0.34	119.3436917	14242.92	2.421296

0.7mm nozzle with AFR 1.5lb/min at 138MPa test data

Dish no	Abrasive wt (g)	Velocity (m/s)	V^2 $(m/s)^2$	Energy(J)
2	0.32	3.788688626	14.35416	0.002297
3	0.32	5.68303294	32.29686	0.005167
4	1.1	7.577377253	57.41665	0.031579
5	1.64	9.471721566	89.71351	0.073565
6	3.6	11.36606588	129.1875	0.232537
7	6.36	13.26041019	175.8385	0.559166
8	5.02	15.15475451	229.6666	0.576463
9	6.16	17.04909882	290.6718	0.895269
10	5.98	18.94344313	358.854	1.072974
11	7.08	20.83778745	434.2134	1.537115
12	7.36	22.73213176	516.7498	1.901639
13	14	24.62647607	606.4633	4.245243
14	11.4	26.52082039	703.3539	4.009117
15	13.74	28.4151647	807.4216	5.546986
16	12.06	30.30950901	918.6663	5.539558
17	15	32.20385333	1037.088	7.778161
18	16.5	34.09819764	1162.687	9.592168
19	16.4	35.99254195	1295.463	10.6228
20	15.04	37.88688626	1435.416	10.79433
21	15.66	39.78123058	1582.546	12.39134
22	12.86	41.67557489	1736.854	11.16797
23	13.66	43.5699192	1898.338	12.96565
24	17.16	45.46426352	2066.999	17.73485
25	19.2	47.35860783	2242.838	21.53124
26	16.84	49.25295214	2425.853	20.42568

27	10.7	51.14729646	2616.046	13.99585
28	14.66	53.04164077	2813.416	20.62234
29	14.14	54.93598508	3017.962	21.33699
30	16.8	56.8303294	3229.686	27.12937
31	16.68	58.72467371	3448.587	28.76122
32	14.6	60.61901802	3674.665	26.82506
33	13.18	62.51336234	3907.92	25.7532
34	17.18	64.40770665	4148.353	35.63435
35	17.38	66.30205096	4395.962	38.20091
36	17.5	68.19639528	4650.748	40.69405
37	18.7	70.09073959	4912.712	45.93386
38	18.16	71.9850839	5181.852	47.05122
39	16.14	73.87942822	5458.17	44.04743
40	18.38	75.77377253	5741.665	52.7659
41	16.64	77.66811684	6032.336	50.18904
42	15.78	79.56246116	6330.185	49.94516
43	13.88	81.45680547	6635.211	46.04837
44	12.16	83.35114978	6947.414	42.24028
45	10.96	85.2454941	7266.794	39.82203
46	9.84	87.13983841	7593.351	37.35929
47	8.8	89.03418272	7927.086	34.87918
48	7.52	90.92852704	8267.997	31.08767
49	6.28	92.82287135	8616.085	27.05451
50	5.22	94.71721566	8971.351	23.41523
51	4.54	96.61155998	9333.794	21.18771
52	8.5	98.50590429	9703.413	41.23951
53	3.76	100.4002486	10080.21	18.95079

54	3.24	102.2945929	10464.18	16.95198
55	3.06	104.1889372	10855.33	16.60866
56	2.8	106.0832815	11253.66	15.75513
57	2.02	107.9776259	11659.17	11.77576
58	1.62	109.8719702	12071.85	9.778198
59	1.46	111.7663145	12491.71	9.118948
60	1.06	113.6606588	12918.75	6.846935
61	0.76	115.5550031	13352.96	5.074124
62	0.66	117.4493474	13794.35	4.552135
63	0.96	119.3436917	14242.92	6.8366

APPENDIX G.

EXPERIMENTAL DATA FOR EFFECT OF AFR AT 38MPa

Effect of Abrasive flow rate on material removal at 35MPa

AFR (lb/min)	Time (sec)	Volume (m3)x10^-6
3	15	4.926108374
3	30	8.128078818
3	45	14.28571429
3	60	18.22660099
2	15	6.403940887
2	30	9.60591133
2	45	16.25615764
2	60	18.96551724
1	15	3.448275862
1	30	4.679802956
1	45	5.911330049
1	60	7.881773399

BIBILIOGRAPHY

Alberts, D. and Hashish, M., "Observations of submerged abrasive suspension jet cutting for deep ocean applications," Proceedings of the 8th American Water Jet Conference, August 1995, Houston, Texas, pp. 735- 749.

Anand, U. and Katz, J., "Prevention of nozzle wear in abrasive water suspension porous lubricated nozzles," *Transaction of the ASME,* January 2003, Vol. 125, pp.168-180.

Anon, "New gulf method of jetted particle drilling promises speed and economy," *Oil and Gas Journal*, June 1971, pp. 109-114.

Baker, J.H., "Mining by Hydraulic Jet" Journal of Mining Congress, Vol. 45, No.5, May 1959, pp. 45-46, 52.

Bloomfield, E.J., and Yoeoman, M.J.," DIAJET – a review of progress," *Proceedings 1st Asian Conference on Recent Advances in Jetting Technology, CI- Premier PTE.* Ltd, Singapore, 1991, pp- 21-30.

Bonge, N. and Ozdemir, L., "Development of a system for high speed drilling of small diameter roof bolt holes," Final report on Contract DE-AC01-76ET-12462, Colorado School of Mines, April 1982, 236 pages.

Bortolussi, A., Summer, D.A. and Yazici, S., "The use of waterjets in cutting granite," *Proceedings of the 9th International Symposium on Jet Cutting Technology,* Sendai, Japan, October 1988, pp. 239-254

Bortolussi, A., Ciccu, R., Mance, P.P., and Massacci, G., "Granite Quarrying with Water Jets: A Viable Technique?" Proceedings of the 5th American Water Jet Conference, Toronto, Canada, August 29-31, 1989, pp. 49-58.

Brandt, C., Louis, H., Meier, G., and Tebbing, "Abrasive suspension jets at working pressures up to 200 Mpa," *Jet Cutting Technology – Application and Opportunities*, MEP Ltd, London, UK, 1994, pp. 489-509.

Brandt, C., Louis, H., Meier, G. and Tebbing, G., "Fields of application for abrasive water suspension jets of pressures from 15 -200 MPa," *Proceedings of the 8th American Water Jet Conference,* August 1995, Houston, Texas, pp. 207-217

Brandt, C., Louis, H., Ohlsen, J. and Tebbing, G., "Process control of Abrasive water suspension jets," *Jetting technology, BHR group,* 1996, pp.563-581.

Brandt, C., Louis, H., Ohlsen, J. and Tebbing, G., "Influence of nozzle geometry on abrasive water suspension jets," *Proceedings of the 5th Pacific Rim International Conference of Water Jet Technology,* February, 1998.a, New Delhi, pp. 330-343.

Brandt, C., Brandt, S., Louis, H., Milchers, W., Von Rad, C. and Von Berlepsch, T., "Modeling of abrasive particle acceleration in suspension nozzles," *Jetting Technology, BHR Group,* 1998.b, pp. 110-129.

Chatterton, N.E., "Development of safer more efficient hydraulic based technique for rapid excavation of coal, rock and other minerals," *Final Report on US Bureau of Mines Contract HO232062, Teledyne Brown Engineering*, PB 245 343, April 1975

Deliac, E.P., Messines, J.P. and Thierree, B.A., "Slimhole drilling-1 Mining technique finds application in oil exploration," *Oil and Gas Journal*, May 06, 1991, Volume 89-18

Eckel, J.E., Deily, F.E., and Ledgerwood, L.W.Jr., "Development and testing of jet pump pellet impact drill bits," *30th Annual Fall Meeting Petroleum Branch of AIMME*, New Orleans, October 1955, paper 540

Fair, J.C., "Development of high pressure abrasive jet drilling," *Journal of Petroleum Technology*, Vol. 33, No.8, August 1981, pp. 1379-1388.

Fairhurst, R.M., Heron, R.A. and Saunders, D.H., " DIAJET- A new abrasive water jet cutting technique," *Proceedings of the 8th International Symposium on Jet Cutting Technology*, Durham, England, 1986, pp. 395-402

Fowell, R.J., Martin J.A., Louis, H. and Brenner, V.A., "Primary investigation on the possibility of applying water jets in tunnel excavation," Jetting *Technology, BHR Group*, 2000, pp. 263-274

Gadd, M.W., "The Development of a Concentration Meter for High Pressure Suspensions Using Ultrasonic Attenuation Measurements," *PhD Thesis*, 1996, Cranfield University, School of Mechanical Engineering.

Galecki, G. and Summers, D.A., "Comparison between abrasive fragmentation in conventional high pressure abrasive jetting and the abrasive slurry jet," *Proceedings of the 6th Pacific Rim International Conference on Water Jetting*, October 2000, pp. 148-150

Hai, Z., Ming-Qing, Y., Yi-Lu, W., Mo-Shen, C., "Study of the DIAjet system and its cutting effect," *Proceedings of the 4th Pacific Rim International Conference on Water Jet Technology,* 1995, pp. 273-282.

Hashish, M., Michael, J.K. and Yih-ho, P., "Method and apparatus for forming high velocity liquid abrasive jet," U.S. Patent Number 4,648,215, 1985

Hashish, M., "Aspects of abrasive water jet performance optimization," *Proceedings of the 8th International Symposium on Water Jet Cutting Technology*," Durham, England, 1986, pp. 297-308

Hashish, M., "The potential of an Ultra high pressure abrasive water jet drill," *Proceedings of the 5th American water jet conference*, August 1989.a, Toronto, Canada pp. 321-332.

Hashish, M., "Comparative Evaluation of Abrasive-Fluidjet Machining Systems," *Proceedings ASME 1989 Winter Annual Meeting*, December 1989.b, PED-Vol. 41, pp. 221-228.

Hashish, M., "Cutting with high pressure abrasive suspension jets," *Proceedings of the 6th American water jet conference,* August 21-27, 1991, Houston, pp. 439-454

Hashish, M., "Comparative Evaluation of Abrasive liquid jet Machining Systems," *Transactions of ASME, Journal of Engineering for Industry*, 115, 1993, pp 44-50.

Hashish, M., "Machining of hard materials with abrasive suspension jets," *Proceedings of the 9th American Waterjet Conference,* August 1997, Michigan, pp. 267-280

Hollinger, R.H. and Mannheimer, R.J., "Rheological investigation of the Abrasive suspension jet," *Proceedings of the 6th American water jet conference*, August 24-27, 1991, pp.515-528.

Hoogstrate, A.M., Karpuschewski, B., van Luttervelt, C.A., and Kals, H.J.J., "Modeling of high velocity, lose abrasive machining process," *Annals of the CIRP,* 2002, 51/1, pp. 263-266.

Hoshino, K., Nagano, T., Takagi, K., Narita, Y. and Sato, M., "The development and the experiment of the water jet drill for tunnel construction," *Proceedings of the 3rd International Symposium on Jet Cutting Technology*, 1976, Chicago, E4/41-48

Jenkins, R.W., "Hydraulic mining," The National Coal board Experimental installation at Trelewis Drift Mine in the No3 area of the South Western Division, M.Sc. thesis, University of Wales, 1961

Jiang, S., Yan Xia, Ross Popescu, Cris Mihai and Kim Tan, "Cutting capability equation of abrasive suspension jet," *Proceedings of 2005 WJTA American Waterjet Conference*, August 2005, Houston, Texas, paper- 5A-1

Kolle, J.J., and Marvin, M.H., "Jet assisted drilling with supercritical carbon dioxide," Tempress Technologies Inc, 2000, http://www.tempresstech.com/papers/SC-CO2.pdf.

Labus, T. J., Neusen, K.F., Albert D.G., and Gores, T.J., "Factors Influencing the Abrasive Mixing Process," *Proceedings of the 5th American Water Jet Conference*, Toronto, Canada, August 1989, pp. 205-215.

Laurinat, A., Louis, H., and Tebbing, G., "Premixed abrasive slurry jets - the influence of important parameters," *Jet Cutting Technology*, 1992, pp. 577-591

Lemmon, E.W., McLinden, M.O. and Friend, D.G., "Thermophysical properties of fluid systems," *NIST Chemistry Webbook, NIST Standard Reference Database Number 69,* November 1998, National Institute of Standards and Technology.

Liu, B., Shang, Y., Yao, H. and Zhang, G., "The recent PREMAJET advance in cutting and derusting technology," *Jet Cutting Technology*, 1992, pp. 451-460.

Liu, B-L, Shang, Y., Yao, H. and Zhang, G.," The recent PREMAJET advance in cutting and derusting technology," *Jet Cutting Technology*, Kluwer Academic Publishers, Dordrecht, NL, 1992, pp. 451-460.

Maurer, W.C., "Advanced deep drilling technology," *Proceedings of the 30th annual Petroleum Mechanical Engineering Conference*, Tulsa, Oklahoma 1975.

McHugh, M., and Kukronis, V., "Supercritical Fluid extraction,", *2nd edition*, 1994, Butterworth-Heinemann, Boston, MA.

Ming-quing, Y., Hai, Z. and Zi-Pu, C., "Study of Direct Injection Abrasive Jet System," *Proceedings of 7th American Water Jet Conference*, August 1993, Seattle, Washington, pp. 295-305.

Mingqing, Y., Yufeng, D., Wei, L., and Moshen, C., "A study of DIAJET nozzle wear," *Proceedings of the 13th International Conference on Jetting Technology*, 1996, pp. 45-46.

Ofengenden, N.E., and Dzhvarsheishvili, A.G., "Technology of Hydromining and Hydrotransportation of Coal," (initially published in Russian by Nedra Press, Moscow, 1980) translated by A.L. Peabody, Terraspace Inc., 304, N. Stonestreet Avenue, Rockville, MD., 20850

Okita, Y. and Nakamura, K., "Performance of abrasive water suspension jet nozzles with a single annular conduit," *Proceedings of the 6th Pacific Rim International Conference on Water Jet Technology,* October 200, pp. 111-114.

Parkes, D.M. and Fisher, M., "Underground Coal Mining in Western Canada," Mining Engineering, Vol. 35, No.4, April 1983, pp. 313-316.

Rach, N.M., "Particle-impact drilling blasts away hard rock," *Oil and Gas Journal*, February 12, 2007, Vol. 105.6, pp. 43-48.

Savanick, G., A. and Krawza, W.G., "An Abrasive Water Jet Rock Drill," Proceedings of the 4th U.S. Water Jet Conference, Berkeley CA, August 1987,pp. 129-132.

Seiji, S., "Effects of nozzle shapes on the structure and drilling capability of premixed abrasive water jets," *Jetting Technology, BHR Group*, 1996, pp. 13-26

Shimizu, S., "Erosion due to premixed abrasive water jet under submerged condition," *Proceedings of the 4th Pacific Rim International Conference on Water Jet Technology*, Kajima Institute Publishing Co., Japan, 1995, pp. 71-82

Shimizu, S., Miyamoto, T. and Aihara, Y., "Structure and drilling capability of abrasive water suspension jets," *Jetting Technology, BHR Group,* 1998, pp. 109-117

Shimizu, S. and Nishiyama, T.," Drilling capability of submerged abrasive water suspension jet," *Jetting Technology, BHR Group*, 2002, pp. 509-521

Snyder, R.E., "US firms could follow Canada's lead in coiled tubing drilling," World Oil Magazine, February 2005, Vol. 226, No.2

Summers, D.A, "Disintegration of rock by high pressure jets," Ph.D. thesis, Mining Engineering, University of Leeds, UK, 1968.

Summers, D.A. and Bushnell, D.J., "Preliminary investigation of the waterjet drill device," *Proceedings of the 3rd International Conference on Jet cutting technology*, Chicago, 1976, E2/21-28

Summers, D.A., Yao, J., and Wu, W.Z., "A further investigation of DIAjet cutting," *Proceedings of the 10th International Conference on Jet Cutting Technology*, 1991, pp.181-192

Summers, D.A.,"Waterjetting Technology,", Chapman and Hall, 1995.

Summers, D.A., 31 March 2008, *Personal Communication*.

Tabitz, A.Q., Parsy, F. and Abriak, N., "Theoretical analysis of the particle acceleration process in abrasive waterjet cutting," *Computational Materials Science*, Vol. 5, N 1-3 Feb- Mar 1996. p 243-254

Tan, R., B., H. and Davidson, J.F. "Cutting by sand-water jets from a fluidized bed," *Proceedings of the 10th International Conference on Jet Cutting Technology*, 1991, pp.235-251

U.S DOE, National Energy Technology Laboratory, "Multi-Seam well completion technology: Coal bed methane production," September 2003, *DOE/NETL-2003/1193*.

Veenhuizen, S.D., Cheung, J.B. and Hill, J.R.M., "Waterjet drilling of small diameter holes," *Proceedings of the 4th International Conference on Jet cutting technology*, Canterbury, England, 1978, C3/29-40

Wakabayashi, J. "Slurry pumped 3,000 ft vertically," Coal Age, June 1979, pp. 84-87.

Wang, F-D., "Status of Hydraulic Coal Mining in the People's republic of China," Proceedings of the 2nd U.S water Jet Conference, Rolla, MO, 1983, pp. 263-268.

Weng, Y.Q., Fang, L.Z., Ling, Y. and Aihua, F., "Flow dynamics about underwater DIAjet," *Jetting Technology, BHR Group,* 1996, pp. 299-306.

Wolgamott, J.E., and Zink, G.P., " Self rotating nozzle heads," *Proceeding of the 6th American Water Jet Conference*, Houston, Texas, August 1991, pp. 603-612.

Yazici, S., "Abrasive jet cutting and drilling of Rocks," *Ph.D. Dissertation*, Department of Mining Engineering, University of Missouri Rolla, June 1989a, 191 pp

Yazici, S., and Summers, D.A., "The Investigation of DIAJET cutting of granite," *Proceedings of the 5th American WaterJet Conference*, August 1989b, Toronto, Canada.

You, M., Zhang, H., Chai, Z., "Study on a direct injection abrasive jet system," *Proceedings of the 7th American Waterjet conference,* August 1993, Seattle, Washington, pp. 295-305.

Zakin, J.L., and Summers, D.A., "The effect if visco-elastic additives on jet structure," *Proceedings of the 3rd International Symposium on Jet Cutting Technology*, Chicago, IL, May 1976, A4-47- A4-66.

Zhang, H., You, M.Q., Wang, Y.L. and Cui, M.S., "Study on the DIAJET system and its cutting effect," *Proceedings of the 4th Pacific Rim International Conference on Water Jet Technology*, Kajima Institute Publishing Co., Japan, 1995, pp. 273-282.

Zhang, S., "Three dimensional milling using and abrasive waterjet," *Ph.D. Dissertation*, Department of Mechanical and Aerospace Engineering, University of Missouri Rolla, May 2006.

VITA

Pradeep Nambiath was born on December 15th 1978 in India. After receiving his primary and secondary education in Kerala, he studied at VLB JACET in India. He received his bachelor's degree in June 2001 in Mechanical Engineering.

After his graduation, he received his master's degree in Mechanical Engineering specializing in Discrete Event Controls, at the University of Missouri-Rolla in 2004. Mr. Nambiath began his PhD degree in Mining Engineering in January 2005 and has served as a Graduate Research Assistant at Rock Mechanics and Explosives Research Centre. He received his PhD degree in May 2008.